NOTICE

The quality of this microform is heavily dependent upon the quality of the original thesis submitted for microfilming. Every effort has been made to ensure the highest quality of reproduction possible.

If pages are missing, contact the university which granted the degree.

Some pages may have indistinct print especially if the original pages were typed with a poor typewriter ribbon or if the university sent us an inferior photocopy.

Previously copyrighted materials (journal articles, published tests, etc.) are not filmed.

Reproduction in full or in part of this microform is governed by the Canadian Copyright Act, R.S.C. 1970, c. C-30.

AVIS

La qualité de cette microforme dépend grandement de la qualité de la thèse soumise au microfilmage. Nous avons tout fait pour assurer une qualité supérieure de reproduction.

S'il manque des pages, veuillez communiquer avec l'université qui a conféré le grade.

La qualité d'impression de certaines pages peut laisser à désirer, surtout si les pages originales ont été dactylographiées à l'aide d'un ruban usé ou si l'université nous a fait parvenir une photocopie de qualité inférieure.

Les documents qui font déjà l'objet d'un droit d'auteur (articles de revue, tests publiés, etc.) ne sont pas microfilmés.

La reproduction, même partielle, de cette microforme est soumise à la Loi canadienne sur le droit d'auteur, SRC 1970, c. C-30.

Canada

THE UNIVERSITY OF ALBERTA

MODELLING OF ACCELERATING MOVEMENTS IN ROCK SLOPES

by

© JAMES WILLIAM CASSIE

A THESIS

SUBMITTED TO THE FACULTY OF GRADUATE STUDIES AND RESEARCH

IN PARTIAL FULFILMENT OF THE REQUIREMENTS FOR THE DEGREE

OF MASTER OF SCIENCE

DEPARTMENT OF CIVIL ENGINEERING

EDMONTON, ALBERTA

FALL, 1987

ISBN 0-315-40986-X

THE UNIVERSITY OF ALBERTA

RELEASE FORM

NAME OF AUTHOR JAMES WILLIAM CASSIE

TITLE OF THESIS MODELLING OF ACCELERATING MOVEMENTS IN ROCK SLOPES

DEGREE FOR WHICH THESIS WAS PRESENTED MASTER OF SCIENCE

YEAR THIS DEGREE GRANTED FALL, 1987

Permission is hereby granted to THE UNIVERSITY OF ALBERTA LIBRARY to reproduce single copies of this thesis and to lend or sell such copies for private, scholarly or scientific research purposes only.

The author reserves other publication rights, and neither the thesis nor extensive extracts from it may be printed or otherwise reproduced without the author's written permission.

(SIGNED) .....

PERMANENT ADDRESS:

531 Boreank St.

Winnipeg, Mb

R3N 1C8

DATED Oct. 15 1987

THE UNIVERSITY OF ALBERTA

FACULTY OF GRADUATE STUDIES AND RESEARCH

The undersigned certify that they have read, and recommend to the Faculty of Graduate Studies and Research, for acceptance, a thesis entitled MODELLING OF ACCELERATING MOVEMENTS IN ROCK SLOPES submitted by JAMES WILLIAM CASSIE in partial fulfilment of the requirements for the degree of MASTER OF SCIENCE.

.....

Supervisor

.....

.....

Date 87-10-15

Abstract

The decrease in frictional resistance along the sliding surface with progressive displacement is proposed as a mechanism to explain the accelerating behaviour of the rock slopes of western Alberta open pit coal mines.

The buckling failure of the Gregg River Resources NO Pit in 1985 is used as a case history. Representative slope movement parameters are obtained from the displacement-time record of the wall movement using the computer program CPACK.

Footwall sandstone samples are repeatedly tilt-tested to obtain a relationship between the frictional resistance and the displacement. The tilt-test results exhibit variability in the absolute values and in the amount of sliding angle decrease with successive displacement. The various sliding angle(strength)-displacement behaviours of the samples is classified using the brittleness index concept and the majority of the cases displayed a decreasing angle trend.

The sliding block theory, using regression coefficients from the tilt-tests results, qualitatively modelled the velocity increase behaviour of the NO Pit example. It is therefore concluded that the decrease in frictional resistance with progressive displacement, may be an adequate mechanism to explain the accelerating movements in these western Alberta coal mines.

Acknowledgements

The author would like to thank his thesis supervisor, Dr. D. Cruden, for his topic suggestion and his enthusiasm throughout the research. His expertise, guidance, and patience were all geatly appreciated.

The author would also like to thank Dr. K. Barron and Dr. D. Chan for their useful suggestions and criticisms.

Appreciation should be extended to Mr. R. Casey and the Department of Zoology for the use of the profiler and to Mr. D. Booth of the Department of Mineral Engineering for assistance in the use of the digitizing table and the Shore Scleroscope.

Thanks must also go to Mr. R. Karst and Gregg River Resources for supplying the wall movement information.

The assistance from the technical staff of the Civil Engineering Department, especially Mr. G. Cyre and Mr. S. Gamble, was extremely helpful.

Special thanks must go to my fellow graduate students, notably Christopher Neville, Sam Proskin, and Wim Van Gassen, for their interesting and always challenging discussions, their enthusiasm for géotechnique, and their friendship.

The financial assistance provided by Dr. Cruden and the Department of Civil Engineering allowed the author the opportunity for advance studies and is gratefully acknowledged.

Finally, my deepest appreciation goes to my family for their continued support, encouragement, and love.

Table of Contents

List of Tables

List of Figures

1. Introduction

1.1 Background

The north-central Foothills of western Alberta have abundant deposits of coal. These deposits of Cretaceous age are found in a series of asymetrical synclinal structures which are removed by open pit mining methods.

The combination of the geological structure and the extraction process lead to the development of steep, high footwalls. These walls deform due to loss of support as coal is removed from the hinge area of the syncline. The movement of these slopes may accelerate; the rate of the wall displacement increasing with time until total collapse occurs.

When this process occurs in a temporary excavation, the wall is allowed to deform with constant monitoring (usually employing survey techniques) to ensure the safety of the men and the machinery.

Some western Alberta mines have now accumulated a body of experience regarding strain rate limits for forecasting failure. Little work though, has been done on the mechanism responsible for these accelerating movements. Therefore, the aim of this thesis is to investigate the effect of frictional changes along the sliding surface as a viable mechanism.

1.2 Purpose and Scope

This thesis will attempt to determine whether or not the loss of frictional resistance along the sliding surface as it moves, is an adequate mechanism to cause these accelerating movements.

The method of analysis for this research has three major sections:

1. Firstly, an accelerating movement case history is analysed to determine representative slope movement parameters.

2. Secondly, a laboratory testing program is undertaken on sliding blocks to address the question of strength changes of the sliding surface as the amount of displacement progresses.

3. Thirdly, the results of the case history and the laboratory program are compared to determine their relationship.

Chapter 2 is an analysis of an accelerating buckling failure in the Gregg River Resources Mine south of Hinton, Alberta. The analysis consists of fitting a wall displacement record to two power law representations through the use of the computer program CPACK.

Chapter 3 contains the details of the sliding block testing program. A description of the rock samples used is also included. The rock samples are smooth in comparison to the field conditions. Therefore, some of this chapter discusses the roughness of these samples, the measurement and the characterization of this roughness, and the applicability of small-scale roughness work to larger wavelengths.

Chapter 4 links the work of the previous two chapters together by considering an accelerating rigid block model. A relationship between friction and displacement is proposed to which the results of the tilting tests are fit. Integration of the displacement rate equation used in Chapter 2 and solution of the differential modelling equation by finite difference approximation provides a common basis for comparison of the results.

The final chapter contains a listing of significant conclusions, and some recommendations.

2. Accelerating Movement Case History

2.1 Introduction

The Hinton-Cadomin area of Western Alberta has five operating coal mines in Lower Cretaceous coal-bearing strata of the Luscar Group in the northern and north-central Foothills of Alberta. Stratigraphic terms used follow Langenberg and McMechan (1985).

Both the Cardinal River Coals and Gregg River Resources operations, located adjacent to one another 40 km south of Hinton, extract coal from the Grande Cache Member of the Gates Formation, mining the 10 m thick Jewel Seam.

The Lower Cretaceous coal strata form a series of en echelon folds. Later glacial erosion has removed the tops of the anticlines leaving behind a series of parallel, asymmetric-to-overturned synclines which are mined by open pit methods.

The open pits have steep, high footwalls during the coal extraction. Men and machinery work below the footwall removing the bottom coal. Bedding planes in the footwall unit parallel the footwall face. Therefore steeply dipping-to-overturned sedimentary rocks may lose some of their support by the removal of the synclinal bottom coal and footwall movements are induced.

A dominant failure mechanism in this combination of geology and geometry is by buckling. A buckle can be divided into a planar slab slide between the crest and the

inflection point of the slope (also refered to as the "roll-over point") and a topple of the overturned beds between the inflection point and the toe of the slope.

Cavers (1981) provided some simple methods to analyze flexural and three-hinge buckles.

These movements are not instantaneous but are characterized by premonitory movements which accelerate until the wall collapses. The wall displacements are monitored as an aid in predicting the time to failure.

On March 6, 1985, at 07:22, the Gregg River Mine experienced such a buckling failure in the southeast corner of its NO pit along the south wall on a straight footwall slope between elevations 1620 and 1680. Slope displacements were monitored continuously to allow mining to continue until four hours before the failure occurred. This case history is examined in detail to illustrate the characteristics of an accelerating slope movement.

2.2 Gregg River Mine

The Gregg River Mine began production in 1983 after a coal sales agreement was reached with several Japanese companies. In 1985, the mine produced 2.2 million tonnes of high quality coking coal with approximately 12 million m^3 of material being excavated by truck and shovel. The mine is operated by Gregg River Resources Ltd. and employs 390 people.

The coal is found in a series of parallel, asymmetric synclines. Each successive outcropping of the Jewel Seam of each syncline is assigned an alphabetic designation starting from the northeast end of the property. Hence the name of the NO pit.

2.2.1 Pit Geology

The Lower Cretaceous coal is part of the Luscar Group whose stratigraphy and nomenclature have been recently discussed by Langenberg and McMechan (1985). Coal mining is centered on the Jewel Seam of the Grande Cache Member of the Gates Formation. This member has an abrupt contact with the underlying Torrens Member sandstone which forms a hard footwall unit. The overlying, softer, hangingwall unit of the Gates Formation consists of interbedded shales and siltstones. Karst and Gould (1985) discussed the mine's geology in relation to mine planning and economics while McLean (1982) discussed the various lithologies in detail as well as suggesting possible depositional environments.

The coal thickness increases locally at the fold hinges from typically 10 m along the limbs to 30 m or more due to the weaker, softer coal migrating along the limbs during folding as suggested by Karst and Gould (1985). Therefore synclinal hinges are prime areas for coal removal.

Karst and Gould (1985) reported that the hard footwall sandstone had an unconfined compressive strength of 160 MPa while the interbedded siltstones and shales had a strength

of 50 MPa. The overlying Gates Formation is easily drilled and blasted while the Torrens sandstone forms a hard pit wall. Generally, south walls are benched into the footwall rock while north walls follow the coal-footwall contact. Bench face angles range from 50° to 90°.

The bottom coal is removed by a deep-range (14 m below grade) backhoe and transported by truck.

2.2.2 NO Pit Failure

The buckling failure in the NO pit occured at 07:22 on March 6, 1985 bringing down 11,000 m^3 of rock onto the active mining area. The failure took place on the east end of the south wall on an unbenched slope from elevation 1680 to the pit bottom as illustrated in the cross-sectional view of Figure 2.1. A deep-range backhoe sitting at elevation 1638 digging at elevation 1625 was removed before the failure. The overall slope height of the footwall was 55 m with the strike length of the wall being 75 m.

The straight footwall section dipped into the pit at 58° N at the crest of the slope but the angle steepened at lower elevations. The roll over point where the beds began to overturn was at elevation 1642. The dip of the beds below this point was found to be 80° S. The Gregg River Resources failure report described the final event in the following way:

> "As the last of the supporting coal below the 1638 elevation was removed, a 5 m thick slab of

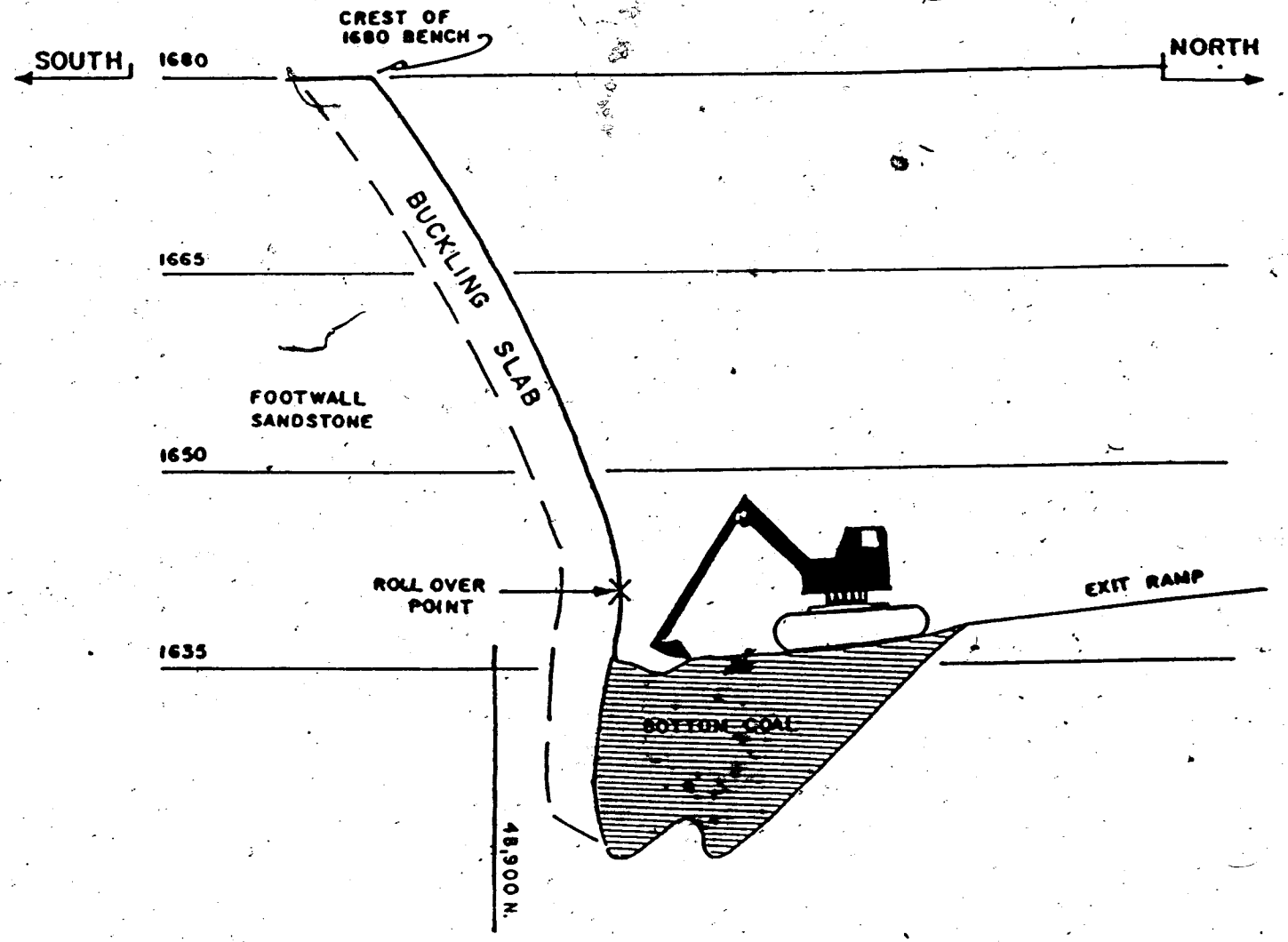

Figure 2.1 Cross-section of the NO pit during the buckling failure.

overhanging footwall buckled and fell into the pit."

The rupture surface was a bedding plane located 4 to 5 metres behind the coal-sandstone contact. The western boundary of the slide mass was an open cut while a fairly continuous joint surface (strike 180°/ dip 60° E) provided the eastern boundary.

The first indication of wall movement was a hairline crack noticed on March 2, 1985 at 09:00. The crack, approximately 0.8 m in depth, was located at the east end of the footwall and proceeded up and to the right for a length of about 20 m. At 10:00 on March 3, the crack had progressed right across the face with a length of 50 m and had a width of 5 to 10 mm. Overturning of the lower footwall at the toe was then measured.

At 13:30 on March 3, a reflector prism was installed in the crack in order to facilitate remote displacement monitoring.

It is assumed in default of more exact information that the reflector was attached to the upper translating block of a three-hinge buckling movement and that the movement recorded was essentially a translation along a bedding plane. Other models of movement, such as ploughing at the toe or buckling of a plane slab are found in these foothill coal mines and cannot be excluded with the observations available.

On March 5 at 22:00, the surveyor detected 2.5 mm movement between 15 minute readings and the backhoe was

pulled out. The slope then stabilized and the backhoe was sent back in. At 03:30 on March 6, 4.5 mm of movement was detected and machinery was removed and kept out of the pit. By 05:45, the wall was moving 6 mm every 15 minutes. At 07:05 another crack developed on the face and at 07:20, the prism fell out. Finally, the wall failed at 07:22. Karst (1985) provided a more detailed sequence of events.

Johnson (1982) stated that the radial survey method using a theodolite-EDM system was the standard method used by the mining industry for wall monitoring. The three dimensional position of a prism were calculated using measured values of the slope distance and the vertical and horizontal angles. The vectors of movement were computed from changes in the three dimensional position.

Monitoring of the failure was initially done from an instrument station located on the north side of the pit at the corner of the 1650 bench. After 18 hours of readings, no definite movement was recorded and the instrument station was changed to the east side of the pit access ramp located on the far north side of the pit. This location offered greater sensitivity to wall movements.

Masoumzadeh (1985) found that the total resultant of the displacement vectors better represented these slope movement processes rather than the components such as the slope distances or the cumulative horizontal displacements. Figure 2.2 provides a graphical view of the cumulative total displacements versus elapsed time for the NO pit failure.

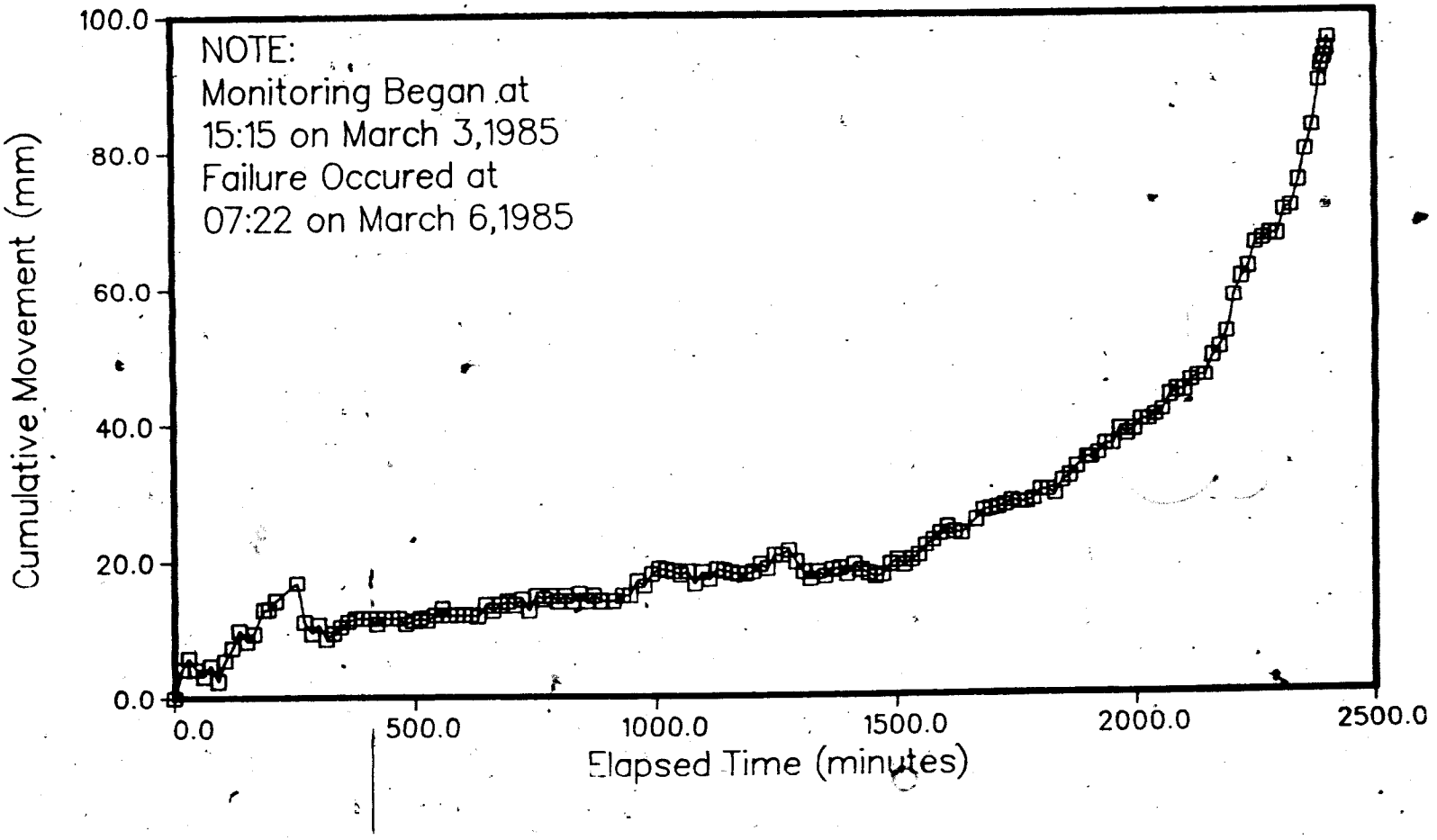

Figure 2.2 Cumulative total displacement versus elapsed time for the GRR NO Pit failure.

For the most part, the curve displays an accelerating displacement with time except for early in the displacement record when there is a jog. This decrease in displacement may have been due to some drainage affecting the slope movement.

2.3 Computer Analysis of the Displacement Record

Materials under a constant load exhibit deformation with time referred to as creep. Varnes (1982) discussed the general characteristics of creep curves. Firstly, there is some instantaneous strain followed by rapid deformation which decreases in rate which was refered to as primary creep. This creep phase transitions into a steady-state or secondary creep. Finally, it may accelerate into tertiary creep until failure ultimately occurs.

Many equations have been proposed to describe the various creep phases. Varnes (1982) discussed three laws for accelerating creep. These included;

1. the Saito relation,
2. exponential laws, and
3. power laws.

Also, Zavodni and Broadbent (1980), after examining failures in copper porphyry open pit mines, recognized two principal failure stages and produced an empirical relationship for failure prediction. Masoumzadeh (1985) reviewed the above four equations in detail and discussed their usefulness in relation to the Luscar Mine failure case history.

All the above equations are basically curve fitting techniques, which fit separate equations to the two different phases (decelerating and accelerating) independently. There is no consideration for the actual physical processes which are occurring. Varnes (1982, p.114) stated that:

> "In working with curves showing both primary and tertiary creep, I found that the tertiary portion often could not be analyzed satisfactorily by itself because the process responsible for primary creep continued beyond the point of inflection. "

Unfortunately, he presented no further insight (or equations) which could be used to link the two phases of creep.

Cruden *et al.* (1986) provided a method for estimating the parameters necessary to describe a complete creep curve for coal samples in laboratory creep tests. The following relationship between the strain rate, $\dot{\epsilon}$, and the elapsed time, t (in minutes) was proposed:

$$\dot{\epsilon} = At^B + Ct^D \qquad [2.1]$$

where A, B, C, and D were constants. The first term of the equation was used to describe the decelerating portion where A was the displacement at unit time and $0 > B > -2$. The second term described the accelerating portion with $C << A$ and $D > 0$, up to values as large as 9 for laboratory creep

experiments.

The observations, absolute time and displacement, were used to calculate elapsed times and strain rates which were smoothed by the recursion formulae outlined by Cruden (1971) to account for minor extraneous variations. The smoothed data was then fitted by a weighted least squares method to a decelerating creep power law. This power law was integrated to obtain estimates of the decelerating creep strains. The accelerating strains were calculated by subtracting the decelerating strains from the observed strains. Therefore the decelerating creep phase has an influence on the strain values used for the determination of the accelerating creep parameters which is unlike any of the previous equations such as those of Saito or Zavodni and Broadbent.

An interactive package of computer programs, CPACK, was coded to fit the data of creep movements to power laws.

2.3.1 CPACK

The main program of CPACK outlines the steps of the analysis by calling five subroutines: CRED, BFIT, CFIT, and CPLOT. A flow chart and listings of the above are provided in Appendices A and B.

The fit of the data to the proposed straight lines is assessed by two tests. The first is a test for serial correlation in the residuals for which the Durbin-Watson statistic, dw, is calculated as suggested by Durbin and Watson (1951). The second is the test of slope significance

which examines the null hypothesis that the fitted line does not have a slope significantly different from zero or that the data could have been represented by its mean.

The functions of the subroutines and the goodness of fit parameters are discussed in more detail in Cruden *et al.* (1986). In this paper, the creep data of a right rectangular prism of subbituminous coal which failed after 159 days at 19.4 MPa was found to fit the equation:

$$\dot{\epsilon} = 4650\ t^{-1.01} + 0.588\times10^{-53}\ t^{9.90}. \qquad [2.2]$$

where the units of time is still in minutes.

Cruden and Masoumzadeh (1986a) used an updated version of their program, CPACKI, to determine slope movement parameters for the displacement record of the 51-B-2 pit failure at the Luscar Mine. The equation relating the displacement rate, $\dot{x}$, to the elapsed time, t, was:

$$\dot{x} = 0.280\times10^{-9}\ t^{1.23} + 0.129\times10^{-24}\ t^{4.17}. \qquad [2.3]$$

which actually defined two accelerating phases.

Displacement rate rather than strain rate was used in this case because the slope is given an initial length of unity in the CPACKI program. Hence, the displacement over a certain time interval divided by the original length results in a displacement rate, not a strain rate.

The first term parameters gave a reasonable fit of the initial data to the power law, but the accelerating data did not fit the second term well. They stated that the pit displacement data analyzed using the POW program identified three stages of accelerating creep rather than the two stages computed using the CPACKI program.

The Gregg River displacement record was input into CPACK2 (details regarding the testing of this new version are located in Appendix C) to determine its movement parameters. The input file (given in detail in Appendix D) was derived from survey coordinates obtained from Gregg River Resources Ltd. and the cumulative total displacements were used. The strain record was started at 15:15 on March 3 and lasted for 2405 minutes. The maximum total wall displacement was 96.2 mm.

2.3.2 Results

The CPACK2 output files are located in Appendix F. The resultant equation for the entire data set is:

$$\dot{x} = 0.130\times10^{1}\ t^{-0.84} + 0.332\times10^{-14}\ t^{3.99}. \qquad [2.4]$$

The two terms of the equation are represented by the two straight lines on Figure 2.3.

The first term of the equation with a power coefficient of -0.838 (indicating decelerating creep) provides a good fit to the initial data. The dw value of 1.748 exceeds the

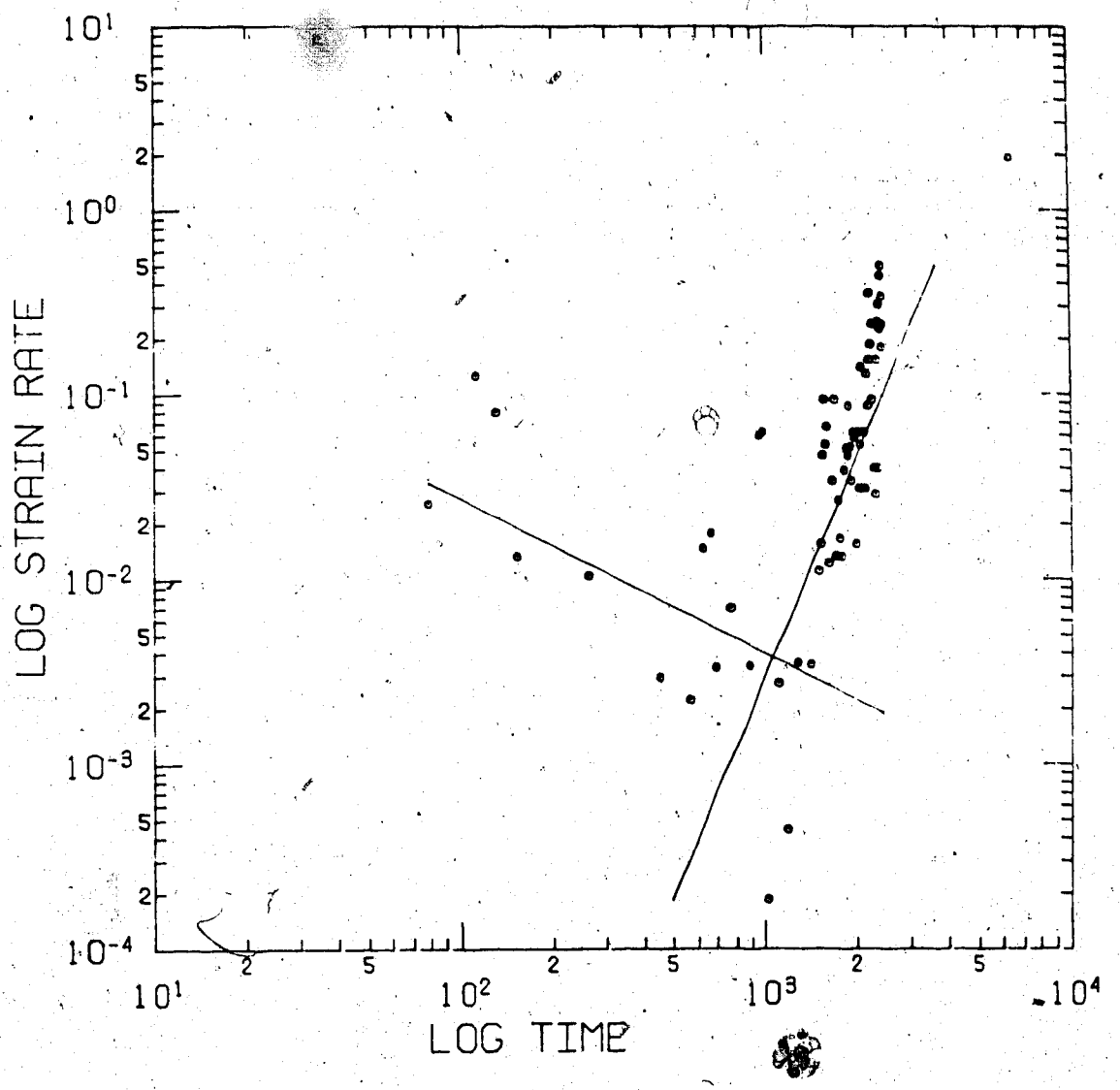

Figure 2.3 Log strain rate vs log time for GRR full data set.

upper bound value of 1.690 indicating no positive serial correlation while the slope significance value is 26.96.

The second term of the above equation with D=3.985 has a dw value of 1.391 which is less than both the upper and lower bound values (1.690 and 1.650 respectively) indicating positive serial correlation. Hence the data points are similar in deviation direction from the fitted line.

Intuitively, we sense that once the sliding mass has begun to move, there are few reasons why the mass should stabilize. The experience of Cruden and Masoumzadeh (1986b) indicated that the slide at the Luscar Mine had three accelerating phases. No decelerating components were found.

An attempt was made to truncate the data set from the beginning in order to remove the observations in the initial decelerating creep phase. Table 2.1 provides a summary of the results.

The first occurrence of two accelerating phases occurs with the Trun5 data set where B=1.573 and D=4.178. But the Durbin-Watson statistic for the second phase indicates positive serial correlation.

The Trun6 data set with an initial time of 195 also has two accelerating phases. The first term with B=2.14 is a good fit for the data range of 1 to 56. The second term has a large exponent, D=25.78 and the coefficient C, is reported as 0.221×10^{-87}. The dw value, 1.666, while not greater than the upper bound value of 1.690, is larger than the lower bound value of 1.650 suggesting that positive correlation

Table 2.1 Summary of CPACK results for truncated data sets.

Data Set	Initial Time (min.)	Number of Points	A B	dw UB	Data Range	R1	C D	dw UB	Data Range	R1
Full	15	160	0.130E01 -0.838	1.748 1.690	1-99	26.96	0.332E-14 3.985	1.391 1.690	13-159	301.71
Trun1	105	154	0.754E00 -0.759	1.772 1.686	1-93	13.26	0.939E-10 2.600	1.014 1.690	10-153	193.34
Trun2	120	153	0.668E00 -0.751	2.006 1.682	1-91	11.71	0.603E-09 2.329	0.930 1.690	9-152	92.73
Trun3	150	151	0.128E01 -0.868	2.045 1.674	1-87	11.95	0.128E-10 2.874	1.076 1.690	6-150	184.7
Trun4	165	150	0.692E01 -1.146	2.230 1.658	1-79	11.11	0.120E-10 2.869	1.133 1.690	5-149	113.5
Trun5	185	149	0.201E-06 1.573	2.022 1.614	1-58	10.24	0.310E-15 4.178	1.519 1.690	18-148	235.6
Trun6	195	148	0.611E-08 2.135	2.115 1.608	1-56	24.36	0.221E-87 25.78	1.666 1.690	48-147	4848.8
Trun7	210	147	0.106E-06 1.568	1.965 1.642	1-71	9.12	0.221E-08 2.066	1.098 1.690	2-146	37.37

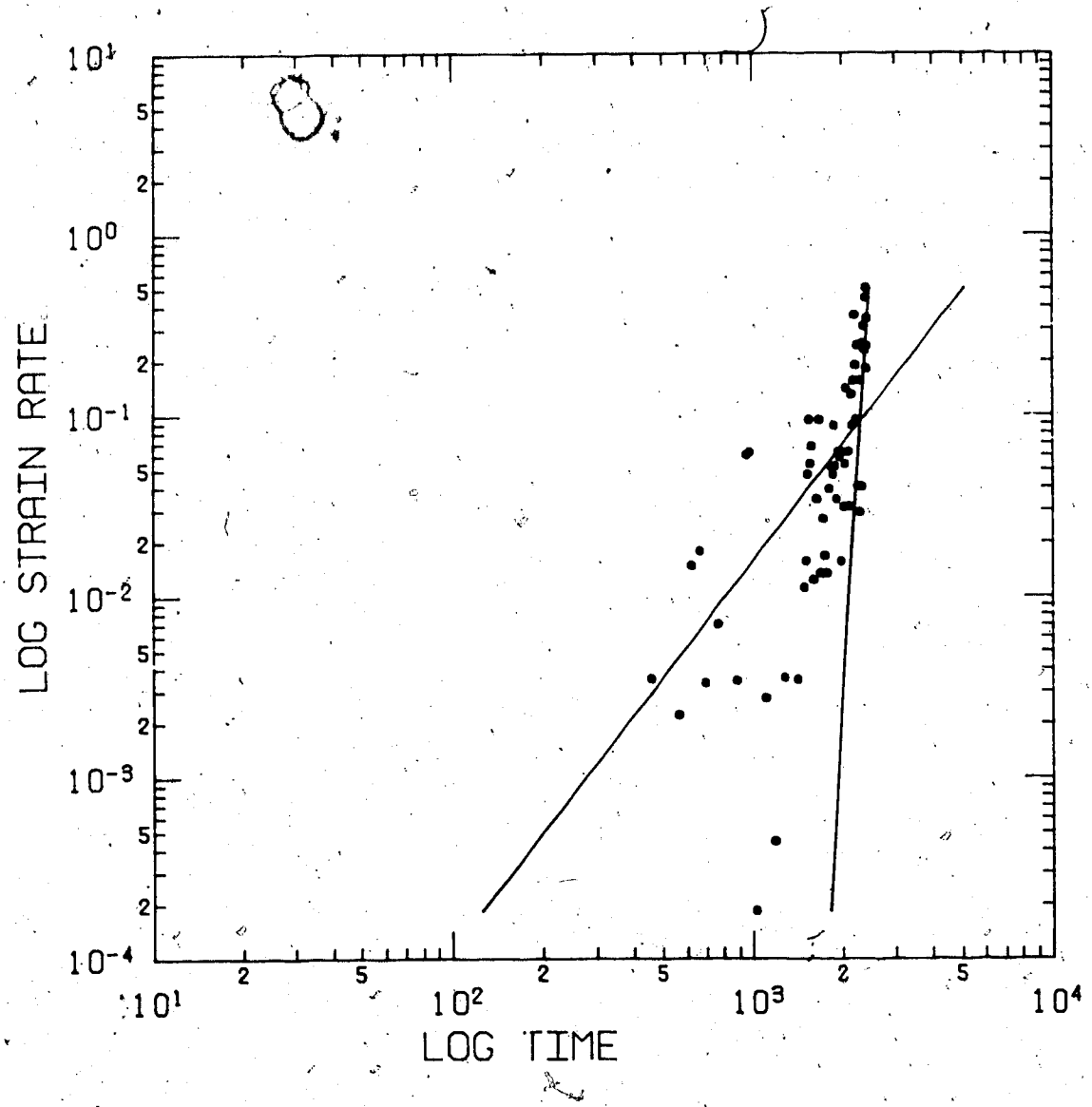

Figure 2.4 Log strain rate vs log time for GRR truncated data set.

may possbly exist. The slope significance value for the data range 48 to 147 is very large at 4849. Hence, the following equation, displayed in Figure 2.4 may be a more realistic representation of the accelerating portion of the Gregg River displacement record;

$$\dot{x} = 0.611\times10^{-8}\ t^{2.14} + 0.221\times10^{-87}\ t^{25.78}. \qquad [2.5]$$

It is now apparent that the CPACK program will have to undergo some modifications. The increasing experience with fitting these coal mine deformation records indicates the need for a program which fits three (or more) accelerating phases as was the conclusion of Cruden and Masoumzadeh (1986a). Future versions of this program should therefore attempt to implement this procedure.

3. Laboratory Determination of Model Parameters

3.1 Introduction

The shear-deformation behaviour of rock discontinuities is influenced by such factors as normal stress, infilling, geometry and roughness, past displacement history, and strength and deformability of asperities (related to mineralogy and weathering).

Shear stress-shear displacement curves typically consist of two main regions as illustrated in Figure 3.1:

1. the pre-peak region, where a large increase in shear stress over a small displacement occurs, up to a maximum stress τ_{peak} and

2. the post-peak section where the shear stress decreases with increasing displacement, until it reaches a constant value.

Experimental results indicate that both the shear strength and the dilation of discontinuities are functions of the normal force and the shear displacement.

The movements in these western Alberta pit walls show an accelerating displacement with time leading to the failure of the wall. This acceleration suggests a mechanism which produces decreasing frictional resistance along the rupture surface because the driving force of the movement,

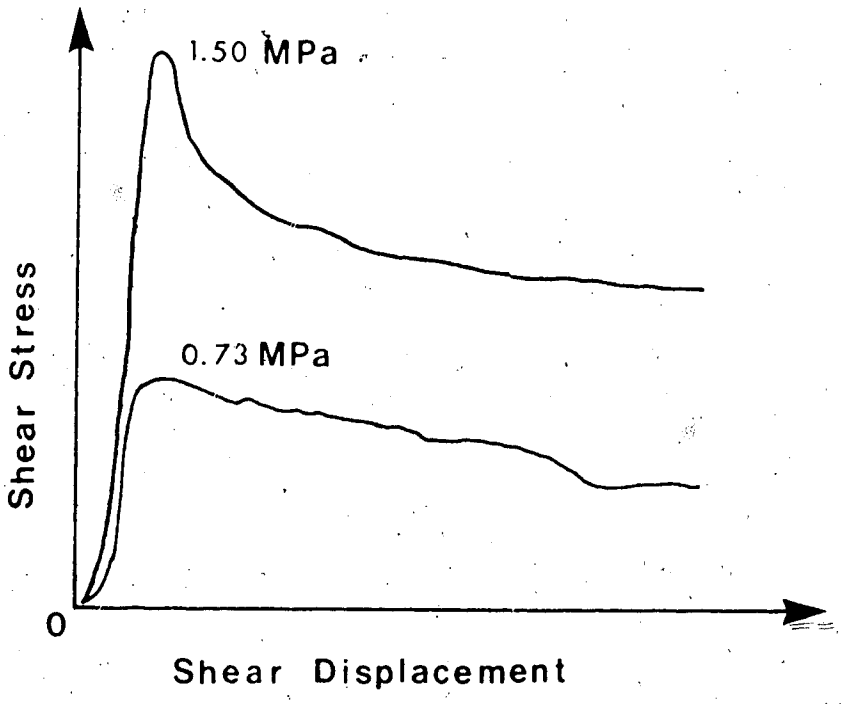

Figure 3.1 Typical shear force-shear displacement curves as a function of the normal stress level displayed.

the sliding block weight, is assumed to be constant here in the absence of observations to the contrary. As the displacement along the rupture surface (usually a bedding plane) proceeds, surface irregularities are sheared off, roughness decreases, and therefore the frictional resistance of the surface decreases.

A laboratory program was set up to determine a relationship between the frictional resistance and the displacement of a model sliding block of sandstone. Rather than using the more conventional direct shear test to measure the frictional resistance, a tilt-table apparatus was used. A series of tilting tests were done on the same sample to determine how the sliding angle (*i.e.* frictional resistance) changed with successive sliding events (*i.e.* increasing displacement). The experimental set-up allows concurrent surface roughness measurements to be made to examine how the sample roughness was changing.

There is, of course, several differences between the two tests. An important difference is the application of normal force during displacement. The tilt-test uses only self-weight of the top sliding block which results in a normal stress application of approximately 0.6 KPa.

This low normal force does not invalidate the usefulness of the tilt-test for several reasons:

1. The tilt-test does occur at a much lower normal force than the insitu conditions, but the roughnesses of the

two surfaces controlling deformation also differ by several orders of magnitude.

An example shall follow to illustrate the concept. The slope is inclined at 60° and the thickness of the failing slab is 5 m. Therefore, the sliding surface is under a normal pressure of 250 KPa. Divide the normal stress by the roughness height controlling roughness, say 2 cm and the ratio of normal stress to roughness is 125.

Applying the same principle to the tilt-tests, the normal stress of 0.6 KPa divided by the roughness, 0.001 cm (400 microinches) results in a ratio of 600.

It seems from this quick quantitative analysis, that the ratio of normal force to controlling roughness height for the field and the tilt-test conditions are within the same order of magnitude. In comparison, it is the tilt-test which actually has the higher ratio.

2. The basic friction angle of rock, ϕ_b, is relatively insensitive to normal force as found by Coulson (1972), within the stress range range significant for surface workings.

3. The tilt-test system models a dilated slab after some movement has sheared off the larger asperities on the rock surface. Bruce *et.al.* (1986) found that the sliding angle results of tilt-tests on smooth samples were

similar to the friction angle results of the direct shear tests. There is a similitude of results between the two tests which have different operating forces, perhaps in part to the above normal stress ratio concept.

The frictional characteristics of a flat rock surface are dependent upon the surface preparation. Coulson (1972) found that the smoother the sample, the lower the frictional resistance, which suggested a correlation between the two parameters. The work of Rengers (1970), Barton (1971a), Krahn and Morgenstern (1979), and Tse and Cruden (1979) all suggest a correlation between surface roughness and rock joint shear strength. If a functional relationship could be obtained between roughness and frictional resistance, then extrapolation of the correlation or insight into possible mechanisms might be important in predicting rock joint behaviour.

3.2 Literature Review

Byerlee (1967) developed a theory of friction for geological materials based on brittle fracture rather than plastic deformation of asperities. Sliding of a surface would then occur when asperities fail by brittle fracture. Evidence for the theory were that;

1. true crystalline plasticity can be ruled out at temperatures under 500° C for rocks containing typical

silicate minerals (quartz, feldspar, olivine, or pyroxene) even at high pressures such as 500 to 1000 MPa, and

2. the tensile strength is a very small fraction of the compressional strength.

Direct evidence suggesting this type of friction was the presence of a fine white debris on the sliding surface after shearing. The amount of debris and the size of the debris particles increased with the roughness of the surfaces in contact. Byerlee found for ground surfaces of Westerly Granite that the coefficient of friction decreased as the roughness of the sample decreased, even though the roughness values for the surface were quite variable.

Coulson (1972) performed shear tests on flat rock surfaces of 10 different lithologies with roughnesses ranging from nearly polished to sandblasted at normal forces from 70 to 7000 KPa. He found four different types of strength-displacement curves;

1. Type #1 occurred in 4% of the tests and showed no change in shear strength with displacement. Normal pressures were always less than 420 KPa.

2. Type #2 exhibited a decrease in shear strength with displacement. These occured at low pressures on dry surfaces and at all stress levels on wet surfaces.

3. Type #3 and #4 curves both had increasing shear strength with displacement with type #3 displaying an initial decrease. These two curves accounted for 60% of the tests and appeared at medium to high stress levels.

He also examined the sliding surfaces and correlated types of surface damage: generation of minor rock flour, formation of gouges with compacted rock flour, polishing, and formation of an indurated crust with these different classes of curves. Coulson stated that the generation of small amounts of rock flour were most often associated with type #2 curves. Since particle interference was low, rolling friction of the debris helped to decrease the shear strength. Type #3 curves appeared as more flour was generated and particle interference increased.

Krahn and Morgenstern (1979) performed direct shear tests on artificially prepared limestone surfaces and made surface roughness measurements with a Talysurf instrument. These traces were digitized for plotting purposes and for analysis. Statistical analysis of digitized profiles indicated a change in the roughness profile after shearing. Frequency-amplitude graphs, before and after shearing displayed an increase in the frequency of amplitudes on the positive side of the mean while there was a decrease in the frequency of the highest asperities. This confirmed the peak truncation and formation of plateaus conclusions made after

viewing the profiles. They also obtained a correlation of 0.881 between Z_2, the root mean square gradient, and the ultimate friction angle, ϕ_u.

Zongqi (1985) also performed direct shear tests (on granite) with profile measurements before and after shearing. He attributed the minor decrease in the RMS surface slope values to wear of the upper asperities during shear.

3.3 Rock Sample Chosen

The coal removed from the Hinton area mines is taken from the Jewel Seam which is located in the Grande Cache Member of the Gates Formation. Overlying the coal seam are interbedded mudstones, siltstones, and fine-grained argillaceous sandstones.

The unit below the Jewel Seam is the Torrens Member sandstone. It is a massive to thick to medium-bedded sandstone which coarsens upward in grain size. Hill (1980) describes the Torrens Member in the Luscar Mine as medium-grained, light grey, non-calcareous, and containing rare conglomeratic lensoids of chert pebbles.

The stratigraphy was similar at both the Gregg River Resources pit and the Luscar Mine studied by Masoumzadeh (1985). Sandstone samples were collected by Masoumzadeh in August, 1983 at four different locations from the Luscar 51-B-2 pit located approximately 320 km west of Edmonton.

The sample used for this testing program was taken from the location of 101700 N and 104700 E on the Luscar Mine grid at an elevation of 5220 (Masoumzadeh, 1983). It was removed from approximately 3 m below the coal seam at a bend in the access road. This sample was assumed to be from the Torrens Member.

These samples were stored in the Civil/Electrical Engineering Building at the University of Alberta for use in future testing programs.

3.3.1 Sample Preparation

Test specimens were cut from a sample taken from location #2C which had an average thickness of 9 cm. Figure 3.2 shows where the specimens were cut from the top half of the sample. The sample was described as a fine to medium grained sandstone, light grey, carbonate-free (tested for effervescence with 10% HCl), laminated and containing occasional thin shaly partings.

The initial cuts were made by a 60 cm diameter, diamond-tipped saw which was water lubricated. The sliding surface cut was made parallel to bedding by a smaller hand controlled saw as were the final top and bottom cuts. Final sample size was approximately 5 x 5 x 2 cm.

Three samples were wet-lapped for one hour on the lapping table with 100 grams of grit being added initially. Afterwards, they were checked for flatness with a straight edge. Various sizes of grits, #80, #220, and #400 were used

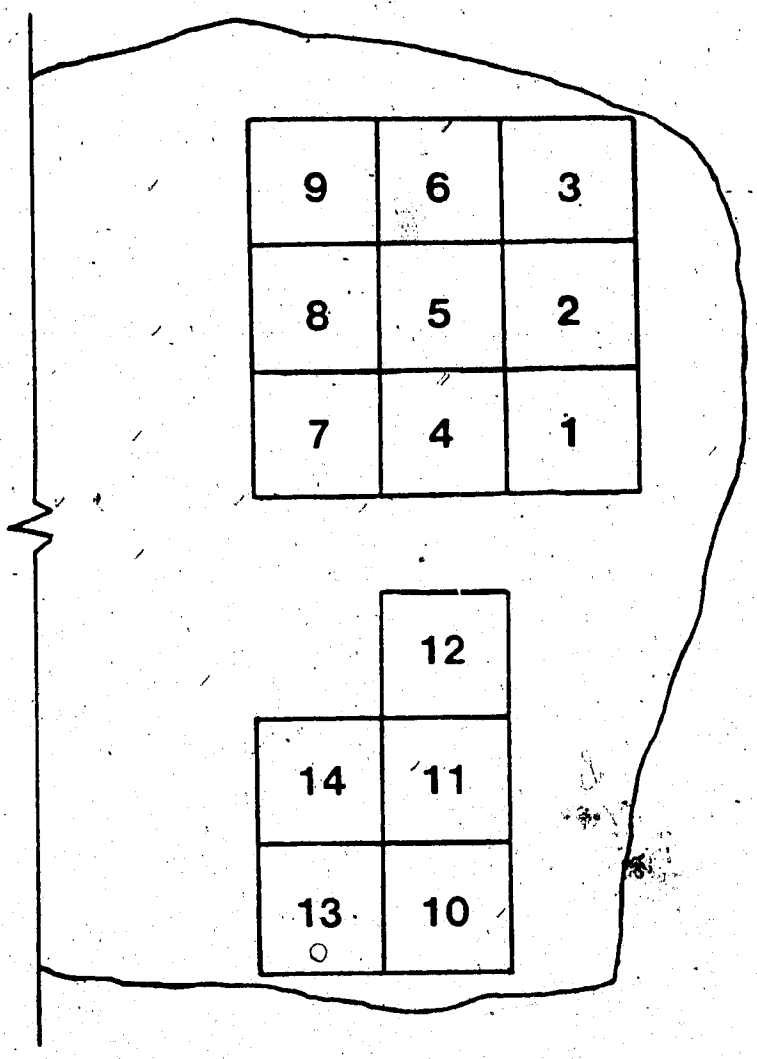

Figure 3.2 Location of specimens from the top half of sample #2C. Individual blocks are 5 X 5 cm, for scale.

to prepare the roughness desired. Fifty grams of grit were added with each successive lapping set and the grit was used for 3 sets (3 hours) before being changed. Bruce *et al.* (1986) provides a detailed discussion of lapping equipment and procedures and sample roughness results.

3.4 Roughness Measurements

Roughness measurements were taken during the tilt-testing program for two purposes;

1. to determine if and how the surface roughness changed during tilt-testing, and
2. to look at the question of scaling of surface roughness and determine whether a general scaling law exists.

Recently, there has been an interest in prediction and modelling of rock joint properties (normal and shear stiffness, closure behaviour, and hydraulic conductivity properties) from roughness measurements in such papers as Swan (1981,1985), Dight and Chiu (1981), Swan and Zongqi (1985), Zongqi (1985), and Brown and Scholz (1986).

3.4.1 Previous Work in Surface Topography

Patton (1966) found from roughness profiles and from evaluation of slopes that there were three orders of roughness on failure surfaces: first order irregularities with wavelengths of 60 cm, second order irregularities with wavelengths of 6 to 10 cm, and third order roughnesses of less than 1 cm. He concluded that first order irregularities

were good estimates of the asperity angle i, and that second order irregularities were not a factor when shearing or overriding of these asperities had occurred.

Piteau (1973) considered that there were two orders of topography: "macroscopic" resistance or waviness and "microscopic" resistance or roughness. Piteau (1973, p.7) states:

> "Irregularities which are of such dimension that they are unlikely to shear off are defined as waviness. Roughness is defined as irregularities sufficiently small as to be sheared off during movements of the surface."

Another approach to topography is the random process theory as suggested by Peklenik (1967), Whitehouse and Archard (1970), and Nayak (1971). Instead of two orders of topography where small scale roughness is superimposed on the larger scale waviness, the surface topography is considered as a continuous spectrum of wavelengths down to atomic dimensions. Roughness would therefore be composed of the smallest and shortest wavelengths while waviness would consist of larger and longer wavelengths. Errors of form will have the longest wavelengths and the largest amplitudes.

Therefore the sizes, shapes, and heights of the surface features also formed continuous distributions dependent on this spectrum (Nayak (1971)). Rather than discussing waviness and roughness in terms of fixed wavelengths, Sayles

and Thomas and Brown and Scholz (1985) thought of them in terms of bandwidths of a spectrum.

3.4.2 Surface Characterization Methods

The Talysurf roughness measuring device is a commercially available instrument which drags a 4 sided, 0.0025 mm wide diamond stylus supported by a reference skid across an irregular surface. The device can provide a paper trace of the profile or it can provide a center-line average (CLA) value. American National Standard (1978) B46.1-1978 provides a review of the use and the interpretation of tracer instruments such as the Talysurf.

This instrument traverses a standardized length with the stylus in order to obtain the CLA values. These lengths, referred to as cutoff values are: J, 0.25 mm, K, 0.8 mm, and L, 2.5 mm. The CLA is a commonly used parameter in tribology and is defined as:

$$CLA = \frac{1}{L} \int_{x=0}^{x=L} |y| \, dx$$

where y = amplitude of the roughness about a mean of zero,

L = the sampling length,

dx = a constant distance between amplitude readings.

The CLA value is recorded in units of microinches.

Samples #1 and #2 were both prepared using #80 grit. These samples were then measured for roughness by traversing the stylus perpendicular to the sliding direction but they were too rough for the upper CLA limit of the instrument, 400 microinches. Consequently another method, the profiler, had to be used to quantify the roughness of these samples.

The profiler apparatus consists of a stylus mounted to a spring-arm attachment which is dragged over the surface by a screw mechanism powered by a small electric motor. The stylus, oriented in an inclined position is attached to an LVDT. As the stylus traverses horizontally and rises up and over asperities, voltage changes in the LVDT are recorded on a paper plotter. This device therefore gives an analog profile on paper, of the rock surface.

The Civil Engineering Profiler has been previously discussed by Krahn (1974) and Tse (1978).

Possible problems with this apparatus were:

1. The stylus is not in a vertical position which is the standard on other profilers such as the Talysurf.

2. The downward force of the spring-arm is greater than that of the Talysurf and its magnitude is unknown. This heavier stylus force might lead to the stylus ploughing through the surface material rather than overriding asperities.

3. The stylus on the Civil Engineering profiler (1.00 mm) is 400 times larger than the Talysurf stylus (0.0025 mm) which conforms to the British Standard and as such might miss vital roughness information.

4. No shoe or skid is provided for a datum like the Talysurf.

5. No lateral support is provided for the spring-arm so stylus deviations out of the traverse plane are possible.

Use of the profiler has one major advantage in that the length of the surface trace taken is variable. Thereby a longer profile can be taken which may better quantify the surface roughness.

The profiler used in this study was made available by the Department of Zoology. This profiler is very similar to the Civil Engineering profiler except it has a much smaller stylus and it has no vertical calibration and therefore profiles were only relative.

The first two samples, #1 and #2 (lapped with #80 grit) were profiled with the zoology instrument. Three traces were taken after each sliding event for sample #1 and after every second event for sample #2. A total of 60 analog traces were taken. A quantitative term was required for each profile,

even if it was only a relative one. In order to do this, the analog traces had to be digitzed into discrete X and Y coordinates for computer analysis. This step in the process was done on the CalComp 9000 Digitizer located in Room 280, Chemical/Mineral Engineering Building.

The CalComp Digitizer converts analog traces into discrete X and Y coordinates. This can be done one point at a time, by incrementing X and/or Y values, or continuously on scan mode. The Digitizer also allows an origin and a scale to be set up for each trace and the input format of the data can be varied in a user created file.

The first attempt at digitizing the traces was in the increment mode using a relatively small X increment (5 discrete amplitude readings per mm or every 0.5% of the full X scale) and a large Y increment (every 120% of the full arbitrary scale). This was for later convenience when computing the parameter Z_2. As it turned out, the X increment was not constant for every increment.

The digitizing was accomplished by placing the trace under a plastic covering on the digitizing table. The origin, the scale, and the data input format were then entered for each trace. Then the analog profile was traced by moving a set of cross-hairs over the entire length of the profile by hand. Obviously this method of tracing the profiles was subject to error especially on sharp high peaks. Two common errors were;

1. the Y value of the sharp peak might be missed if the X

increment value did not correspond exactly with the X coordinate of the tip, and

2. when tracing the sharp peak, some "backtracking" might occur, *i.e.* the X values might start decreasing due to poor hand tracing technique.

When the digital files were listed and visually examined for backtracking, some of the tips (maximum Y values) of sharp peaks were seen to be missed.

3.4.2.1 Results From the Profiler

After the files had been examined and corrected for backtracking, the data from sample #1 was run through a computer program to calculate a relative roughness parameter, Z_2^*. This parameter was only relative because the profiler had no vertical calibration and the voltage transducer exhibited some nonlinearity (Casey, 1986).

The root mean square gradient, Z_2 is defined as:

$$Z_2 = \sqrt{\frac{1}{L}\int_{x=0}^{x=L}\left[\frac{dy}{dx}\right]^2 dx}.$$

with the parameters being discussed earlier in reference to the CLA.

The assumption was made in the program when calculating Z_2^* that the step increment of the digitizer could approximate dx, the constant distance between amplitude readings.

A fine to medium grained limestone sample (Jy 31-4) lapped with #80 grit was obtained from the specimens

used by Eaton (1986). Its surface was smoother in comparison to the much rougher sandstone sample (1F-1). Figure 3.3 illustrates this fact even through the asperity heights were only relative and the scales were distorted. The limestone sample, the smoother surface had a Z_2^* value of 0.05 while the rougher sandstone surface had a value on 1.96. The smooth value was less than the rough one by an order of magnitude even though the number of data points, 162 and 173 respectively were about equal. Hence it was assumed that the program could quantify changes in roughness. Unfortunately, the values were only relative to one another and they could not be compared with other authors' work.

Sample #1 was tilt-tested with profiles taken at the back, middle, and front of the specimen. These were digitized and Z_2^* was computed. Table 3.1 provides a summary of these values from the back and the front portions of sample #1. Although the sliding angles decreased from 28° to about 24° after 18 sliding events, the expected decreasing trend in the Z_2^* values was not observed.

A test was done to determine how the calculation of Z_2^* was affected by the width of the X increment of the Digitizer. Profile 1F-1 was initially digitized using a X increment of approximately 0.2 mm which gave 195 data pairs and a Z_2^* value of 13.58. The same profile was digitized using a much smaller X increment of 0.05 mm.

Table 3.1 Relative root mean square gradient values for sample #1

SAMPLE #1			
Front		Back	
1F-1	1.96	1B-1	13.58
-2	1.63	-2	2.89
-3	22.21	-3	12.29
-4	9.74	-4	6.25
-5	1.69	-5	8.89
-6	23.56	-6	40.43
-7	———	-7	3.04
-8	4.08	-8	31.35
-9	9.35	-9	1.40
-10	6.23	-10	20.91
-11	6.76	-11	3.44
1F-12	9.42	1B-12	15.54

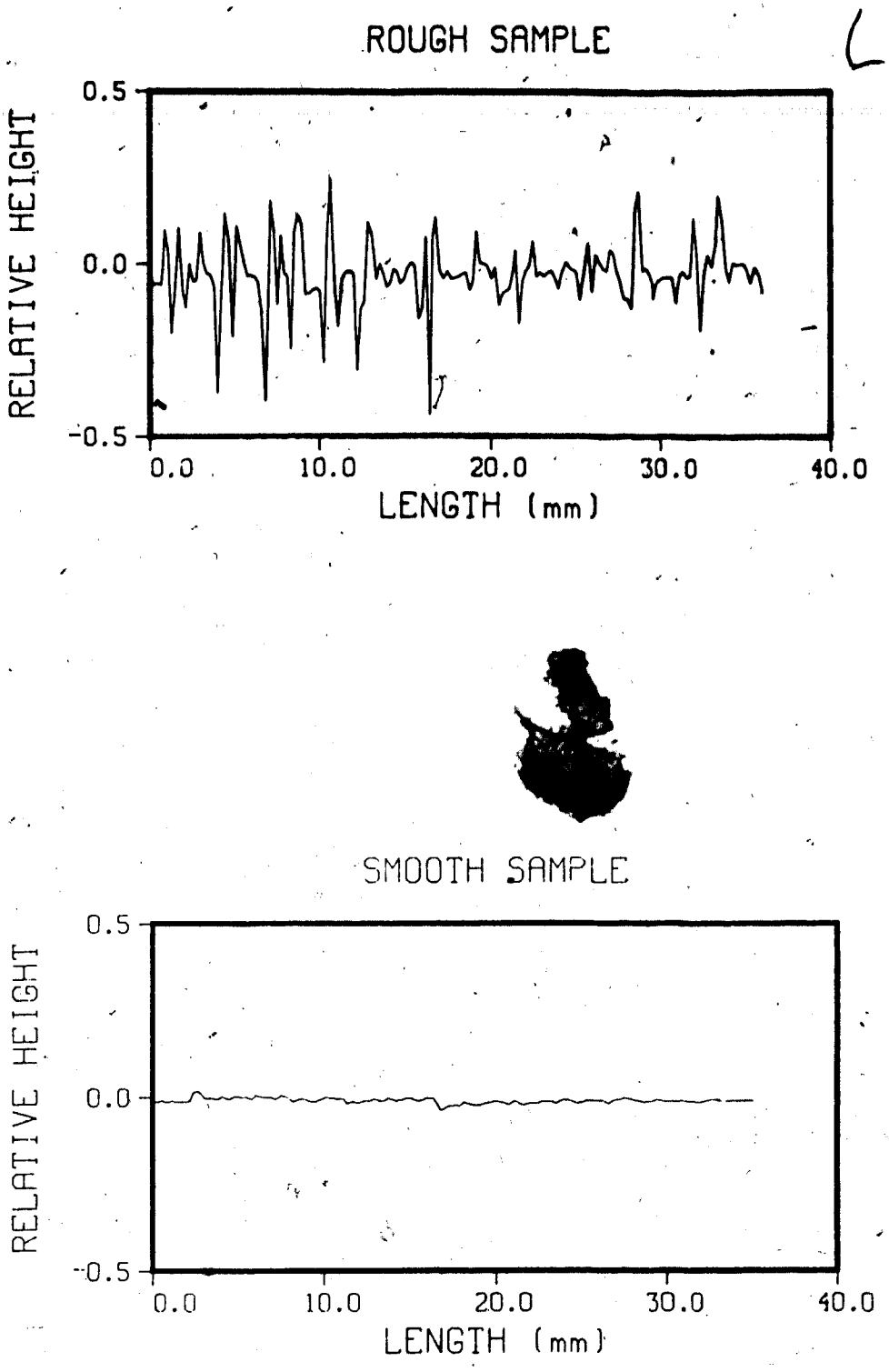

Figure 3.3 Comparison of profiles from a rough and a smooth sample.

This data file had 539 sets of data and a relative roughness value of 83.17.

3.4.2.2 Discussion of the Profiler Results

The procedure of profiling, digitizing, and computing roughness parameters had the ability to differentiate between a smooth and a rough sample as discussed earlier. It has been successfully used by previous authors, specifically Krahn (1974) and Tse (1978).

The inconclusive Z_2^* results from sample #1 indicated that this procedure was inappropriate for this rock type and equipment. The Zoology Profiler had no vertical calibration and exhibited nonlinearity, both of which prevented the calculation of an absolute roughness parameter (*e.g.* CLA or Z_2). The digitizing process created errors in that maxima of some profile peaks were missed and backtracking of the X values had to be corrected. Also, the computed values of Z_2^* were dependent upon the sampling interval dx which was also the experience of Reeves (1985).

The problem in both using a profiler or a digitizing system is deciding upon a sampling interval dx that will be sufficiently small to characterize the roughness without creating unnecessary data points. Reeves (1985, p.431) states that:

"Failure to include either high or low frequencies may lead to poor estimates of the

RMS height (Z_1), gradient (Z_2), and curvature (Z_3) statistics."

These parameters are dependent upon dx and care must be taken in their interpretation.

The decision was made to use finer grits (#220 and #400) on the lapping table to achieve smoother surfaces and to return to the Talysurf instrument for roughness quantification. Although there were still some problems with this procedure, the Talysurf gave a direct measurement of roughness in a quick and convenient manner without the possibility of errors due to extraneous data manipulation.

3.4.3 Results from the Talysurf Characterization

Sample #4 was lapped with #220 grit while sample #6 was lapped with #400 grit. Both of these samples were tested on the Talysurf and CLA values were obtained. These samples were then put through the tilt-table tests and the surfaces were measured again after the sliding incidents. Tables 3.2 and 3.3 summarize the CLA and the sliding angle values. Even though the tilt-table results showed a general decrease in the sliding angle (representative of the frictional resistance), the before and after Talysurf measurements showed no decrease in roughness.

American Standard B46.1-1978 pointed out that if the cutoff value was too small to include the coarser irregularities of a surface, the measurement would not agre

Table 3.2 CLA values (microinches) and sliding angles for sample #4.

SAMPLE #4	Top	Bottom
Cutoff	Not Recorded	
Initial (recorded at various locations)	315, 230, 250, 355, 255, 210 n=6, x=269 s=55	340, 270, 325 n=3, x=312 s=37
Sliding Angles in Sequence (degrees)	26.6, 23.4, 25.7, 22.3, 22.7, 21.1, 20.1, 19.1, 19.5, 19.2, 19.7	
Cutoff	L	
Final (two traces each at the back, middle, & front)	280, 250, 250, 260, 320, 220 n=6, x=263 s=34	350, 280, 270, 310, 250, 320 n=6, x=297 s=37

Table 3.3 CLA values and sliding angles for sample #6.

SAMPLE #6	Top	Bottom
Cutoff	Not Recorded	
Initial (recorded at various locations)	130, 140, 155 n=3, x=142 s=13	180, 225, 185 n=3, x=197 s=25
Sliding Angles in Sequence (degrees)	35.5, 31.7, 31.4, 26.6, 26.0, 24.8, 24.0, 24.0, 26.6, 27.4, 22.9, 27.4	
Cutoff	L	
Final (two traces each at the back, middle, & front)	270, 250, 240, 170, 250, 130 n=6, x=202 s=52	215, 140, 265, 215, 205, 145 n=6, x=198 s=48

with those taken with a larger cutoff. When samples #4 and #6 were measured after displacement, using cutoff lengths, L, 2.5 mm, and K, 0.8 mm, in every case, the longer cutoff L gave the higher CLA value as shown in Table 3.4.

Sample #3, lapped with #220 grit, was also tilt-tested and the roughnesses measured by the Talysurf. The sliding angle decreased from 28.1° to 26.5° after six slides and to 27.4° after 12 events. Six Talysurf traces were done after each sliding event, two at the back, the middle, and the front of the sample. The average of the six measurements was then calculated as was the standard deviation. Table 3.5 shows these results. Although the CLA for both the top (T3) and bottom blocks (B3) show a decrease from the initial value, the value does not decrease with increasing displacement consistently but it oscillates. The CLA value decrease was minor, 6.5% for T3, and 5.1% for B3.

3.4.3.1 Distribution of the CLA Results

Whether a sample of CLA readings from a freshly lapped surface would be normally distributed would become important for later statistical analyses of the roughness data.

Sample #12 was used for this testing. The surface was lapped for one hour with #220 grit and the roughness was measured on the Talysurf. Thirty readings were taken in one direction, all parallel (#T12A) and then 31 more (one reading exceeded the upper limit of 400 microinches) were taken perpendicular to the previous

Table 3.4 Comparison of CLA values (microinches) using different cutoff lengths.

SAMPLE #4 (#220 grit)	Top L	Top K	Bottom L	Bottom K
Back	270	195	330	305
	260	260	260	205
Middle	320	250	285	250
	280	255	285	250
Front	280	255	240	240
	240	220	245	240
$\bar{x}$	275	239	271	247
s	27	26	33	33
SAMPLE #6 (#400 grit)	**Top L**	**Top K**	**Bottom L**	**Bottom K**
Back	155	170	225	175
	180	180	220	120
Middle	125	120	175	120
	190	150	210	145
Front	160	120	130	130
	175	160	155	110
$\bar{x}$	164	150	186	133
s	23	25	39	24

Table 3.5 CLA values and sliding angles for sample #3.

SAMPLE #3 (#220 Grit)							
Event	CLA Values (Cutoff=L)	Back	Middle	Front	x	s	Angle
Initial	T B	380,320 320,370	320,330 295,335	380,295 330,230	321 313	34 48	28.1
2.	T B	350,265	315,385	265,290	312	48	26.4
3.	T B	350,335	290,395	315,300	331	38	27.9
4.	T B	290,360	320,260	330,285	308	36	28.2
5.	T B	320,320	295,360	290,290	313	27	27.2
6.	T B	350,385	265,260	320,250	305	55	26.5
7.	T B	315,315	240,330	270,305	296	34	26.5
8.	T B	375,360	300,270	275,290	312	45	28.1
9.	T B	330,305	290,245	315,330	303	32	29.4
10.	T B	320,320	275,315	250,300	297	29	28.4
11.	T B	310,315	340,315	290,280	308	21	27.4
12.	T B	340,315	315,250	310,250	297	38	27.4
Final	T B	285,320 315,290	250,300 280,330	350,295 295,270	300 297	34 22	——

Table 3.6 Statistics from the CLA data set for T12A.

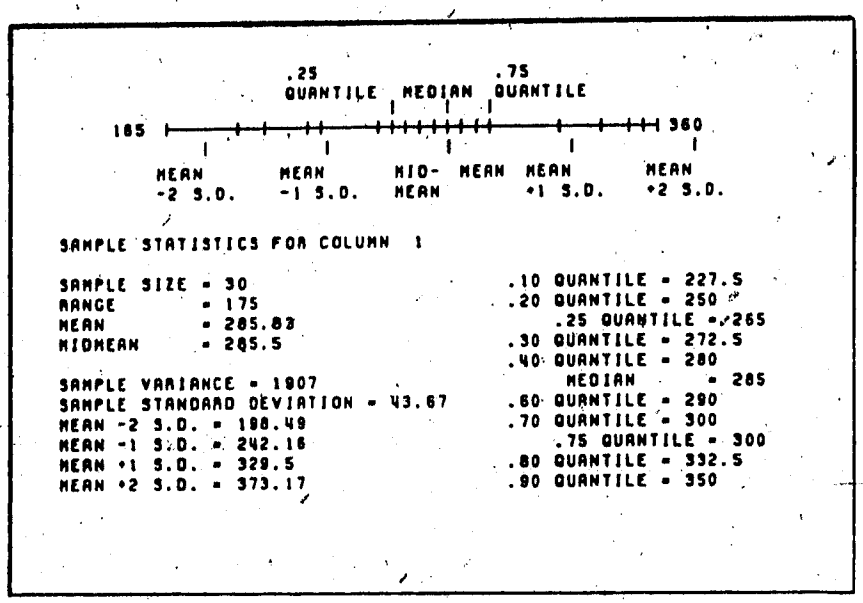

Table 3.7 Statistics from the CLA data set for T12B.

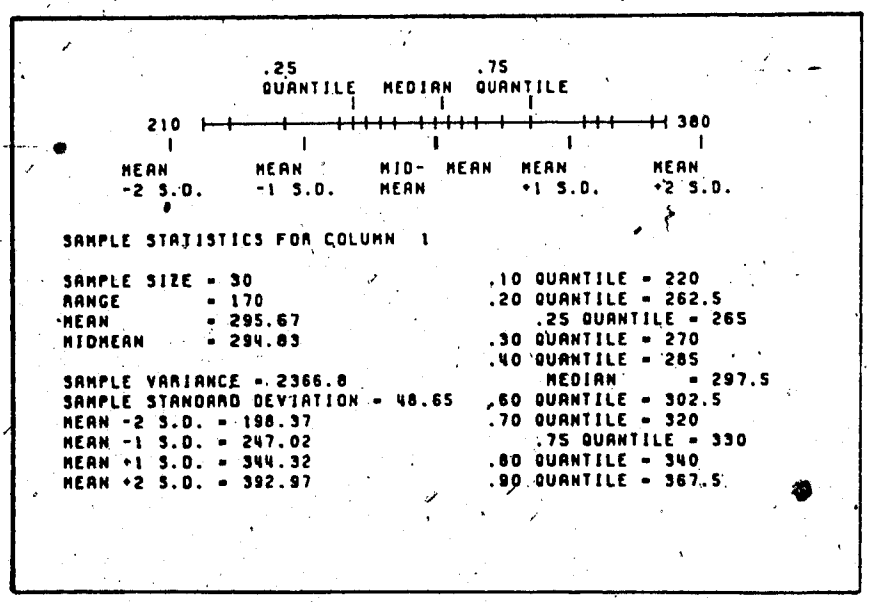

set (#T12B). Tables 3.6 and 3.7 show the statistics from the two sample sets as calculated by the program *STPK. Figures 3.4 and 3.5 give histograms for the two data sets and the normal distribution curves fitted by the program.

The two samples have similar means, 285.83 and 295.67 respectively for T12A and T12B and similar standard deviations, 43.67 and 48.65. These values, from perpendicular directions, indicate that there is no directional anisotrophy in the surface roughness.

The size of the standard deviation is relatively large in this case and in the following results because the stylus does not resample in the same track every time.

A χ^2 test compares the observed grouped distribution with the fitted normal distribution for the data set T12A, as described by Hald (1952). The calculated χ^2 for the data was 2.63 which was not significant compared to the $\chi^2_{.95}$ value of 3.84 with one degree of freedom. Therefore the observed distribution did not differ significantly from the fitted normal distribution.

Ten samples were relapped with #220 grit and tilt-tested. Talysurf roughness measurements and surface cleaning, removal of debris from the sliding surface with the use of compressed air, were performed during testing to

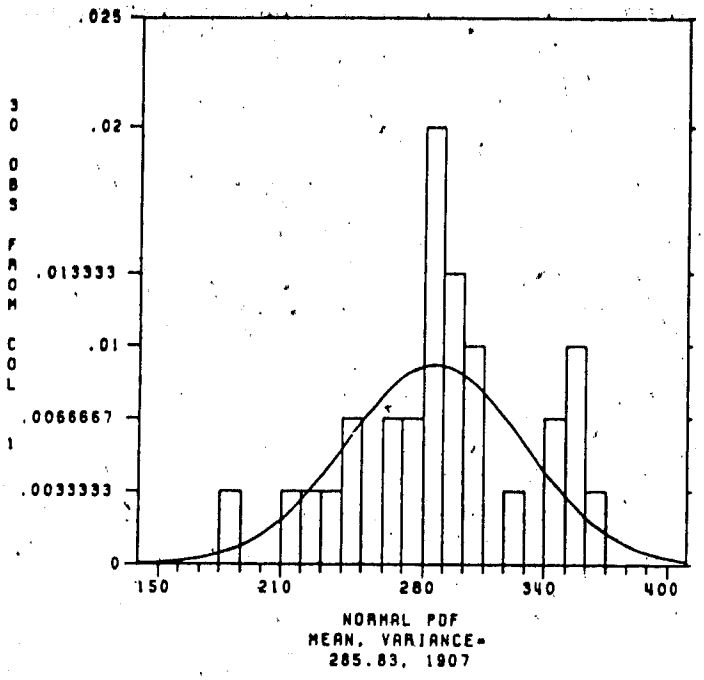

Figure 3.4 Histogram and fitted normal distribution for T12A.

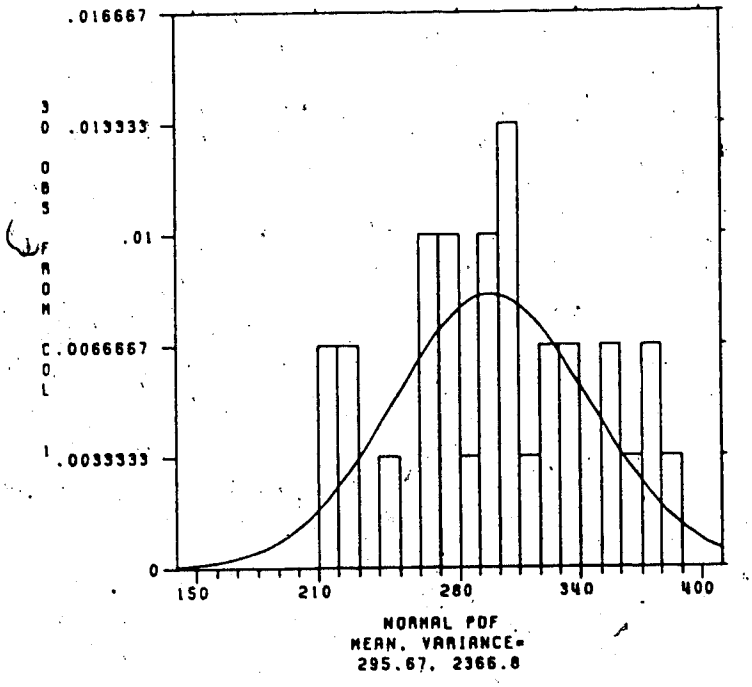

Figure 3.5 Histogram and fitted normal distribution for T12B.

determine its effect.

The testing procedure followed is discussed in 3.5.1.

The results from this testing are located in Tables 3.8 to 3.17. These tables contain the mean roughness, $\bar{x}$ of the six traces and the estimated standard deviation, s. If more than six traces were done per sample, the number of traces used in determining the distribution parameters is indicated.

In some cases, a CLA reading exceeded the 400 microinch upper limit and therefore the specific value of that reading was unknown. Hald (1952, Sec, 6.9) describes a procedure for estimating the distribution parameters $\bar{x}$ and s for a one-sided censored normal distribution. This procedure was followed for the aforementioned cases and these results are marked with an '*' symbol in the tables.

Four different roughness hypotheses were proposed by an asperity model. The values from the ten tables were examined to test these hypotheses using the Student's t-test to determine the significance of the means of the samples' observations.

The Student's t-test has two underlying assumptions according to Hald (1952). Firstly, the observations within each set must be randomly drawn from the same population and secondly, the two populations must be normally distributed. Hald (1952, p.397) stated:

"The first condition is essential to the validity of the t-test, whereas moderate deviations from

Table 3.8 Average CLA values (microinches) for sample #1.2.

SAMPLE #1.2		Top			Bottom		
Cutoff		L	K	J	L	K	J
Initial	x	343	278	214	330	269	190
	s	46	53	33	34	39	42
After 6 Events	x	313	252	190	319	282	203
	s	19	34	23	23	29	16
					5%		
After Cleaning	x	332	284	202	356	293	203
	s	19	38	31	23	32	55
Final					n=8		
	x	333	260	182	375	283	207
	s	47	49	30	*55	39	45

Table 3.9 Average CLA values for sample #3.2.

SAMPLE #3.2		Top			Bottom		
Cutoff		L			L		
Initial	x	276			308		
	s	53			21		
After 6 Events	x	270			284		
	s	14			44		
After Cleaning	x	295			285		
	s	29			40		
Final	x	283			317		
	s	52			41		

Table 3.10 Average CLA values (microinches) for sample #4.2.

SAMPLE #4.2		Top			Bottom		
Cutoff		L	K	J	L	K	J
Initial	x	324	274	204	301	243	181
	s	39	50	29	38	19	13
After 6 Events	x	305	262	212	n=7 273	228	163
	s	18	34	22	*62	33	16
After Cleaning	x	333	268	199	287	238	157
	s	32	55	36	30	31	27
Final	x	298	233	174	252	214	170
	s	42	39	24	46	16	19

Table 3.11 Average CLA values for sample #6.2.

SAMPLE #6.2		Top			Bottom		
Cutoff		L			L		
Initial	x	251			302		
	s	39			14		
After 6 Events	x	283			316		
	s	33 5%			46		
After Cleaning	x	326			289		
	s	28			49		
Final	x s	Sample dropped and scratched. No final measurements done.					

Table 3.12 Average CLA values (microinches) for sample #8.2.

SAMPLE #8.2		Top			Bottom		
Cutoff		L			L		
Initial	x s	269 46			336 19		
After 6 Events	x s	268 46			308 45		
After Cleaning	x s	268 21			341 10 1%		
Final	x s	268 41			303 20 5%		

Table 3.13 Average CLA values for sample #9.2.

SAMPLE #9.2		Top			Bottom		
Cutoff		L			L		
Initial	x s	304 34			320 31		
After 6 Events	x s	n=7 289 *71			310 51		
After Cleaning	x s	305 16			309 49		
Final	x s	314 41			298 33		

Table 3.14 Average CLA values (microinches) for sample #10.2.

SAMPLE #10.2		Top			Bottom		
Cutoff		L			L		
Initial	x	314			n=7 321		
	s	46			*64		
After 6 Events	x	279			n=7 321		
	s	44			*69		
After Cleaning	x	286			303		
	s	33			40		
Final	x	284			296		
	s	47			70		

Table 3.15 Average CLA values for sample #11.2.

SAMPLE #11.2		Top			Bottom		
Cutoff		L			L		
Initial	x	305			288		
	s	36			58		
After 6 Events	x	293			263		
	s	36			43		
After Cleaning	x	300			273		
	s	56			53		
Final	x	315			274		
	s	48			51		

Table 3.16 Average CLA values (microinches) for sample #13.2.

SAMPLE #13.2		Top			Bottom		
Cutoff		L			L		
Initial	x	255			233		
	s	58			39		
After 6 Events	x	202			244		
	s	111			49		
After Cleaning	x	220			256		
	s	31			41		
Final	x	268			243		
	s	36			30		

Table 3.17 Average CLA values for sample #14.2.

SAMPLE #14.2		Top			Bottom		
Cutoff		L	K	J	L	K	J
Initial	x	319	258	194	323	228	173
	s	64	55	38	67	36	33
After 6 Events	x	333	269	192	278	214	168
	s	28	38	10	29	21	12
After Cleaning	n	n=7	n=7	n=7			
	x	308	275	176	289	219	173
	s	*65	43	38	51	35	14
Final	x	301	252	187	317	242	173
	s	28	44	41	40	23	23

normality usually are of no great importance."

Because the t-test assumes that the samples are from the same population, the sample variances cannot be significantly different. Therefore, the F-test was applied to check the variances of the samples before the t-test was applied. If the variances were significantly different, then the t-test was not appropriate. Kennedy and Neville (1976, Chap. 13) discuss a more useful test of significance for the case of nonhomogeneous variables and this procedure was applied in these special cases.

Significant results are marked on Tables 3.8 to 3.17 with a % sign indicating the significance level used, *e.g.* the "5%" in Table 3.11 at the second position indicates that increase in roughness from the sixth to the seventh event after cleaning was significant at the 5% level.

The four possible roughness changes and their occurrence follow (looking at the L-scale results only):

1. Surface roughness decreased after six sliding events from the initial value in 15 out of a possible 20 cases (75%). But none of the cases were significant according to the t-test even at the 10% level. Conversely, of the remaining 25% which displayed an increase, none were significant at the 10% level.
2. The roughness increased, after cleaning in 15 of the cases (75%) with two cases being significant at the 5%

level. None of the cases exhibitting a decrease were significant, even at the 10% level.

3. The sample roughness decreased in the final six sliding events in 9 out of 18 cases (50%) with one being significant at the 1% level. One sample though, #13.2 Top, displayed a significant increase in roughness at the 5% level.
4. Lastly, the roughness decreased from the initial CLA value to the final in 11 of 18 cases (61%). Only one case was significant at the 5% level. None of the cases displayed a significant increase in roughness.

3.4.4 Discussion of Talysurf Results

A simple asperity model consisting of asperity peaks and troughs is proposed to explain the results of the roughness testing. Initially, the troughs may be partially filled with debris from lapping. As sample sliding progressed, asperity peaks would be sheared off by brittle fracture. The material sheared off would fall into the troughs as asperity peaks were truncated. Therefore roughness would decrease as the asperities were sheared off and the troughs filled in (hypothesis #1). Also the frictional resistance (or sliding angle of the tilt-test) should decrease as the sample becomes smoother.

If the surface was cleaned with compressed air, some of the debris would be blown out of the troughs and the roughness would increase (hypothesis #2). Then two possible

results exist. As material is blown from the troughs, increased interlocking of the surfaces may cause the sliding angle to increase over the previous angle before cleaning, but not above the initial sliding angle value due to truncation of the peaks. Alternatively, if interlocking does not occur and sliding occurs as a result of truncated peak sliding on truncated peak, no increase in the sliding angle would be expected.

As the sliding of the two samples progressed, more asperity wear would be expected. Again, roughness and the sliding angle values should decrease slightly (hypothesis #3).

Finally, hypothesis #4 followed that the final roughness would be smoother than the initial value as wear of the asperities occurred.

Of the five statistically valid significant changes in roughness during testing, four were in agreement with the hypotheses proposed by the test model.

The one deviation from the proposed model was for hypothesis #3 regarding a decrease in the roughness from the sixth to the last event. Sample #13.2 Top showed a significant increase which perhaps can be attributed to detritus building-up on the sliding surface. This does not necessarily imply that the sliding angles of the sample would increase; only that the Talysurf measured an increased roughness.

Hypotheses #1 and #2 both occurred in 75% of the possible cases perhaps agreeing with the proposed physical model. The third hypothesis, which results from one of two possible causes (increased interlocking of the surfaces versus truncated peak sliding on truncated peak) occurs in only 50% of the cases possibly reflecting uncertainty and variability in the model and also reflecting variability in the CLA measurements. Another surface model, as suggested by Coulson (1972) indicated that the surface might become smoother or it might become rougher as material breaks off. Hence, multiple surface models which grade into one another might be a better explanation for the variability of the results.

The problem may not lie in the fact that these expected responses did not happen, but in the fact that the method of roughness quantification may have been imprecise.

The Talysurf values may have been imprecise because:

1. the Talysurf did not measure the correct roughness in that the stylus may have ploughed through the frictional surface sensing roughness at depth, and/or
2. the Talysurf did not measure the roughness at the appropriate scale.

The Talysurf instrument, on cutoff value L, traverses a sampling length of 2.5 mm. Perhaps this is sufficient for a finished man-made material (*e.g.* a metal surface) but it may be insufficient for a finished natural rock surface whose composition was variable (hard quartz grains in a fine,

softer matrix). Reeves (1985, p.438) stated that:

"...surface statistics and shear strength should be measured on the same scale."

This would indicate that for a 5 x 5 cm shear box sample, the surface profile trace should be centimetres in length, not millimetres as in the Talysurf.

Eaton (1986) found that the majority of asperity wear occured on the leading one third of the sliding surface. Table 3.4 lists the CLA values for two samples after shearing has occurred. The average of the two front readings is lower than the average of the two back readings in 3 out 4 possible cases when comparing the L-scale results while one case was equal. Looking at Table 3.5 for CLA values as the number of sliding events increased, the front average value was lower than the back in 11 of 13 cases neglecting the initial two readings. Although the means were not tested for significance, the results would seem to indicate agreement with Eaton's work.

Rock sample roughness would therefore vary over the entire surface area. Six Talysurf traces were probably insufficient to properly characterize the surface roughness of the sample. Perhaps if more traces had been taken to quantify the roughness of the entire surface, the differences between the observation means would have been significant according to the t-test.

3.4.5 Surface Scaling

The deformation behaviour of joints is dependent upon the topography of the contacting surfaces. If the topography varies with surface size, then so must the deformation behaviour. Therefore a scaling law for surface roughness would be quite important as it would possibly allow extrapolation of small-scale (lab) measurements to field conditions.

Thomas and Sayles (1975) wrote on the effect of waviness on thermal contact resistance and in 1977, their work was related to the deformation of machine joints. In both cases they assumed the power spectra $G(\omega)$ of the random surfaces to be of the form:

$$G(\omega) = 4a\sigma^2 / (a^2+\omega^2) \qquad [3.1]$$

where a = a constant of decay for the autocorrelation function,

σ^2 = the variance of the height distribution, and

ω = the frequency

as suggested by Whitehouse and Archard (1970).

The power spectra varies with ω^{-2} and because the area under a power spectral density curve $G(\omega)$ equals the variance (σ^2) of the height distribution, the RMS roughness increases as the square root of the profile length. The RMS value should therefore be most heavily influenced by the

longest wavelengths in a sample. Hence, roughness should be related in some way to the length of the sample or to the measured bandwidth.

Sayles and Thomas (1978) proposed a scaling law for characterizing a wide range of different surface structures. They proposed that:

$$G(\omega) = 2\pi k/\omega^2 = (k/2\pi)\,\lambda^2$$

$$\text{or} \quad G(1/\lambda) = k\lambda^2 \qquad [3.2]$$

where k = the "topothesy" of a surface and

λ = wavelength.

The topothesy value was a unique value which defined the statistical geometry of an isotropic surface for any given range of wavelengths. In their paper, they show many different surfaces whose roughness data lies along a ω^{-2} curve.

Roughness data from Table 3.8 for sample #T4 was used for comparison to the work of Sayles and Thomas (1978). The roughness values, which were CLA readings in microinches, were converted to RMS values in meters. An RMS value is 11% greater in magnitude than a CLA value for the same surface. The cutoff values used were those of the Talysurf; J (0.25mm), K (0.8 mm), and L (2.5 mm).

Thomas and Sayles (1975) made roughness measurements on a shot-blasted bar of mild steel which was known to be a good example of a random isotropic surface. Figure 7 of this

reference illustrates a log-log plot of RMS roughness versus the diameter of the contact area, d, which was assumed to be equal to the cutoff value divided by two (or λ=2d).

Figure 3.6 plots these 13 data points on a plot of normalized roughness (RMS roughness divided by the square root of the topothesy value) versus the cutoff length. Sayles and Thomas (1978) found the topothesy value for this surface to be 1.7×10^{-8} m. The solid line on the plot represents the theory given by the equation:

$$\sigma^2 = k\lambda_o$$

where $\sigma/\sqrt{k}$ = the normalized roughness and

λ_o = the cutoff wavelength.

Also plotted on Figure 3.6 are the three data points for the roughness measurements made at three different scales for sample #T4. The sandstone was considered fine to medium grained, and assuming an average grain size of 0.5 mm (5×10^{-4} m), the E-scale on the Talysurf was slightly greater than the average grain size.

The topothesy value for the sandstone was found to be 4.1×10^{-6} m which similar to the value for the shot-blasted surface; k= 1.7×10^{-8} m. The #T4 points plot in close proximity to the theory line proposed by Sayles and Thomas (1978) as do the other points.

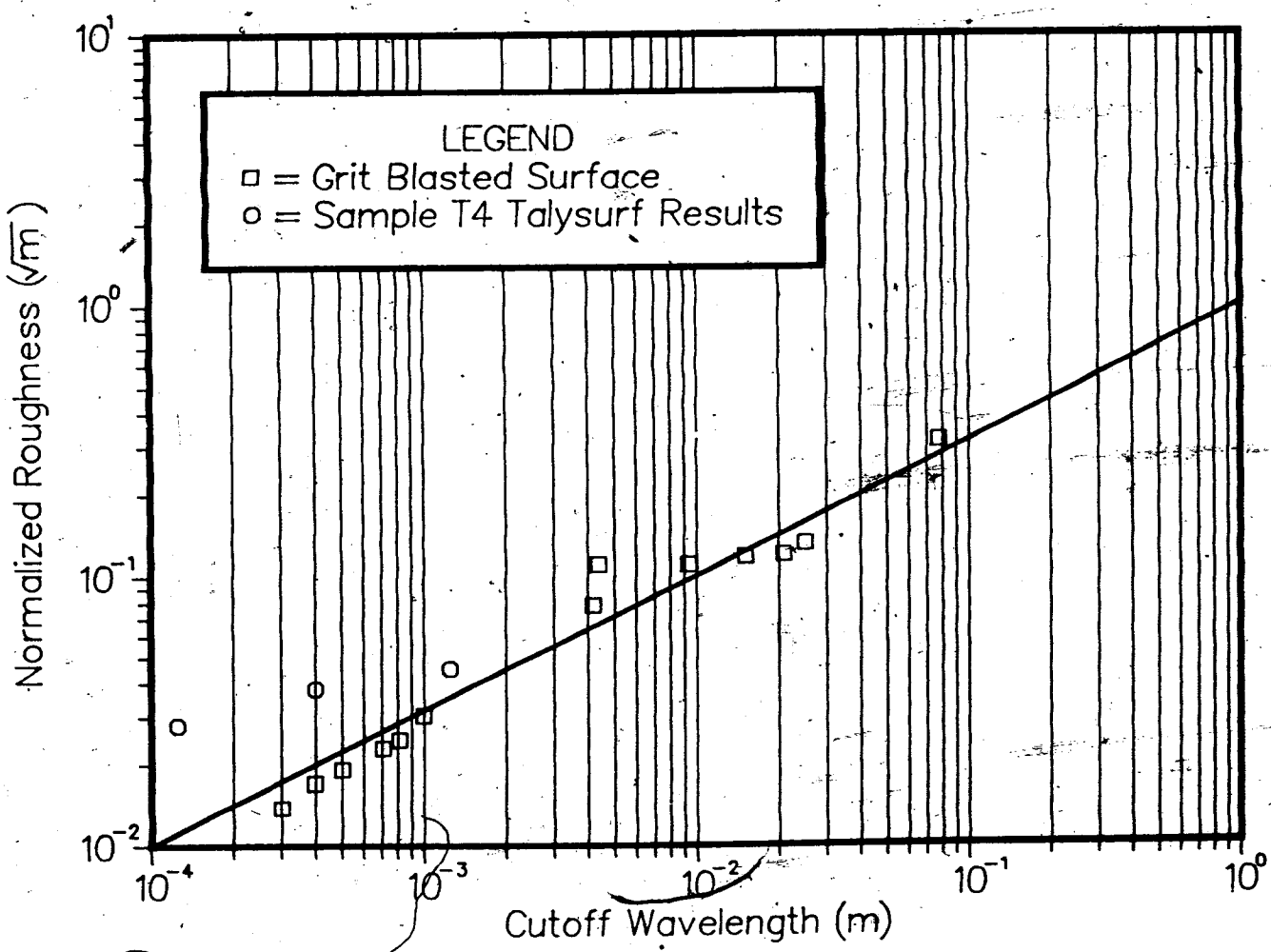

Figure 3.6 Comparison of T4 initial roughness data to the results of Sayles and Thomas (1978).

Berry and Hannay (1978) in a following discussion paper stated that Sayles and Thomas forced the data to follow a ω^{-2} curve and that each surface had a spectrum with a different slope.

Mandelbrot (1977, 1983) developed a new geometry of nature and identified a family of shapes called "fractals". The concept of fractals can be thought of as a class of mathematical functions which are continuous but nowhere differentiable. Fractals tend to be scaling which implies that the degree of irregularity and/or fragmentation is identical at all scales.

The fractal dimension D is a parameter which describes the "size" of the roughness as the scale changes. It can also be thought of as a fraction lying between the lower bounds of topological geometry ("rubber-sheet geometry") and the upper bounds of Euclidian dimensions. The parameter D describes the degree to which a fractal function fills up Euclidian space.

As D approaches 2, a surface will have a high degree of correlation between points and approaches being differentiable. As D increases, the surface becomes much more jagged and nearby points more independent. When the fractal dimension becomes greater than 2.5, overhangs may appear.

The fractal dimension D is therefore a parameter which describes the scaling properties of surface topography. Brown and Scholz (1985b) investigated the applicability of

using the fractal dimension in the study of natural rock surface topography.

From stylus measurements, power spectra were computed for each profile using a fast Fourier transform algorithm. Then an ensemble average for each surface was made by averaging the power at each frequency for all profiles (in an earlier paper, 28 profiles were taken per 5 X 5 cm surface) to produce a single smooth spectrum which represented the average character of the surface.

These spectra have the characteristic that power falls off rapidly with spatial frequency ("red noise" power spectra) and each spectrum is approximately linear in log-log space. From the plots of the power spectra, the slopes can be computed by least squares fitting and then the fractal dimension D can be backcalculated.

From figures in Brown and Scholz (1985b), it can be seen that the slopes were not constant but gradually decreased from high to low frequencies. Brown and Scholz suggested that two subjective breaks in the slopes could be seen.

In comparision to natural rock surfaces, studies of flat ground and lapped surfaces (Brown and Scholz (1985a)) show a tendency for the power to flatten out as the frequency decreases. Granite lapped with #80 grit and glass lapped with #80 grit flatten out to white noise below a "corner frequency" which corresponds approximately to the diameter of the grinding powder. This corner frequency may

be caused by the two-stage process of surface grinding and grit lapping.

Conclusions from the Brown and Scholz work were;

1. natural rock surfaces have a red noise power spectrum over the entire frequency band studied,
2. the slope of the power spectrum is not constant for a given surface and therefore no simple relationship between roughness and surface size exists,
3. no single fractal dimension D can be used to describe the topography of natural rock surfaces. This parameter varies significantly with the frequency band considered, and
4. extrapolation of this scaling parameter D to other scales must be done carefully.

3.5 Tilt-Testing

A tilt-testing program was carried out on the Torrens Member sandstone to examine the change in frictional resistance of the sample with increasing displacement. The 5 x 5 cm samples were to act as a model for the accelerating slab movements.

The tilt-table was chosen rather than the direct shear test because of its better suitability. The driving force in the tilt-test is gravity, similar to the sliding block in an actual wall movement, in comparison to an applied mechanical force in a shear test. Also there are end-effects in the direct shear test due to constraint of the sample by the

shear box while the tilt-test had a free sample sliding on a clamped base.

The tilt-test is performed at low normal stresses. Both Coulson's (1972) and Bruce's (1978) results indicated that ϕ_b did not change significantly over the limited stress range of surface workings. Eaton (1986) found that surfaces lapped with #80 grit approached the ultimate frictional resistance after 50 cm displacement even at normal stresses below 0.6 KPa.

The tests were carried out on a tilting table built by the Department of Civil Engineering Workshop for Eaton (1986) which is shown in Figure 3.7. A rigid frame supports a hinged table and an electric motor assembly. This drive assembly rotates a drum which has a wire cable attached to the hinged tilting table.

A linear voltage displacement transducer (LVDT) is mounted on the table against the top sliding block to monitor displacements. To record angular changes, a rotary voltage displacement transducer (RVDT) is mounted on the end of the hinge of the tilting table. A protractor is also mounted here to provide a quick visual reference.

The output voltages from the RVDT and the LVDT are recorded on an X-Y plotter. Scales of 1 cm = 0.5° on the X axis and 1 cm = 0.1 mm on the Y axis allow sufficient accuracy ($\pm$ 0.1° for the RVDT and $\pm$ 0.01 mm for the LVDT).

The bottom half of the sample, the plate, is clamped with brackets to the table. A line level and the three

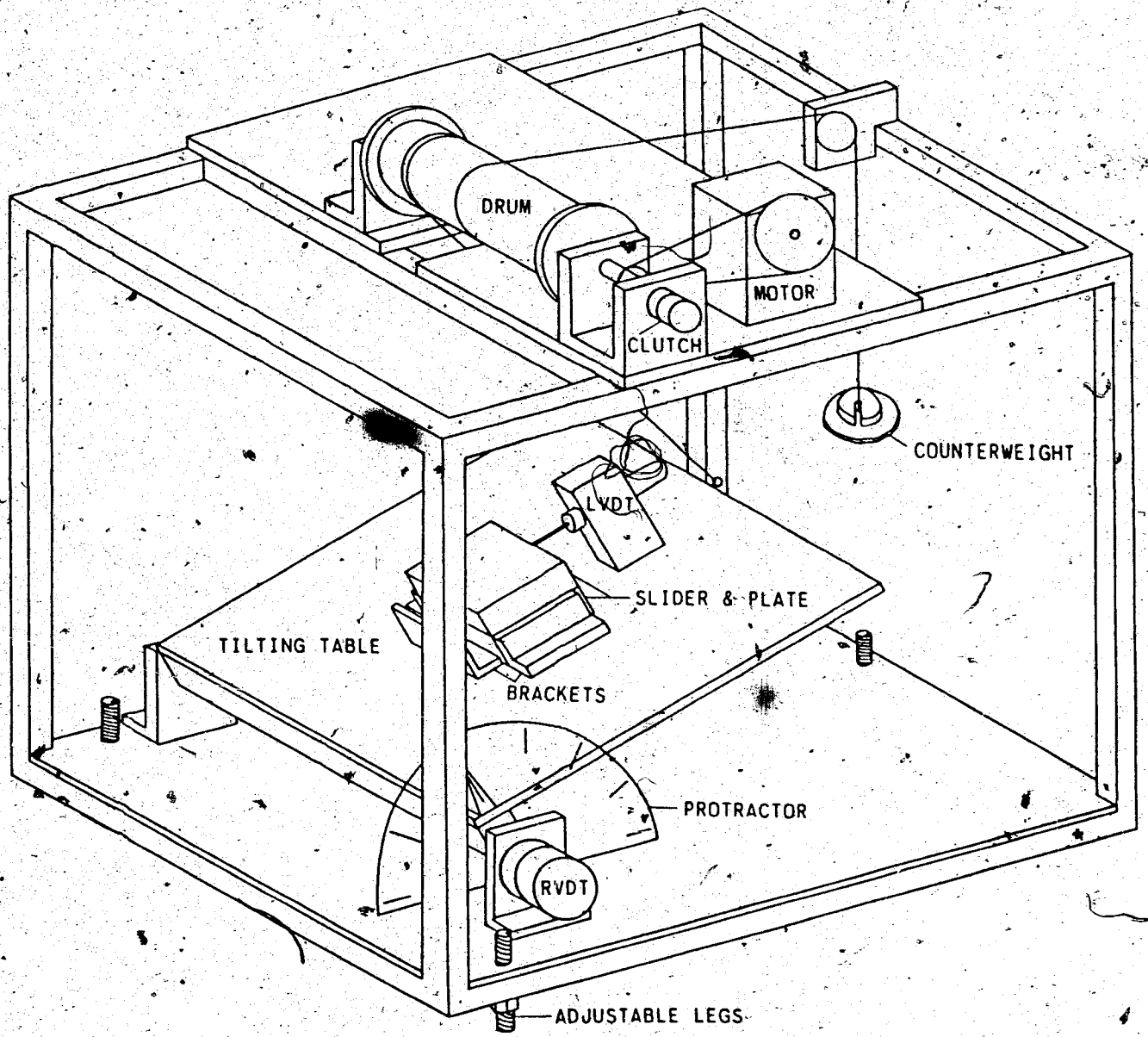

Figure 3.7 Isometric view of the tilting table.

th[redacted] legs are used to level the surface of the plate and at 90° to it. The top half, the slider, is placed on top of the plate. The table is inclined to 15° by hand and then the motor is switched on. A 5:1 gear ratio provides rotation at 8° per minute. The front bracket allows the slider 2 cm of displacement.

The failure or sliding angle was estimated as the angle when greater than 1.0 mm of displacement occurred and acceleration of the slider was continuous. This negates minor block movements due to external vibration sources. Most of the samples exhibited sudden acceleration and sliding but some of the samples showed a slow creeping movement while others displayed a step-like, st[redacted]ck-slip movement.

Some of the tests were performed without surface cleaning while others were cleaned with compressed air after a certain number of sliding events.

The tilt testing program was completed between July and October, 1986.

3.5.1 Results

The first series of tilt-tests done were on samples #1 and #2 which were lapped with #80 grit. These surfaces were measured on the Talysurf but in all cases, the CLA values exceeded the upper limit of 400 microinches. Table 3.18 gives a listing of the sliding angles from the initial to the final values while Figure 3.8 provides a graphical

representation.

Sample #1 had an initial value of 28.0° which decreased to 25.2° after 10 events and after some oscillation, decreased to a final value of 24.5° after 18 events. Sample #2 had a higher initial value of 36.0°, which after 6 events decreased to 26.8° and then stabilized at approximately 28 to 29° for the remaining events.

Samples #4 and #6 were lapped with finer grits, #220 and #400 respectively which produced smoother surfaces. Initially sample #4 slid at 26.6° and then decreased consistently (except for one angle of 25.7°) over 6 events to 20.1. Afterwards, the sliding angles stabilized at approximately 19°. The supposed smoothest sample, #6 slid initially at the high value of 35.5°. It decreased to 24.0° after 8 events and then the sliding angle increased and fluctuated for the remaining 4 events.

Sample #3 (#220) was also tested without surface cleaning. Table 3.16 shows that the sample initially slid at 28.1° and decreased to 26.5° after seven slides. The sliding angles varied over the remaining events with no general decreasing trend exhibited.

This specific test was different from the other uncleaned test as the slider was removed after each displacement to measure the roughness on the Talysurf. The slider was repositioned on the clamped bottom half and testing continued. As a result, this test was carried out in its entirety in the Mechanical Engineering Building.

Table 3.18 Sliding angles for uncleaned tilt-tests.

SAMPLE	#1	#2	#4	#6	#3
Grit #	#80	#80	#220	#400	#220
Date	07/15	07/16	08/12	08/13	09/4
Event	Sliding Angles (degrees)				
1	28.0	36.0	26.6	35.5	28.1
2	30.0	31.0	23.4	31.7	26.4
3	26.5	31.0	25.7	31.4	27.9
4	28.5	27.9	22.3	26.6	28.2
5	26.5	27.5	22.7	26.0	27.2
6	26.4	26.8	21.1	24.8	26.5
7	26.2	28.5	20.1	24.0	26.5
8	26.3	26.5	19.1	24.0	28.1
9	25.5	28.8	19.5	26.5	29.4
10	25.2	28.1	19.2	27.4	28.4
11	26.0	28.1	19.7	22.9	27.4
12	26.5	28.8	—	27.4	27.4
13	29.0	28.9	—	—	—
14	24.8	29.5	—	—	—
15	23.2	—	—	—	—
16	26.5	—	—	—	—
17	23.5	—	—	—	—
18	24.5	—	—	—	—

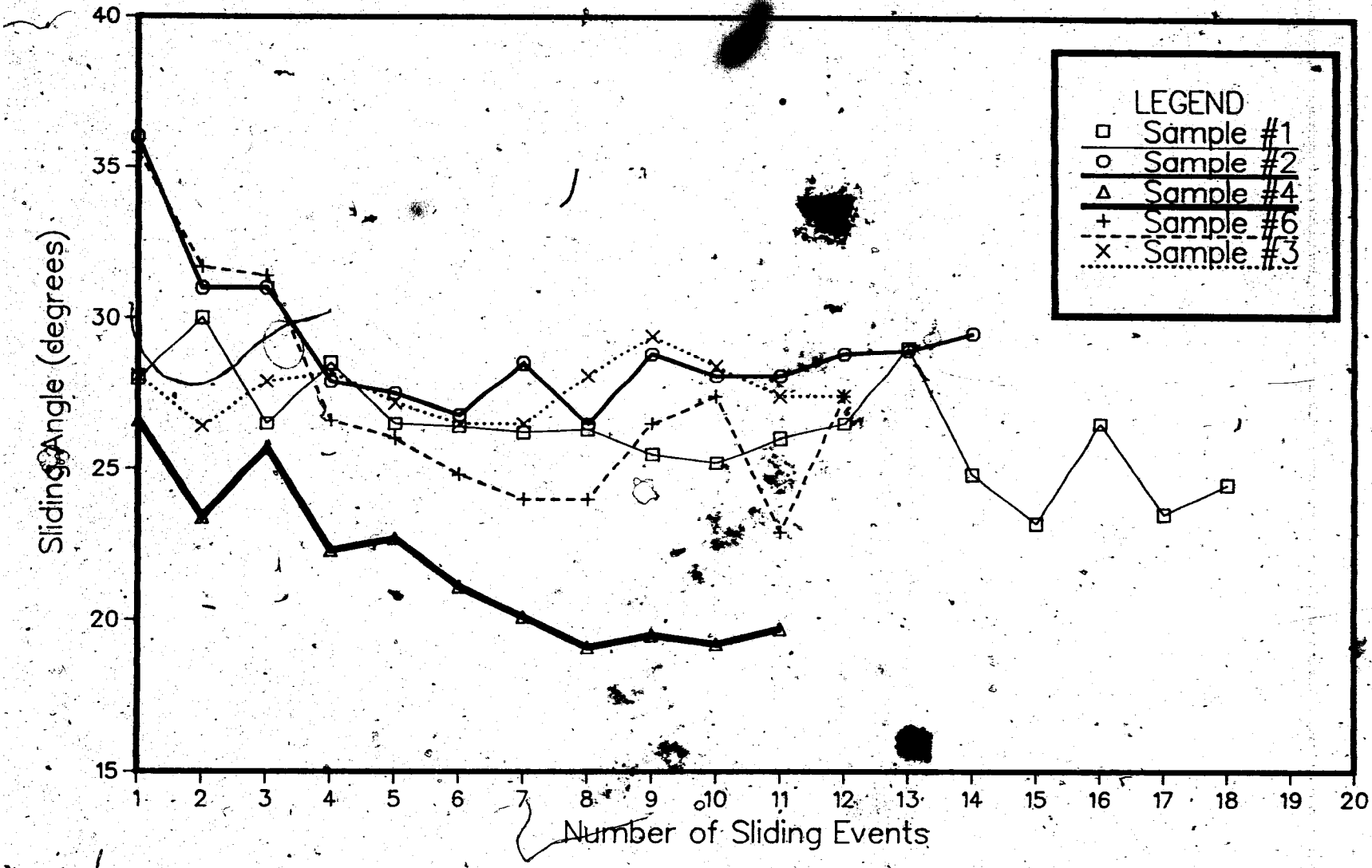

Figure 3.8 Sliding angle versus number of events for the uncleaned tilt-tests.

Another set of tilt-tests were performed but with surface cleaning. After five sliding events had occurred, samples #3.1 and #4.1 were cleaned (both top and bottom) with compressed air to determine cleaning's effects on the frictional resistance. Table 3.19 shows that both samples decreased in frictional resistance on their first five sliding events. After cleaning, #3.1 increased from 26.7° to 29.3° while sample #4.1 exhibited no increase and oscillated in sliding value over the last four events.

Because no conclusions could be drawn from the [illegible] two cleaned samples, a more ambitious tilt-testing p[illegible] was undertaken. Ten samples were lapped with #220 gri[illegible] two different sets; 4 specimens in [illegible]on Sept. 22 and 6 in set #2 on Oct. 10. The testing p[illegible] followed was:

1. Init[illegible] roughness traces were measured on the Talysurf by taking six traces at various scales on both the top and bottom halves of the sliding surface.

2. The sample was slid six consecutive times on the tilt-table.

3. Talysurf measurements were done again.

4. The sliding surface was cleaned with compressed air.

5. Roughnesses were mea[illegible]red again after cleaning.

Table 3.19 Sliding angles for cleaned samples #3.1 and #4.1.

SAMPLE	#3.1	#4.1
Grit #	#220	#220
Date	09/16	09/16
Event	Sliding Angles	
1	30.2	31.1
2	28.6	29.0
3	26.5	27.[illegible]
4	27.6	24.9
5	26.7	19.4
	Surfaces	Cleaned.
6	29.3	19.0
7	24.7	24.1
8	24.6	19.5
9	24.5	21.1

6. The sample was slid another six times for a total of twelve sliding events.

7. Final Talysurf measurements were done.

Tables 3.20 and 3.21 and Figures 3.9 and 3.10 provide a summary of the results for both sets.

The first set tested consisted of four samples. Two of the samples, #3.2 and #6.2 had high initial angles of 33.1° and 34.4° which decreased after the first four sliding events. On the sixth event, both of the samples' sliding angles increased fairly dramatically (>2°). The other two samples in the set started at much lower initial angles, 25.3° for #1.2 and 29.6° for #4.2. Over the next four events, #4.2 decreased to 24.1° while #1.2 increased and then decreased to 24.4° on the fifth slide. Again, both samples had an increase in the sliding angle, but only slightly (<2°) after the fifth event.

After cleaning the surfaces with compressed air, three out of four samples decreased in angle. Sample #1.2 changed from 25.1° to 20.0° (5.1° change), #3.2 changed from 30.4° to 27.2° (difference of 3.2°) and #6.2 decreased from 35.2° to 26.9° (8.3° change). Only #4.2 increased in value from 25.9° to 27.5°, an increase of 1.6°.

Sliding angles for the remaining sliding events did not exhibit any obvious increasing or decreasing trends. Sample

Table 3.20 Sliding angles for cleaned samples from set #1.

SAMPLE	#1.2	#3.2	#4.2	#6.2
Grit #	#220	#220	#220	#220
Date	09/23	09/24	09/25	10/3
Event	Sliding Angles (degrees)			
1	25.3	33.1	29.6	34.4
2	26	28.1	27.9	29.2
3	25.9	27.7	25.1	30.9
4	24.8	27.1	24.8	28.5
5	24.4	27.7	24.1	28.4
6	25.1	30.4	25.9	35.2
		Surfaces Cleaned		
7	20.0	27.2	27.5	26.9
8	21.3	27.5	25.2	26.1
9	22.5	26.7	27.0	25.3
10	21.2	26.6	25.7	Sample
11	20.4	27.2	25.6	not
12	21.0	27.1	27.1	Tested

Table 3.21 Sliding angles for cleaned samples from set #2.

SAMPLE	#8.2	#9.2	#10.2	#11.2	#13.2	#14.2
Grit #	#220	#220	#220	#220	#220	#220
Date	10/17	10/20	10/21	10/21	10/22	10/22
Event	Sliding Angles (degrees)					
1	30.9	26.6	34.1	27.6	29.9	24.6
2	30.5	26.2	31.6	34.3	32.6	28.8
3	31.5	31.3	31.6	30.0	27.3	25.4
4	30.1	30.8	29.6	30.0	30.7	27.0
5	27.4	28.7	32.9	27.5	33.9	26.4
6	27.5	28.4	35.8	31.7	32.0	31.1
			Surfaces Cleaned			
7	27.4	31.8	30.1	31.6	30.4	28.6
8	26.1	26.8	31.0	34.5	28.9	22.8
9	24.8	28.0	30.2	29.2	28.4	21.3
10	23.3	27.6	31.5	29.6	28.6	24.5
11	24.5	28.4	28.5	31.6	28.6	20.1
12	23.7	30.1	30.6	29.5	28.7	25.7

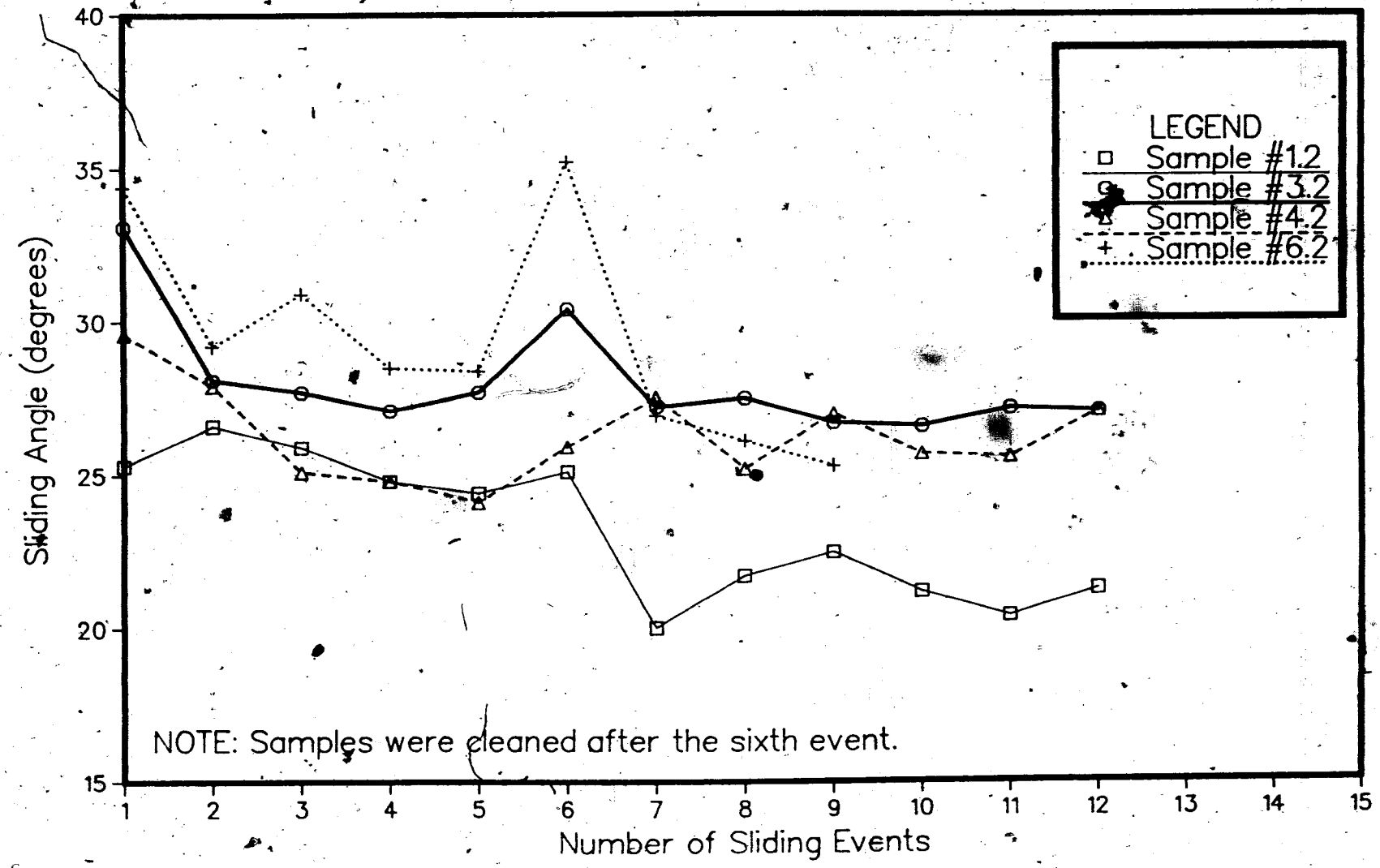

Figure 3.9 Sliding angles versus number of events for cleaned set #1.

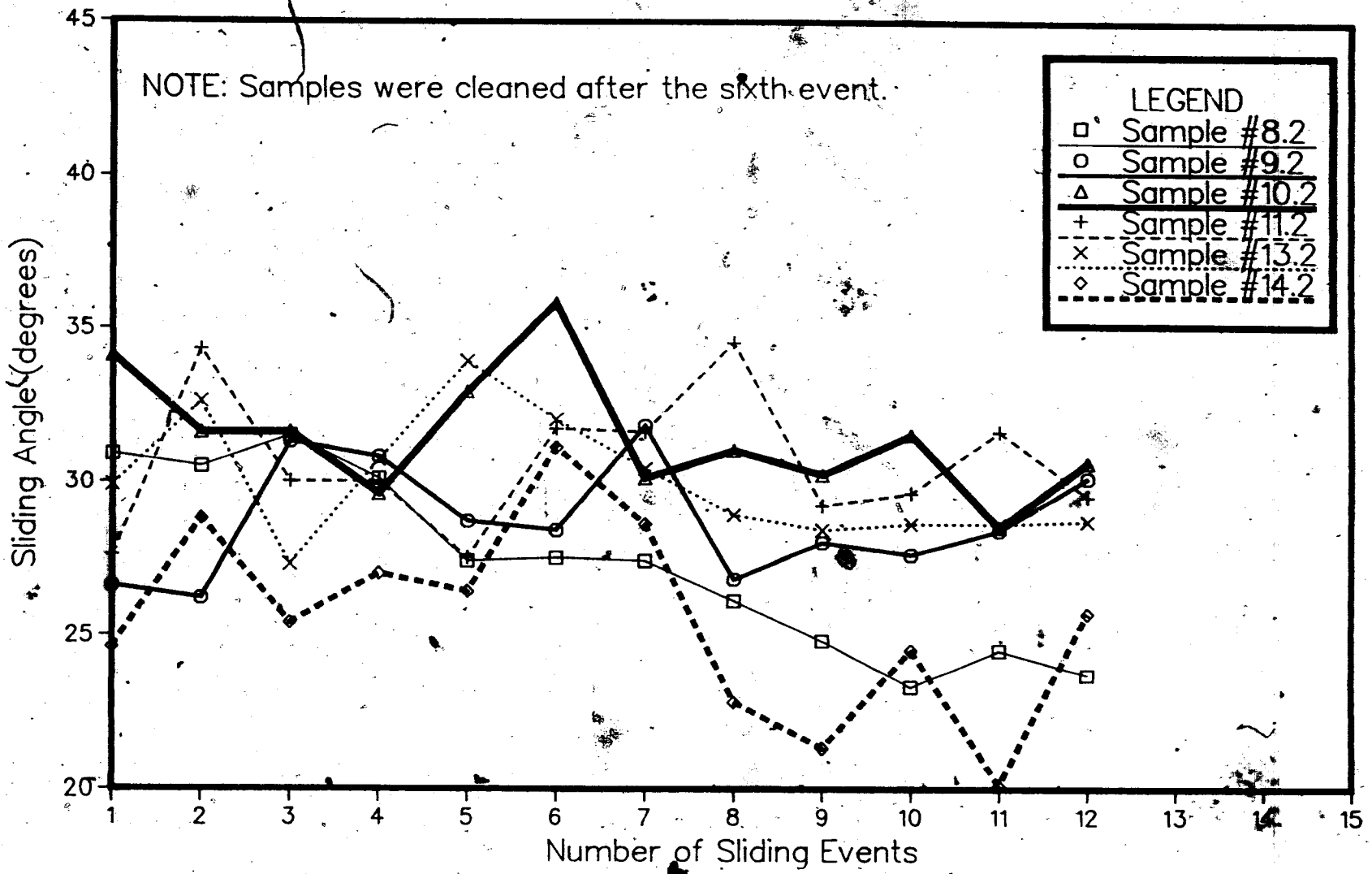

Figure 3.10 Sliding angles versus number of events for cleaned set #2.

#1.2 oscillated around 21 to 22° while #4.2 fluctuated around 26°. Sample #3.2 seemed to stabilize around the 27° mark with only minor variations. Only #6.2 exhibited a decreasing trend but only three sliding events were done as the sample was dropped and scratched. Hence, testing was discontinued.

Set #2 contained six samples which had a wide variation in initial sliding angles. Two of the samples, #8.2 and #10.2 had initial angles greater than 30°, while the other four were less, with #14.2 sliding at the lowest value of 24.6°. Sample #10.2, which had the highest initial angle of 34.1°, decreased to 29.6° after three slides and then increased to 32.9° and then to 35.8° on the sixth event. The other high initial sample, #8.2 after a minor increase on the third slide, decreased to 27.5° on the sixth slide. The other four samples in the set did not exhibit a decreasing trend as did the two high initial angle samples. These four all had a medium to low value initial angles which increased dramatically (>2°) on the second or third sliding event. They then decreased in angle with additional events except for #11.2 and #14.2 which had increases after the fifth slide of 4.2° and 4.7° respectively.

Five of the samples decreased in angle after cleaning with a range of changes from 0.1° to 5.7°. Only #9.2 exhibited an increase after cleaning of 3.4°.

Sample #8.2 showed a decrease from 27.4° to 23.7° over the remaining six sliding events while #13.2 exhibited a

minor decrease from 30.4° on the seventh slide to approximately 28.5° where the angle seemed to stabilize. The other samples exhibited no obvious trends. Sample #9.2 oscillated over the last six events with the final angle being less than the seventh value but higher than the initial. Sample #10.2 also fluctuated around 31° while #11.2 increased dramatically on the eighth slide. Then it bounced between 29.5° and 31.5° for the last four events. The final sample, #14.2 oscillated greatly but it did not show an overall decrease in the sliding angle.

For set #1, the final angle was less than the initial angle for all cases (excluding results for #6.2) while set for #2, it occurred in 3 out of 6 samples. If the final angle was compared to the second angle measured, the reduction observation occurred in five out of six events.

3.5.2 Discussion

Sample #1, lapped with #80 grit exhibited a decreasing sliding angle trend over the first ten events. Then the values began to fluctuate over the remaining 8 events with an overall decreasing trend being shown. The other rough sample, #2 slid initially at 36.0° and then reduced to 26.8° after 6 slides. Afterwards, the sliding angle value began to oscillate until it stablized around 28.5° with a slightly increasing trend being observed.

Sample #1 decreased in value 7.8° from the initial to the seventh event while #2 decreased 9.2° between the intial

and the sixth event. Then the sliding angles began to oscillate and deviate from the decreasing trend.

This behaviour may have been a result of surface asperities wearing off during the initial sliding events (causing the roughness and the sliding angle to decrease) and then accumulating on the sliding surface. The debris, probably being angular as a result of the shear failure of the asperities, would decrease the frictional resistance if the particles acted as rollers. Conversely, the debris may have increased the resistance as it built-up and increased the interlocking of the surfaces. Hence, the behaviour of the surfaces was dependent upon the shape, the amount and distribution, and the compaction of the gouge material. These multiple surface models will be transitional, a concept first proposed by Coulson (1972).

Sample #4, which had a smoother surface preparation slid initially at an angle of 26.6° which was less than the initial values of the rougher samples, #1 and #2. It displayed a continuous and pronounced decreasing trend with a loss of approximately 7° from the initial to the final value.

The sample prepared with the finest grit, #6 had the second highest initial sliding angle of 35.5°. This value rapidly decreased to a value of 24.0° after 8 events and then the value began to oscillate.

Sample #3 displayed a variation in angles but no definite decreasing trend was observed.

The tilt-test results for these samples were quite variable in the absolute values of the initial through final angles, in the form of the sliding angle-number of sliding events (each event is equal to 20 mm displacement) behaviour (*e.g.* continuously decreasing, oscillating, no obvious trends, *etc.*), and in the amount of sliding angle decrease (if displayed) over its sliding history.

The factors and their significance affecting these results include:

1. The surface preparation method would alter the heights of the surface asperities and hence control the amount of interlocking and/or peak to peak contact. The rougher surface preparation may have produced more detritus upon shearing which would have compacted and increased the surface interlocking whereas smoother surfaces with small amounts of detritus would have a decrease in resistance as the particles acted as rollers.

2. Climatic conditions, especially moisture would alter the results of the tilt-tests as found by Eaton (1986). The tilt-tests were done at different times of the summer and in different buildings. Therefore the moisture content of the air may have been different. This would have affected only the absolute, not the relative values of the sliding angles.

3. Test conditions and procedures may have been responsible for some of the variation between tests.

The first two rough samples tested, #1 and #2 were the first two tests carried out by the author; nonfamiliarity with the tilt-table and recording devices may have had some minor contributions.

Also, in some of the tests the upper slider of the halved sample was completely removed from the tilt-table for roughness measurements; in other cases the slider was simply lifted off the bottom half and returned to its original position in preparation for another sliding event. The excessive handling of the block may have caused alteration to any detritus upon the sliding surface.

When replacing the top slider upon the bottom block, care had to be taken not to apply too much normal force which may have caused more interlocking of the surfaces in contact.

4. Definition of the failure angle was at an arbitrary movement of 1 mm as previously explained. Most of the samples displayed an instantaneous acceleration and sliding which made the selection of the failure angle obvious. Other samples displayed a creeping movement while others exhibited a "step-like" movement on the rotation versus displacement recording. The selection of the failure angle in these cases had to be in accordance

with the criterion set earlier.

5. Slight mineralogical differences between samples would have affected its sliding angle values and its amount of decrease. A sample with more clay content would achieve a lower sliding angle than a more sandy sample where harder and stronger quartz grains would be more prominent at the sliding surface rather than having clay particles being in contact. This factor was thought to be significant and will be looked at in more detail in the next section.

Two sets of samples were prepared for tilt-testing to see if some of the previous factors could be eliminated or minimized;

1. all the samples were prepared at the same time and in a similar manner (with #220 grit),
2. the tilt-tests were all done within a narrow time range (about one week for each set) to minimize moisture content effects,
3. the author was now familiar with all the apparatus and had a definite test procedure to follow,
4. definition of the failure angle remained, and
5. subtle differences in mineralogy would be examined for after testing was completed.

The results from the cleaned tests also exhibited a wide variation. Four of the samples had initial sliding angles between 35° and 30°, five were between 30° and 25°, and one was less than 25°; the range of values was 9.8°. The final angles had a similar range of 9.3° with a distribution of two samples between 35° and 30°, five between 30° and 25°, and two less than 25°.

Only four of the samples exhibited a decrease in angle between the initial and the sixth event. This observation changed to seven out of ten samples when the difference between the first and fifth events were examined. The fifth event seemed to be a limiting amount of displacement which ended the decreasing angle trend. Six sliding events may have caused sufficient debris to build-up on the sliding surface that increased interlocking and hence the strength of the interface.

Seven of the samples decreased in value between the initial and the final angles. The range of reductions were between 1.2° and 9.1° with an average decrease of 4.8°. Three of the samples showed an average increase of 1.9° between the two values. This increase may have been an actual behaviour of the samples or it may have been a result of an abnormally low initial sliding angle such as exhibited by sample #14.2. These results concur with the expected behaviour of the proposed asperity model where surface asperites were worn off with successive sliding events and hence the sliding angle deceased.

The cleaning of the samples after six events lead to a decrease in the angle in eight of the ten samples. The average decrease was 3.3° with a range of 0.1° to 8.3°. An increase in the angle was observed in two of the samples.

The sliding angle behaviour of these samples were quite variable as illustrated by Figures 3.9 and 3.10. Some of the samples initially slid at high angles and then decreased, others started at slightly lower angles but then increased, while others had low initial values which deceased in value thereafter.

A parameter was required which could quantify the decrease (or increase) in sliding angles and which would assist in classifying the behaviours of these samples.

Bishop (1967) proposed the brittleness index I_B, to quantify the post-peak behaviour of soils and rockfill which was defined for drained conditions as:

$$I_B = \frac{\tau_f - \tau_r}{\tau_f} \qquad [3.3]$$

where τ was the resistance to shear on the sliding surface for a given effective stress value and the suffixes f and r related to the failure (peak) and residual states.

Brittleness indices were calculated for the above ten samples. The peak value was assumed to be the initial sliding angle because the roughness would have been the greatest during this event. The final angle was taken to be the residual value as this was when the greatest

displacement of the sample had occurred.

Three methods were investigated in calculating I_s to account for minor variations in the sliding angle results:

I. The first method used the initial point as the peak value and the final angle as the residual value.

II. The peak value was used as previously defined but the residual value was taken as the average angle of the final six sliding events. This was done to negate variations due to debris build-up on the sliding surface. Hence, trends would be filtered-out to use for the residual value since multiple sliding events had occurred on that sample. The decreasing sliding angle trend which tended to increase on the sixth event seems to agree with this observation.

III. The peak value was taken as the average of the first two sliding events and the residual value was taken as the average of the last two. Again, this was another filter method used to identify trends.

The results from this analysis were used to classify the behaviours of the samples into three proposed classes;

1. the initial sliding was medium to high in value which

deceased upon sliding,

2. the initial sliding angle was as above but exhibited an increasing trend upon sliding, and
3. the initial sliding angle was low in value and decreased upon sliding.

Table 3.22 indicates the results of classifying the behaviour of the samples according to the initial sliding angle and the brittleness index.

The first method tested obtained a range of five positive values for I_B for class #1, two negative values for class #2, and two positive and one negative value for class #3. This method differentiated between class #1 and #2 on the basis of the relative values of the initial angle and that the class #2 results were negative (because the final angle was greater than the initial). Class #3 results were selected on the basis of the initial angle values only as the brittleness index results were inconclusive.

The second method had similar results except for all three class #3 results were positive. Therefore the initial angle was greater than the average sliding angle for the last six events. The results could now be classified according to two criteria for all the classes.

The third method determined all the I_B values were greater than 8.3 for classes #1 and #3. Class #2 was defined by values less than 1.3, one positve and one negative. This method also allowed the classes to be selected on the basis of two criteria.

Table 3.22 Brittleness indices and classes of behaviour.

Sample (initial angle)	Brittleness Index (%)		
Method	I	II	III
1. start mid to high and decrease			
3.2 (29.0)	18.1	20.2	10.4
6.2 (31.1)	26.5	24.1	19.2
8.2 (29.7)	23.3	19.1	21.5
10.2 (32.6)	10.3	11.1	10.0
13.2 (31.1)	4.0	3.0	8.3
2. start mid to high and increase			
9.2 (28.7)	-13.2	-8.3	10
11.2 (30.2)	-6.9	-12.3	1.3
3. start mid to low and decrease			
1.2 (25.4)	15.8	16.2	19.7
4.2 (26.2)	8.5	10.8	8.3
14.2 (27.2)	-4.5	3.3	14.2

The brittleness indices and the initial sliding angles allowed the behaviour of these samples to be classified into three different types. This particular series of tests were done with the intention of minimizing the factors responsible for variation in the results. Hence, it was felt that the variation in the results must have been due to differences in the samples.

The samples were all prepared at the same times except for the amount of rock flour in the lapping grit would have increased with time. Additional grit was added to the lapping fluid to try and compensate for dilution effect. Therefore, the surface roughness of the samples varied but probably only on the order of 100 microinches or so. This was not a major difference between the samples.

Subtle differences in mineralogy would have had a pronounced effect on the sliding behaviour of the samples. The two basic components of this sandstone were quartz gains and an argillaceous matrix. This topic is discussed in more detail in the following section.

3.6 Material Characterization

The variation in the sliding behaviour of the samples was thought to be due to differences in the mineralogy. The hypothesis was proposed that the clay content of the samples varied and hence the samples with a higher clay content would exhibit the decreasing behaviour (due to the low residual angle of friction for clays) while class #2 samples

with its increasing behaviour were an indication of samples with a higher quartz content.

Three nondestructive tests were utilized to identify any mineralogical differences;

1. density measurements,
2. sonic velocity measurements, and
3. hardness testing.

Other methods were also available such as thin section analysis, X-ray diffraction, or scanning electron microscopy but were not used because of complexity, time requirements, and cost.

3.6.1 Density Measurements

Set #1 was measured for density differences before tilt-testing, while set #2 was measured afterwards. They were measured at the local room humidity initially by the caliper method. Two lengths were taken in each of the three orthogonal directions, with calipers accurate to 0.05 mm, which were averaged. These three average measurements were used to calculate the bulk volume of the block to an accuracy of 0.01 cm^3. The samples were then weighed on a scale to the nearest 0.01 grams. The density was calculated to one hundredth of a g/cm^3.

The results of the initial density measurements are collected in Table 3.23 for the top and bottom halves in their respective behaviour classes.

Table 3.23 Density results for the different classes of behaviour.

Sample	Density (g/cm^3)	
	Top	Bottom
1. start mid to high and decrease		
3.2 (29.0)	2.56	2.51
6.2 (31.1)	2.60	2.51
8.2 (29.7)	2.56	2.55
10.2 (32.6)	2.47	2.58
13.2 (31.4)	2.57	2.52
2. start mid to high and increase		
9.2 (28.7)	2.58	2.56
11.2 (30.2)	2.63	2.53
3. start mid to low and decrease		
1.2 (25.4)	2.57	2.53
4.2 (26.2)	2.57	2.51
14.2 (27.2)	2.66	2.31

Table 3.24 Densities for different states for samples #6.2, #9.2, and #11.2.

Sample	Atmospheric Condition		Saturated Condition		Dried Condition
	Dens.	M.C.	Dens.	M.C.	Density
T6.2	2.587	0.13%	2.603	0.75%	2.583
B6.2	2.501	0.13%	2.517	0.80%	2.497
T9.2	2.580	0.13%	2.595	0.72%	2.576
B9.2	2.557	0.14%	2.575	0.83%	2.554
T11.2	2.629	0.14%	2.647	0.84%	2.625
B11.2	2.529	0.13%	2.547	0.86%	2.525

If the densities of the samples were ranked in value, both #9.2 and #11.2 from class #2 were third and first heaviest respectively, looking at the top halves. The bottom halves of the two previous samples were second and fourth highest also. This observation tends to agree with the hypothesis that the class #2 behaviour was a result of higher density samples perhaps reflecting a higher quartz content. The other two classes had lower densities between 2.47 and 2.60 g/cm^3.

Three of the samples, #6.2, #9.2, and #11.2 were selected for water absorption and drying tests. After being previously oven dried for some measurements, the samples were left in the testing room to determine the moisture content for the testing room conditions. The samples were then saturated in water for an hour under a suction of 25 KPa. The surface water was wiped from the samples and the saturated weights were taken. Afterwards the samples were dried in a 115° C oven for 24 hours in order to obtain the dried weight. Table 3.24 provides a summary of the densities and the moisture for the various states.

All three samples exhibit a similar moisture content under room atmospheric conditions after the samples had initially been dried. The saturated water contents displayed slightly more variation with #11.2 having the highest average content. The final dried densities only confirmed the previous density rankings with #T11.2 having the highest value.

If a sample contained more clay than another sample, the water absorping capacity and hence the water content should have been higher than a more sandy sample. The results from Table 3.24 do not indicate such a trend. Perhaps the time required to remove air bubbles form the pore spaces and to saturate the clay minerals was greater than the one hour time suggested by the ISRM (1979) standards.

3.6.2 Sonic Measurements

Sonic testing was tried as a method of determining the amount of homogeneity between the samples. A sonic pulse from a tranducer is sent through a sample and received at the other end. The primary wave velocity, V_p is calculated by measuring the arrival time of the P-wave (as the first deviation from the straight line on an oscilloscope) and the length of the sample is known.

Set #1, consisting of four samples was tested in the direction perpendicular to bedding. Table 3.25 provides a summary of the results. The velocities were in the range between 2025 m/s and 2760 m/s with an average velocity of 2373 m/s for the eight samples. The first three samples indicate a correlation with the higher densities having the higher sonic velocity also. The last sample, #6.2 does not fit into this trend though.

The second set of samples were tested parallel to bedding, in both directions on the samples. Unfortunately,

this did not allow a comparison of sonic velocities between sets but perhaps inhomogeneities such as fractures or mineralogical changes within the samples could be identified. The two directions tested were oriented with the direction of sliding during the tilt-tests;

1. direction A which was parallel to sliding and
2. direction B which was perpendicular to the previous direction.

Table 3.26 compiles the results.

Looking at the velocities for the top halves only, the average A velocity was 3903 m/s while for B it was 3992 m/s with standard deviations of comparable value. This suggests that for the whole sample set, no major differences in velocities were exhibited and the set could be regarded as homogeneous.

The individual differences between A and B velocities for the top halves ranged from 90 to 290 m/s with an average value of 192. Sample #T11.2 from class #2 had the largest difference and the second highest average velocity. The other class #2 sample, #T9.2 had the third highest difference of 220 m/s between A and B but had the second lowest average velocity.

The bottom half results indicated an average velocity of 4043 m/s and a B velocity of 4197 m/s, both higher than their top halves' counterparts. The estimated standard deviation were 336 for A and 331 for B which were also greater than their corresponding values for the tops.

Table 3.25 Primary wave velocities (m/s) for set #1.

Sample (& class)	T1.2 (#1) B1.2	T3.2 (#1) B3.2	T4.2 (#3) B4.2	T6.2 (#1) B6.2
Primary wave velocity (m/s) (& density)	2580 (2.57) 2040 (2.53)	2580 (2.56) 2025 (2.51)	2760 (2.57) 2570 (2.51)	2030 (2.60) 2400 (2.51)

Table 3.26 Primary wave velocities (m/s) for set #2.

Sample (& class)	T8.2 (#1) B8.2	T9.2 (#2) B9.2	T10.2 (#1) B10.2	T11.2 (#2) B11.2	T13.2 (#1) B13.2	T14.2 (#3) B14.2
Primary wave velocity (m/s) (& density)	A 3550 B 3640 (2.56) A 3800 B 3810 (2.55)	3670 3890 (2.58) 3840 3930 (2.56)	3840 4080 (2.47) 4070 4010 (2.58)	3990 4280 (2.63) 3700 4650 (2.53)	4130 3950 (2.57) 4260 4310 (2.52)	4240 4110 (2.56) 4590 4470 (2.31)

The differences between the bottom A and B individual values had a range from 10 to 950 m/s with a mean of 213 and an estimated standard deviation value of 363. Five of the values were between 10 and 120 but the difference for #B11.2 was extremely large at 950.

The top half of this sample had also exhibited the largest difference at 290 m/s. Sample #T11.2 was found to have the highest density of the top samples but the bottom half density was only fourth highest in the group.

No correlation was seen to exist between the densities and the various velocities taken. The sonic velocities should have been dependent upon the mechanical properties of the rock but perhaps the changes in mineralogy were too subtle to be identified through sonic testing.

Also the direction of testing relative to bedding would influence the results. The second set of tests were done parallel to bedding and hence only features such as fractures or infilled veinlets which cross-cut the bedding at oblique angles would have been identified. The first set of tests were done perpendicular to the bedding (and the sliding) plane but it is mineralogical variation on the sliding surface and to a very minor depth below that which would control the sliding behaviour. Sonic testing would only identify larger scale features not of interest at this scale of testing.

3.6.3 Hardness Testing

The mineralogy of the sliding surface should be reflected in its hardness.

Various tests are available to determine the hardness of rock samples. The Schmidt Hammer test uses a spring-loaded piston to obtain a rebound value, but it can damage weak specimens. The NCB Cone Indenter measures the resistance to indentation of a hardened tungsten carbide cone. A rock chip, 12 X 12 X 6 mm has to be prepared for the instrument though.

The Shore Scleroscope was finally selected for the hardness testing. A 2.32 gram hammer with a diamond tip is allowed to fall freely through a glass tube 25 cm in length upon the specimen. The rebound height is measured on a scale divided into 140 equal increments which is called the First Shore Rebound Number. Because the indenter tip is quite small, at least 20 readings per sample are required to obtain an average value for the usually nonhomogeneous rock surface according to the ISRM (1978) standards.

The samples, #4.2, #6.2, #9.2, and #11.2 were lapped with #220 grit which deviated from the #1800 grit suggested by the above standard, but the surface was flat. All the specimens were greater than the minimum specified thickness of 1 cm.

The sandstone blocks were sampled on a 5 X 5 point grid with a spacing of 10 mm between adjacent points and with a 5 mm spacing from the sample edge. Twenty-five readings were

taken and the averages and estimated standard deviations are reported in Table 3.27.

No correlation can be seen between the density and the hardness of the samples from this data. It was expected that #T11.2 with the highest density would also have the greatest hardness reflecting, perhaps, the larger amount of quartz content. This relationship was not displayed in the results. Sample #T11.2 had a similar hardness value to that of #T4.2 which had a significantly lower density. Samples #T6.2 and #9.2 display similar hardness and density values; although the hardness values are both greater than the heavier sample #T11.2.

The problem with the Shore Scleroscope is the very small contact area tested by the impact hammer. The average hardness number is then a function of the stochastic process whereby the hammer impacts on a hard quartz grain or on the softer argillaceous matrix. It was hoped that this instrument would be able to detect these subtle changes in mineralogy but such was not the case from these results.

3.7 Conclusions

The following conclusions were determined from the work of this chapter:

1. Roughness measurement and characterization of these smooth ground slider blocks is very difficult and must be done at the appropriate scale.

Table 3.27 Shore Scleroscope results.

Sample	Density	Average Hardness	Standard Deviation
T4.2	2.57	49	6.7
T6.2	2.60	56	6.8
T9.2	2.58	56	7.1
T11.2	2.63	48	6.7

2. The roughness values for these surfaces is dependent upon the length of the sample taken.

3. The distribution of CLA readings from these freshly lapped rock surfaces does not differ significantly from a Gaussian distribution and no directional anisotrophy was indicated.

4. The majority of the statistically valid significant roughness changes were in agreement with the proposed asperity model.

5. The Talysurf measurements fit the proposed Sayles and Thomas (1978) scaling law for roughness at various wavelengths.

6. The tilt-test results for the uncleaned and cleaned samples displayed a decreasing angle trend in the majority of cases. These trends were accompanied with extreme variability in both the absolute sliding values and in the amount of strength decrease with increasing displacement.

7. Bishop's concept of a brittleness index was utilized to classify the sliding angle-displacement behaviours of the sliding blocks.

8. Of the three simple material characterization methods tested, density measurements seemed the most useful to detect subtle changes in mineralogy.

4. Comparison of Case History and Laboratory Results

4.1 Introduction

The previous two chapters dealt with an accelerating movement case history and a series of model tilt-tests. Equation 2.5 had two accelerating power law terms, the first to the power of 2.135 and the second term with an exponent of 25.775. The model tilt-tests, although exhibiting some variability, for the most part displayed a decreasing angle trend with successive sliding events.

The purpose of this chapter is therefore to;

1. introduce a sliding block model which has a decreasing frictional resistance,
2. propose a frictional relationship to which the results of the tilt-testing are to be fit,
3. provide a basis for comparison of the sliding block model to the behaviour of the NO Pit failure, and
4. decide whether the loss of frictional resistance with progressive displacement along the sliding surface is an adequate mechanism to explain these accelerating movements.

4.2 Sliding Block Model

Consider a sliding block of weight W on an inclined plane at an angle of β as illustrated in Figure 4.1. The forces tending to cause acceleration of this block will be the excess of the driving over the resisting forces.

Neglecting water pressure, this can be expressed as:

Accelerating Forces = Driving Forces − Resisting Forces, or

$$ma = W \times \sin\beta - W \times \cos\beta \times \tan f,$$

$$m\frac{d^2x}{dt^2} = mg \times \sin\beta - mg \times \cos\beta \times \tan f, \qquad [4.1]$$

where m = the mass,

x = the displacement,

t = the time,

$\frac{d^2x}{dt^2}$ = the acceleration,

g = gravity, and

f = the frictional resistance (in degrees).

Suppose that f, the frictional resistance, is dependent upon the displacement, x. A function is proposed, where the friction decreases as the displacement progresses (shown in Figure 4.2) of the form:

$$f = A\,(1 - Bx^n) \qquad \text{for } x < 220\text{mm} \qquad [4.2]$$

where A = the initial friction angle, and

B, and n = constants derived from tilt-tests.

The 220 mm limit was the maximum amount of displacement imposed upon the sliding block. Equation 4.2 could be substituted in Equation 4.1 in order to model the accelerating movements.

Looking at Equation 4.2 in reference to the sliding angle results of the tilt-tests, it will be assumed that ϕ_1, the initial sliding angle, is equal to A when no

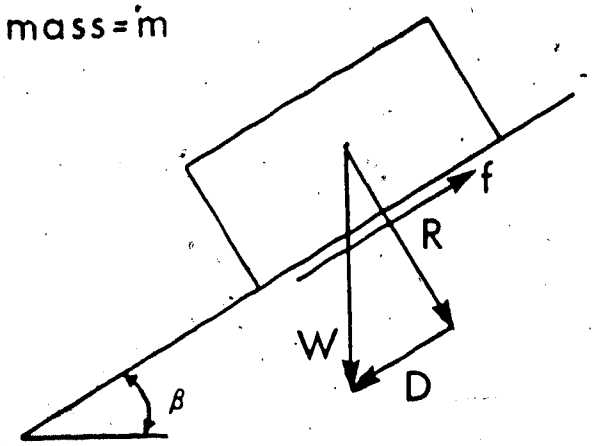

Figure 4.1 Sliding block model on an inclined plane.

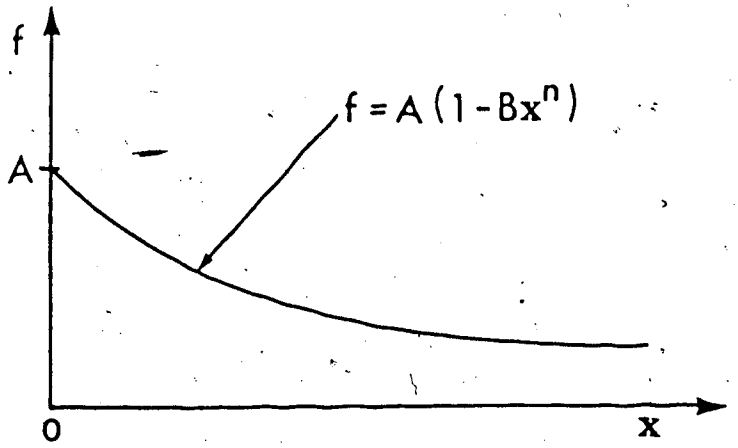

Figure 4.2 Proposed decreasing friction function with progressive displacement.

displacement has occurred (x = 0).

The following formulation is proposed:

Initial Condition $\phi_1 = A$ at $x = 0$;

Relation $\phi_2 = \phi_1 (1-BL^n)$,

where ϕ_2 = the second sliding angle, and

L = the length of displacement during an individual tilt-test which is equal to 20mm.

hence $\phi_1 - \phi_2 = \phi_1 BL,^n$

$\phi_1 - \phi_3 = \phi_1 B(2L),^n$

$\phi_1 - \phi_4 = \phi_1 B(3L).^n$

General Form $\phi_1 - \phi_{i+1} = \phi_1 B(iL)^n$. [4.3]

4.2.1 Regression of Tilt-Test Results

Regression of the tilt-table results was attempted using a modified version of the general form:

$$\log(\phi_1 - \phi_{i+1}) = \log\phi_1 + \log B + n \log(iL) \qquad [4.4]$$

with the friction angle as the indefinite variable. Therefore, the values of the exponent n and the coefficient B could be determined.

The tilt-test results of the class #1 samples from Tables 3.20 and 3.21 for the cleaned data sets were used for the regression analyses. The differences between the initial

sliding angle, ϕ_1 and successive angles, ϕ_i were calculated as were their logarithms. The amount of displacement per sliding event, L (20 ~~mm~~) was accumulated and the logarithms calculated. These displacement values were tabulated along with the sliding angle differences as illustrated for #3.2 in Table 3.1, for example.

The data was input into the public computer program *ST.Package (Computing Services, 1980), which is an interactive statistical graphics package supporting statistical calculations and plotting routines. The polynomial regression feature of the package was utilized to determine the fit of the data to an equation for a straight line with the following form and parameters:

$$Y = b + mX$$

where, in relation to Equation 4.4;

$Y = \log(\phi_1 - \phi_{i+1})$,

$b = \log \phi_1 + \log B$,

$m = n$, and

$X = \log(iL)$.

The logarithmic values were input with the displacement values as the independent variable (X) and the angle differences being the dependent variable (Y).

In some of the samples, especially #13.2, some of the angle difference values were negative (due to later events having higher angle values than the initial). Hence, no

logarithmic values could be obtained at those displacements points. The assumption was made to delete these data points from the regression. This may have lead to some bias in the regression analyses as no increasing trends in the sliding behaviour was accounted for. These samples were selected earlier as having overall decreasing trends by the brittleness indices, although the amount of decrease may have been small.

The regression equations and their correlation coefficients, r, are located in Table 4.2 (the actual plots are located in Appendix G). The equations exhibited a variety of results for both the intercept B, and the slope n; B had a range between 0.000232 and 0.416 while n varies between -0.445 and 1.309. Of the five equations of the class #1 results, four had positive values for n. The negative value obtained for #13.2 was due to the low amount of overall angle decrease (displayed in its very low I_B value) combined with the fluctuating nature of the sliding angle results. The value of n should be positive as this is indicative of an increasing series of difference values.

The fit of the data to the equations was poor in most instances. Two of the five equations showed significant correlation coefficients at the 5% level. Sample #6.2, with n=0.345, showed significant correlation, but with only 7 data points. The other significant sample, #8.2, with an n value of 1.309 displayed a high correlation value of 0.957. The wide variation in values is a result of the poor fit of

Table 4.1 Displacement and sliding angle difference values for the example case of #3.2.

iL (mm)	log(iL)	$\phi_i - \phi_{i+1}$ (degrees)	$\log(\phi_i - \phi_{i+1})$
20	1.3010	5.0	0.6990
40	1.6021	5.4	0.7324
60	1.7782	6.0	0.7782
80	1.9031	5.4	0.7324
100	2.0000	2.7	0.4314
120	2.0792	5.9	0.7709
140	2.1461	9.6	0.9823
160	2.2041	6.4	0.8062
180	2.2553	6.5	0.8129
200	2.3010	5.9	0.7709
220	2.3424	6.0	0.7782

Table 4.2 Regression equations for samples from classes #1 and #3 (#4.2).

Sample Number	# of Points	Regression Equation	B	r	5% r	Sign.
3.2	11	Y=0.5305 + 0.11224X	0.1025	0.280	0.602	No
6.2	7	Y=0.1525 + 0.34538X	0.0413	0.799	0.754	Yes
8.2	10	Y=-2.1445 + 1.3087X	0.0002320	0.957	0.632	Yes
10.2	10	Y=0.0896 + 0.20211X	0.036041	0.371	0.632	No
13.2	6	Y=1.0951 - 0.44503X	0.41642	-0.797	0.811	No
4.2	11	Y=0.3881 + 0.07193X	0.08257	0.142	0.602	No

the data and the different behaviours exhibited by the sliding samples.

Sample #4.2 data, from the third class of sliding behaviours (low initial sliding angle followed by a decreasing strength trend), was also subjected to regression for comparison purposes. The regression equation, displayed in Table 4.2, for this sample determined B to equal 0.08257 and an n value of 0.072, reflecting the small amount of angle decrease from the initial to the final reading, 2.5°. This value compares well with the other small reduction samples such as #10.2 which had a decrease of 3.5° and an n value of 0.202, while #13.2, with an overall decrease of 1.2° displayed a negative slope with n=-0.445.

The recursion formulae proposed by Cruden (1971) was applied in order to smooth the data sets in an attempt to obtain better fitting equations. The sliding angles were smoothed to be continuously decreasing with increasing displacement. An example of the results of this process are displayed in Table 4.3 which can be compared to the original data set. The most noticeable feature is that the number of observations becomes severely reduced.

The resultant equations for the four regressions are located in Table 4.4. The values of B range between 0.000069 and 0.042 while n varies from 0.305 to 1.550. The number of significant correlations increased to three out of four cases, even with the low number of data points per regression, reflecting the influence of smoothing the data

Table 4.3 Original and smoothed data for the example case of #3.2.

Sliding Angle	Cumulative Displacements (mm)	Sliding Angle	Cumulative Displacements (mm)
33.1	0.0	33.1	0.0
28.1	20.0	28.2	54.0
27.7	40.0	27.2	108.0
27.1	60.0	26.2	162.0
27.7	80.0		
30.4	100.0		
27.2	120.0		
23.5	140.0		
26.7	160.0		
26.6	180.0		
27.2	200.0		
27.1	220.0		

Table 4.4 Regression equations for smoothed data.

Sample Number	# of Points	Regression Equation	B	r	5% r	Sign.
3.2	3	Y=0.14565 + 0.3046X	0.04225	0.996	0.997	No
6.2	4	Y=-0.9306 + 0.8618X	0.003411	0.998	0.950	Yes
8.2	7	Y=-2.6696 + 1.5499X	0.000069	0.942	0.754	Yes
10.2	3	Y=-1.0466 + 0.7305X	0.002634	0.999	0.997	Yes

points.

In summary, the n values from significant correlations of class #1 samples ranged from 0.345 to 1.309. After smoothing, the values ranged from 0.731 to 1.550 for n. These values may be regarded as bounds for use in the solution of the modelling equation.

4.2.2 Solution of the Modelling Equation

The sliding block is assumed to be separated from the surrounding rock mass, either by an open cut or by some geological discontinuity and it is also assumed to be initially at rest. After a small initiating acceleration is applied to the block (such as a horizontal acceleration due to blasting or due to rainfall seeping into the separation crack and ultimately draining), the block becomes displaced, the frictional resistance begins to decrease, and the block moves downslope in an accelerating fashion.

The sliding blocks are to be modelled with the equation:

$$\frac{d^2x}{dt^2} = g \times \sin\beta - g \times \cos\beta \times \tan\left[A\ (1-Bx^n)\right]$$

which defines the acceleration in terms of the displacement, x. This second order nonlinear differential equation can be solved by the finite difference method using the following boundary conditions:

1. Initially, the sliding block is at rest,

$$\therefore \text{ at } t=0,\ x=0, \text{ and } \frac{dx}{dt}=0.$$

2. At the next time instant, after some initiating acceleration is applied to the block,

$$\therefore \text{ at } t+\Delta t,\ x>0,\ \frac{dx}{dt}>0, \text{ and } \frac{d^2x}{dt^2}>0.$$

Only a one dimensional finite difference net is required to solve this equation for x and t. The difference in the displacement values over the time-step interval could be used to calculate the velocity. This velocity value could be associated with an average displacement value and a plot of velocity versus displacement could be produced from the modelling equation.

A listing of the finite difference program is located in Appendix H.

For the block to be initially at rest, the driving force must be equal to the resisting force. Hence, the initial friction angle A was made equal to the inclination angle β (equal to 60°, the dip of the NO Pit wall at the crest). The time step variable (T) was kept small, generally less than 0.0005 minutes and the number of points (N) could be adjusted until a sufficient amount of displacement had occurred.

Figure 4.3 displays the finite difference results using the raw coefficient values. For the curve with an n value of 1.309, the velocity changes from 124 mm/min at 1.0 mm displacement to 22860 mm/min after 97.3 mm in a nearly linear fashion. In a relative sense, the equation predicts over two orders of magnitude velocity change in comparison to two orders of displacement change.

The other curve, with n =0.345, displays a pronounced nonlinearity (a concave downwards shape) at lower displacement values and has higher displacement rates than the curve with n =1.309. The velocity ranges from 2180 mm/min to 41510 mm/min after 99.2 mm of displacement, a change of over one magnitude.

Comparing the two curves of Fig. 4.3, as n decreases from 1.3 to 0.3 (and conversely, as B increases from 0.0002 to 0.04), the shape of the function changes from slightly concave upwards to concave downwards, the resultant displacement rates at 1.0 and $\pm$ 100.0 mm is greater, and the relative slope (the number of orders of magnitude velocity change divided by the two orders of displacement change) decreases from over 1 to less than 1.

Figure 4.4 illustrates the predicted velocities using the smoothed coefficients in the finite difference equation. The curve with the higher exponential value, n =1.550, has a slight concave upwards shape with a velocity change from 65.1 mm/min to 20640 mm/min after 97.1 mm displacement. The relative slope of this function is greater than 1.

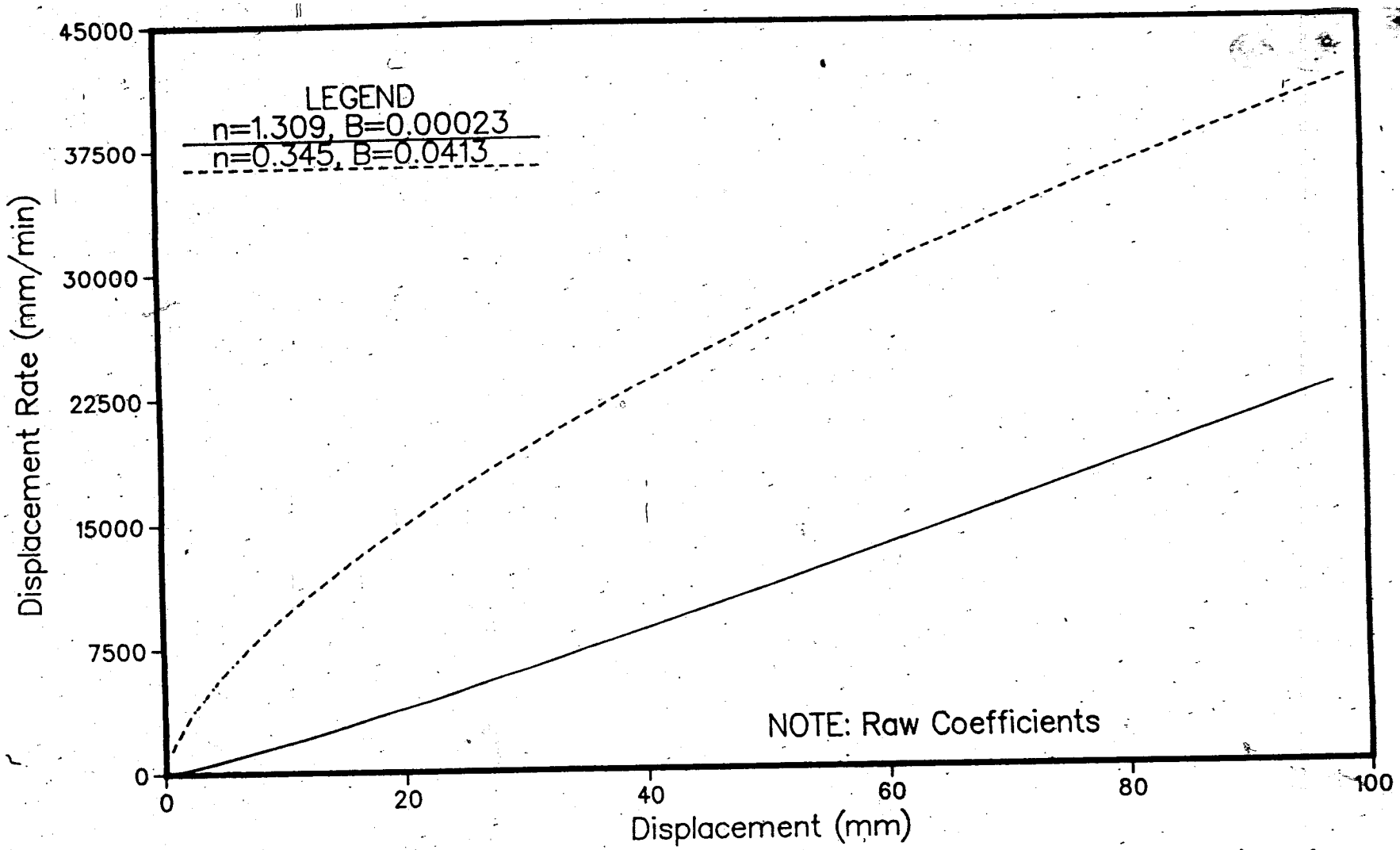

Figure 4.3 Displacement rate versus displacement results from finite difference using the raw coefficients.

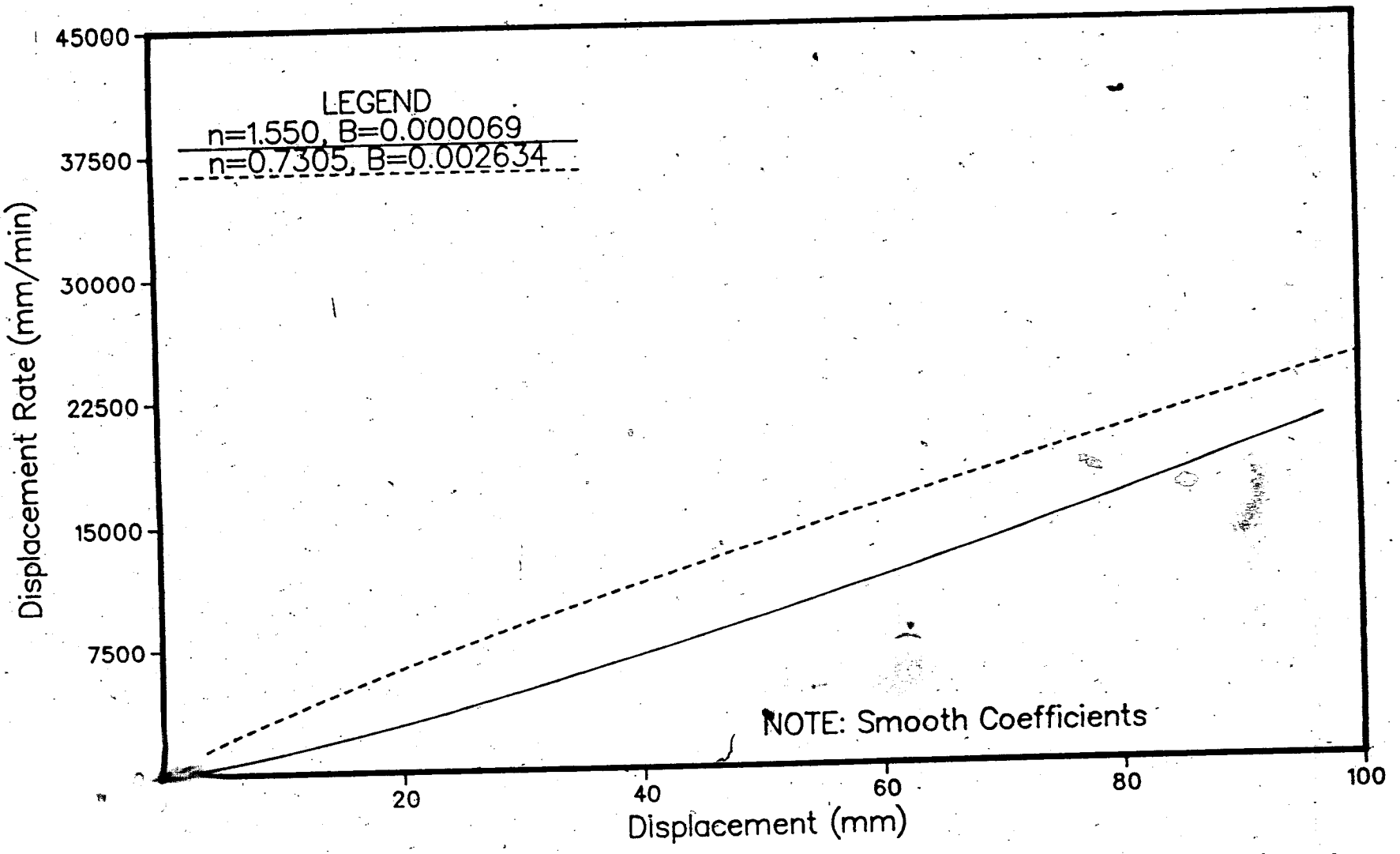

Figure 4.4 Displacement rate versus displacement results from finite difference using the smoothed coefficients.

When n decreases, and B increases as in the second curve on Fig. 4.4, the resultant curve has a slightly concave downwards shape. The displacement rate changes from 487 mm/min to 24410 mm/min after 100 mm of displacement which is a change of over one order of magnitude.

Similar observations as made before can be seen when comparing the two curves; as n decreases, the shape of the resultant function changes to concave downwards, the displacement rates at equivalent amounts of displacement is greater and the relative slope decreases. The two curves of Fig. 4.4 were closer in shape and in displacement rates than the two in Fig. 4.3 presumably due to the two n values being much closer. If these two figures were superimposed upon one another, the curve for n =1.309 would plot down the middle of the two smoothed coefficients curves.

A parametric study was attempted to investigate the influence of each of the variables. The original function chosen was from Fig. 4.3 with n =1.309, B =0.00023, and β =60°. The results are displayed on Fig. 4.5 and can be summarized as follows:

1. As the inclination angle β decreased from 60° to 45°, the displacement rates at 1.0 and $\pm$ 100.0 mm decreased. The function retained its slight concave upwards shape and its relative slope was still greater than 1.

2. As the coefficient B was increased, the resultant

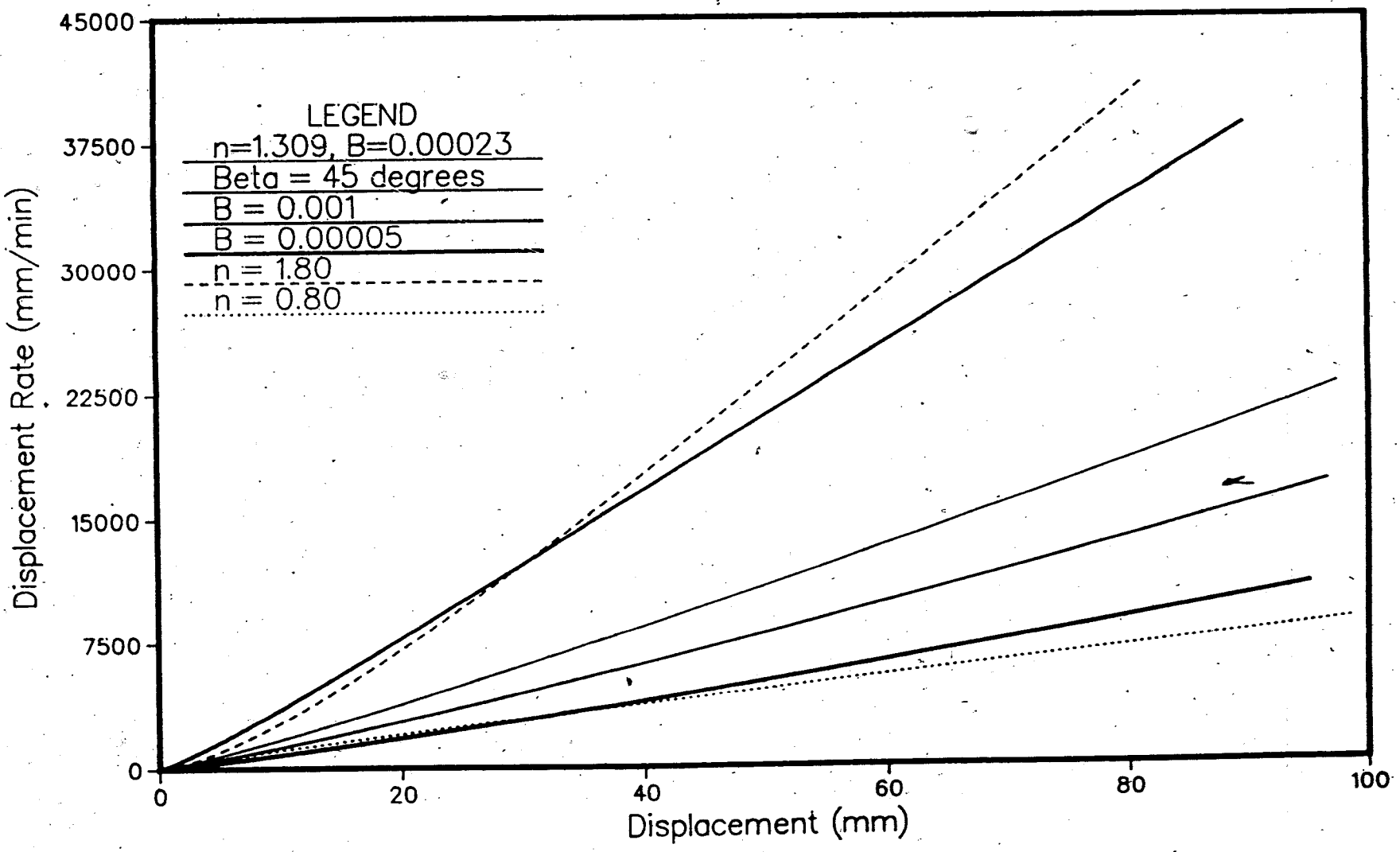

Figure 4.5 Parametric study results with the original curve having n=1.309, B=0.00023, and $\beta=60^{\circ}$.

displacement rates increased with the relative slope remaining greater than 1. When B was decreased from 0.00023 to 0.00005, the velocities decreased but the function still had a relative slope of greater than 1 with its slightly concave upwards shape.

3. More significant changes were found when n was varied. The displacement rate was lower at 1.0 mm and higher at $\pm$ 100 mm when n increased from 1.3 to 1.8. The relative slope was still greater than 1 but the function now displayed a more exaggerated concave upwards form. Conversely, as n decreased to 0.8, the form changed to a nearly linear-to-concave downwards shape with a relative slope less than 1.

The main conclusion was that, while the variables β and B can affect the absolute values of the displacement rates, it is only the exponential term n which can alter the shape and the relative slope of the resultant function. An n value of approximately 0.8 seems to be the boundary between functions which are concave downwards and which are concave upwards.

4.3 Relation of NO Pit Displacement Record

The displacement rate equation of the wall movement from Chapter 2 was in terms of time. In order to compare this equation with the results of previous section where only displacements were measured, it will have to be in

terms of displacement also. Hence, the following derivation is an attempt to alter the equation;

$$\dot{x} = \frac{dx}{dt} = At^B + Ct^D. \qquad [4.5]$$

The two terms in the equation were meant to represent two different creep phases and, arguably, different physical processes occurring in a slope. The first term is dominant at low time values while the second term only becomes significant at larger times. Hence, a simplification of the equation will be made on the grounds that only the process responsible for the acceleration to failure will be considered.

So the derivation considers the second term such that:

$$\dot{x} = Ct^D \qquad [4.6]$$

$$\therefore \quad x = C\int_0^t t^D \, dt = \frac{Ct^{D+1}}{D+1}\Bigg|_0^t$$

$$= \frac{Ct^{D+1}}{D+1} \qquad [4.7]$$

Solving for t:

$$t = \left[(x \times (D+1))/C\right]^{1/(D+1)} \qquad [4.8]$$

Substituting Equation 4.12 into 4.10:

$$\dot{x} = C \left[\left[(x \times (D+1))/A \right]^{1/(D+1)} \right]^{D}$$

$$= C \left[(x \times (D+1))/C \right]^{D/(D+1)}$$

$$= C \left[((x \times (D+1))^{D/(D+1)} \times (1/C)^{D/(D+1)} \right]$$

$$= C \left[((x \times (D+1))^{D/(D+1)} \times C^{-D/(D+1)} \right]$$

$$\dot{x} = C^{1/(D+1)} \left[(x \times (D+1)) \right]^{D/(D+1)} \qquad [4.9]$$

Figure 4.6 illustrates the trend of the function when the constants for the Trun6 data set are placed into it. The function produced is nearly linear (an exponent of 0.963). Over 96 mm displacement (the amount of displacement displayed by the NO Pit wall before failure), the velocity predicted by the equation changed from 0.0126 mm/min to 1.0199 mm/min. This is a velocity change of less than two orders of magnitude over a displacement change of just under two orders, giving the function a relative slope of 1.

4.4 Comparison and Discussion

There would seem to be some difficulty with comparing the results of the sliding block model to that of the accelerating movement. The displacement rates predicted by the sliding block theory using the coefficients from the tilt-tests are much greater than the case history, by several orders of magnitude.

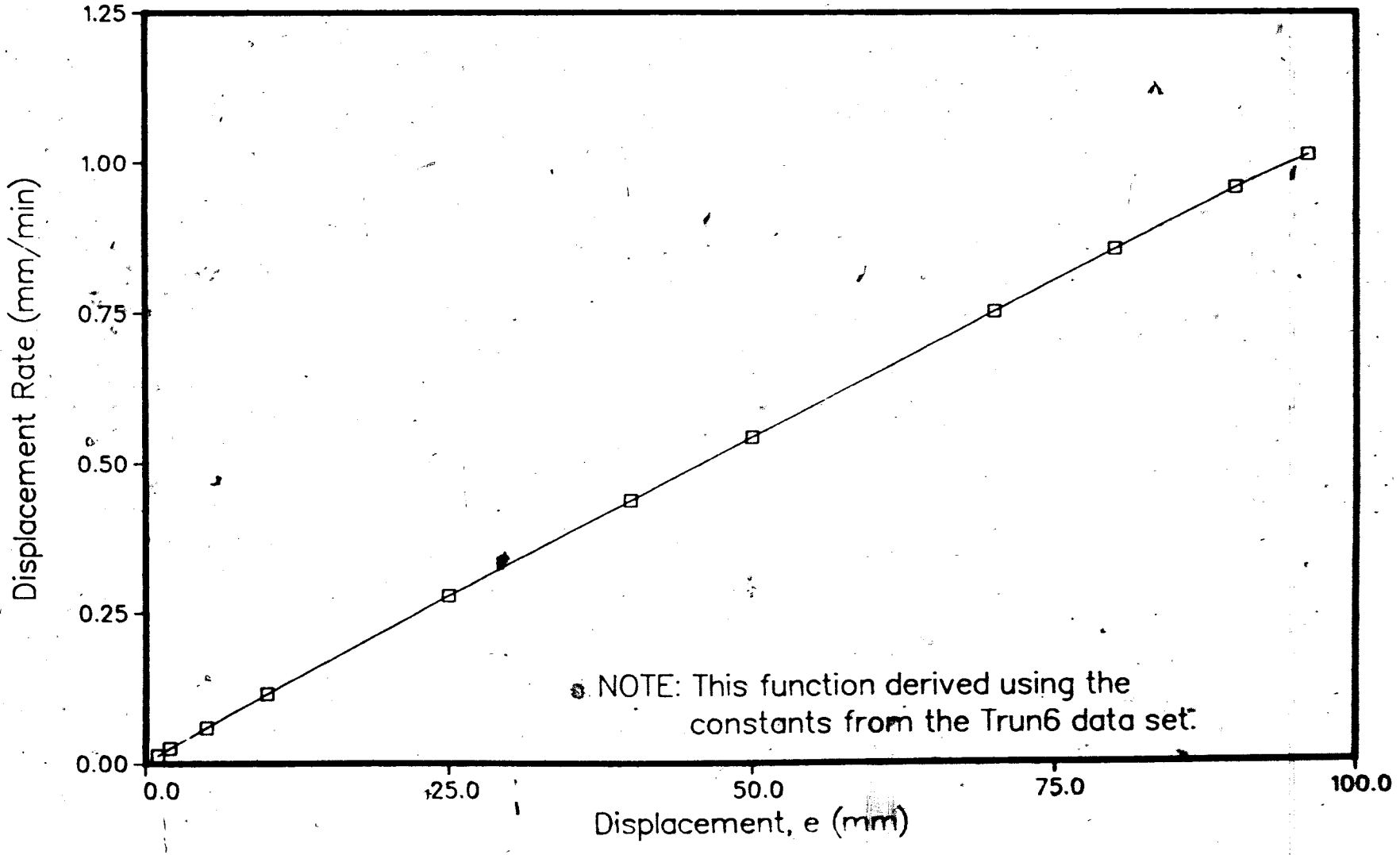

Figure 4.6 Behaviour of the integrated displacement rate equation using the coefficients of the truncated data set, Trun6.

An attempt was made to alter the input coefficients (*e.g.* decrease B) to achieve displacement rates which were of a similar magnitude to those of the case history. Even with values as such, β =45°, B =1×10^{-15}, and n =1.1, the displacement rate was 5.7 mm/min at 1.0 mm displacement, which is still two orders of magnitude off.

The comparison between the two aspects of this study will have to be based on the shapes of the two functions and on the relative slope observations, rather than on the absolute values.

The sliding block theory, for n > 1.3, predicts a displacement rate increase of just over two orders of magnitude in approximately 100 mm of displacement. The NO Pit displacement record displays a similar amount of displacement rate increase over the same displacement range. Hence, this theory, using the friction-displacement parameters from the tilt-tests, appears to qualitatively model the velocity increase behaviour of the accelerating rock movements.

5. Conclusions and Recommendations

5.1 Conclusions

The major conclusions of this study were:

1. The equation;

$$\dot{x} = 0.611\times10^{-8}\ t^{2.14} + 0.221\times10^{-87}\ t^{25.78},$$

was found to be a realistic representation of the accelerating portion of the NO Pit displacement record.

2. The measurement and the characterization of roughness from smooth rock samples is difficult and is dependent upon the sampling length used.

3. The majority of the statistically valid significant roughness changes were in agreement with the hypotheses of the proposed asperity model.

4. The sliding blocks displayed a decreasing sliding angle trend with successive displacement in the majority of the tests. Variability of the results was associated with transitional surface processes in conjunction with subtle differences in mineralogy between samples.

5. Density measurements were found to be the most useful technique to identify these mineralogical differences o the three nondestructive and convenient methods

attempted.

6. The sliding block formulation, using a frictional relationship based on the tilt-test results, appears to qualitatively model the velocity increase behaviour of the accelerating movements. The conclusion to be drawn from this is that the loss of frictional resistance with progressive displacement may be an adequate mechanism to explain accelerating rock movements.

5.2 Recommendations

1. The CPACK program should be altered to allow for three or more accelerating creep phases to be fit to displacement records.

2. More study is required with respect to the fitting ability of CPACK. The fitting procedures of the program may require some modifications to account for the overestimation of the second term exponent.

3. If another Civil Engineering profiler is constructed, it should conform to ANSI B46.1-1978 with regards to a smaller, vertical stylus, a lighter tracking force and other modifications as mentioned in Section 3.4.2.

Interfacing the profiler with a microcomputer would allow for easier data recording and manipulation.

4. Sliding surfaces which decrease in frictional resistance with displacement, require more study as they may be part of the process leading to accelerating rock movements. Surfaces which display an increasing resistance are of less importance as they would not contribute towards a catastrophic rockslide.

5. The sliding block theory may be too simple, especially in assuming the slope inclination angle β to be constant. This angle increases as the slope elevation decreased, until the toe of the slope was overturned. Alteration of the theory could account for a changing slope angle.

6. Rather than a tilt-test, perhaps a creep shear test could be employed to track the frictional resistance of a rock surface with displacement. This relationship could then be substituted into the sliding block model for comparison to the actual movement.

   The creep shear test would allow for the application of normal stress, although at relatively low levels, and for a more continuous deformation of the surface, unlike the tilt-test where the sample was removed after every slide. Problems would still exist,

such as the disturbance of gouge material if the sample was sheared more than one cycle and of course, scale effects.

Bibliography

American National Standard, 1978. Surface Texture: Surface Roughness, Waviness, and Lay. *ANSI B46.1-1978*, 35pp.

Barton, N., 1971. A Relationship Between Joint Roughness and Joint Shear Strength. *International Symposium on Rock Fracture*, Nancy, France. Paper 1-8.

Berry, M.V. and Hannay, J.H., 1978. Discussion of paper by R.S. Sayles and T.R. Thomas, 1978. *Nature*, 273, pp. 573.

Bishop, A.W., 1967. Progressive failure-with special reference to the mechanism causing it, Panel discussion. *Proceedings of the Geotechnical Conference, Oslo*, 2, pp. 142-150.

Brown, S.R., and Scholz, C.H., 1985a. Closure of Random Elastic Surfaces in Contact. *Journal of Geophysical Research*, 90, pp. 5531-5545.

Brown, S.R., and Scholz, C.H., 1985b. Broad Bandwidth Study of the Topography of Natural Rock Surfaces. *Journal of Geophysical Research*, 90, pp. 12575-12582.

Brown, S.R., and Scholz, C.H., 1986. Closure of Rock Joints. *Journal of Geophysical Research*, 91, pp. 4939-4948.

Bruce, I.G., 1978. Field Estimation of Shear Strength in Rock Discontinuities. *Ph.d Thesis*, University of Alberta, 309pp.

Bruce, I.G., Cruden, D.M., and Eaton, T.M., 1986. The Use of A Tilting Table to Determine The Basic Friction Angle of Hard Rock Samples. Paper submitted to the *International Journal of Rock Mechanics and Mining Sciences & Geomechanics Abstracts*. June, 1986, 31pp.

Byerlee, J.D., 1967. Theory of Friction Based on Brittle Fracture. *Journal of Applied Physics*, 38, No.7, pp. 2928-2934.

Casey, R., 1986. Personal communication. Department of Zoology.

Cavers, D.S., 1981. Simple Methods to Analyze Buckling of Rock Slopes. *Rock Mechanics*, 4, pp. 87-104.

Computing Services, University of Alberta, 1980. ST.Package, an Interactive Statistical Graphics Package. R23.0280, 46pp.

Coulson, J.H., 1972. Shear Strength of Flat Surfaces in Rock. *13th U.S. Symposium on Rock Mechanics*, University of Illinois at Urbana, pp. 77-105.

Cruden, D.M., 1971. The form of the Creep Law for Rock Under Uniaxial Compression. *International Journal of Rock Mechanics and Mining Sciences & Geomechanics Abstracts*, 8, pp. 105-126.

Cruden, D.M., Leung, K.,and Masoumzadeh, S., 1986. A Technique for Estimating the Complete Creep Curve of a Sub-bituminous Coal Under Uniaxial Compression. Paper submitted to the *International Journal of Rock Mechanics and Mining Sciences & Geomechanics Abstracts*. 23pp.

Cruden, D.M., and Masoumzadeh, S., 1986a. Models for Monitoring Ground Movements in Coal Mines. Alberta-Canada Energy Research Fund, Report 1985-1986, 20pp. & appendices.

Cruden, D.M.,and Masoumzadeh, S., 1986b. Accelerating Creep of the Slopes of a Coal Mine. Paper submitted to *Rock Mechanics*. 29pp.

Dight, P.M., and Chiu, H.K., 1981. Prediction of Shear Behaviour of Joints Using Profiles. *International Journal of Rock Mechanics and Mining Sciences & Geomechanics Abstracts*, 18, pp. 369-386.

Durbin, J., and Watson, G.S., 1951. Testing for Serial Correlation in Least Squares Regression-II. *Biometrika*, 38, pp.159-176.

Eaton, T.M., 1986. Reconnaissance of Rockslide Hazards in the Kananaskis Country. *M.Sc. Thesis*, University of Alberta, 190pp.

Hald, A., 1952. Statistical Theory with Engineering Applications. John Wiley & Son, Inc., 1952, 783pp.

Hill, K., 1980. Structure and Stratigraphy of the Cadomin Area. *M.Sc. Thesis*, University of Alberta, 191pp.

ISRM, 1978. Suggested Methods for Determining Hardness and Abrasiveness. *International Journal of Rock Mechanics and Mining Sciences & Geomechanics Abstracts*, 15, No. 3, pp.89-97.

ISRM, 1979. Suggested Method for Determining Water Content, Porosity, Density, Absorption, and Related Properties... . *International Journal of Rock Mechanics and Mining Sciences & Geomechanics Abstracts*, 16, No. 2, pp.141-156.

Johnson, R.S., 1982. Slope Stability Monitoring. *4th Canadian Symposium on Mining Surveying and Deformation Measurements*, pp. 363-379.

Karst, R.H., 1985. NO Pit Failure and its Monitoring. Gregg River Resources Inter-office Correspondence, March 15, 1985, 4pp.

Karst, R.H.,and Gould, G.B., 1985. Gregg River Geology: Effect of Mine Planning, Coal Quality, and Economics. Paper presented at the *Second District Five Meeting of the CIM*, Sept., 1985, 21pp.

Kennedy, J.B., and Neville, A.M., 1976. Basic Statistical Methods for Engineers and Scientists. Harper & Row, Publishers, Inc., 490pp.

Krahn, J., 1974. Rock Slope Stability With Emphasis on the Frank Slide. *Ph.d Thesis*, University of Alberta, 244pp.

Krahn, J., and Morgenstern, N.R., 1979. The Ultimate Frictional Resistance of Rock Discontinuities. *International Journal of Rock Mechanics and Mining Sciences & Geomechanics Abstracts*, 16, pp. 127-133.

Langenberg, C.W., and McMechan, M.E., 1985. Lower Cretaceous Group (Revised) of the Northern and North-Central Foothills of Alberta. *Bulletin of Canadian Petroleum Geology*, 33, pp. 1-11.

Mandelbrot, B.B., 1977. Fractals. W.H. Freeman and Company. 365pp.

Mandelbrot, B.B., 1983. The Fractal Geometry of Nature. W.H. Freeman and Company. 468pp.

Masoumzadeh, S., 1983. Letter, with photographs and figures written to Dr. D.M. Cruden, August, 1983.

Masoumzadeh, S., 1985. Accelerating Creep of Slopes of a Coal Mine. *M.Sc. Thesis*, University of Alberta, 189pp.

McLean, J.R., 1982. Lithostratigraphy of the Lower Cretaceous Coal-Bearing Sequence, Foothills of Alberta. *Geological Survey of Canada*, Paper 80-29, 46pp.

Nayak, P.R., 1971. Random Process Model of Rough Surfaces. *Transactions of the American Society of Mechanical Engineers*, 93F, No. 2, pp. 398-407.

Patton, F.D., 1966. Multiple Model of Shear Failure in Rock and Related Materials. *Ph.D. Thesis*, University of Illinois, 282pp.

Peklenik, J., 1967. New Developments in Surface Characterisation and Measurements by Random-Process Analysis. *Proceedings of the Institute of Mechanical Engineers*, 183, pp. 108-126.

Piteau, D.R., 1973. Characterizing and Extrapolating Rock Joint Properties in Engineering Practice. *Rock Mechanics*, Suppl. 2, pp. 5-31.

Reeves, M.J., 1985. Rock Surface Roughness and Frictional Strength. *International Journal of Rock Mechanics and Mining Sciences & Geomechanics Abstracts*, 22, pp. 429-442.

Rengers, N., 1970. Influence of Surface Roughness on the Frictional Properties of Rock Planes. *2nd Congress of the International Society for Rock Mechanics*, Belgrade, 1, pp. 229-234.

Sayles, R.S., and Thomas, T.R., 1978. Surface Topography as a Nonstationary Random Process. *Nature*, 271, pp. 431-434.

Swan, G., 1981. Tribology and the Characterisation of Rock Joints. *22nd U.S. Symposium on Rock Mechanics*, M.I.T., Cambridge, Mass., pp. 432-437.

Swan, G., 1985. Methods of Roughness Analysis For Predicting Rock Joint Behaviour. *International Symposium on the Fundamentals of Rock Joints*, Bjorkliden, Sweden., pp. 153-161.

Swan, G. and Zongqi, S., 1985. Prediction of Shear Behavoiur of Joints Using Profiles. *Rock Mechanics*, 18, pp. 183-212.

Thomas, T.R., and Sayles, R.S., 1975. Random-Process Analysis of the Effect of Waviness on Thermal Contact Resistance. In *Heat Transfer With Thermal Control Applications*, 39, Edited by M.M. Yovanovich, pp. 3-20.

Thomas, T.R., and Sayles, R.S, 1977. Random Process Approach to the Prediction of Joint Stiffness. *Journal of Engineering for Industry*, ASME, 99, pp. 250-256.

Tse, R., 1978. Strength of Rough Rock Surfaces in Shear. *M.Sc. Thesis*, University of Alberta, 164pp.

Tse, R.,and Cruden, D.M., 1979. Estimating Joint Roughness Coefficients. *International Journal of Rock Mechanics and Mining Sciences & Geomechanics Abstracts*, 16, pp. 303-307.

Varnes, D.J., 1982. Time-Dependent Relations in Creep to Failure of Earth Materials. *7th Southeast Asian Geotechnical Conference*, Hong Kong, pp. 107-130.

Whitehouse, D.J., and Archard, J.F., 1970. The Properties of Random Surfaces of Significance in Their Contact. *Proceedings of the Royal Society (London)*, **A316**, No. 1, pp. 97-121.

Zavodni, Z.M., and Broadbent, C.D., 1980. Slope Failure Kinematics. *Bulletin Canadian Institute of Mining*, 73, pp. 69-74.

Zongqi, S., 1985. Asperity Models for Closure and Shear. *International Symposium on the Fundamentals of Rock Joints*, Bjorkliden, Sweden., pp. 173-183.

Appendix A: Flow Charts for CPACK2 Subroutines

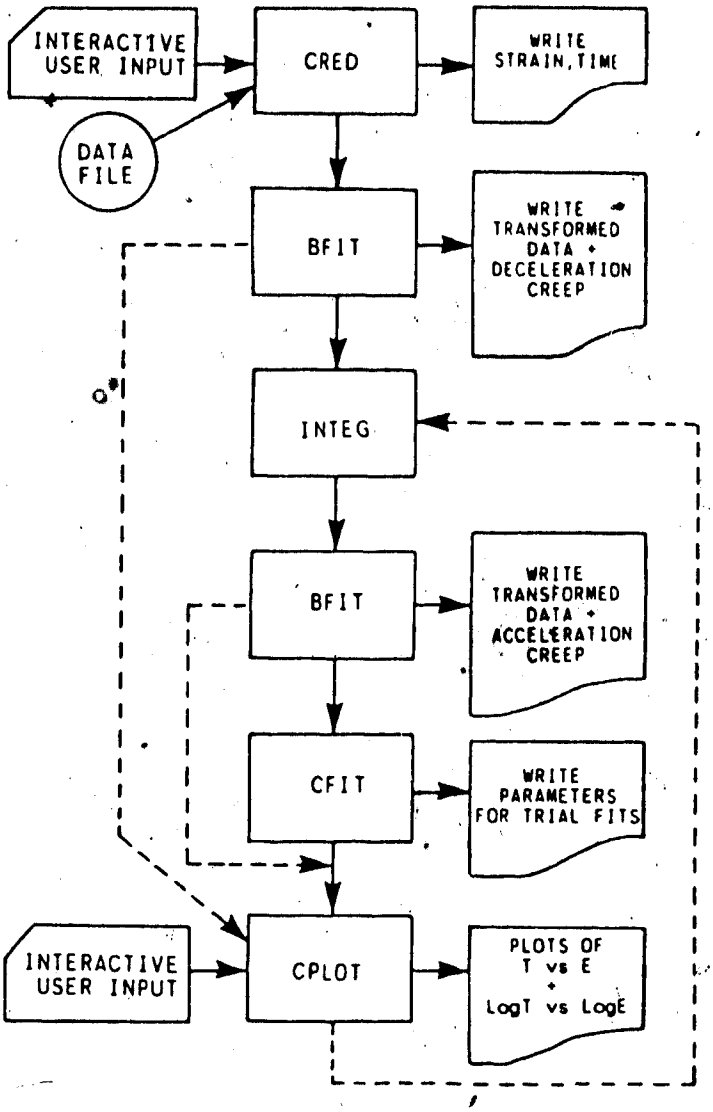

Figure A.1 Flow chart for the main program CPACK2

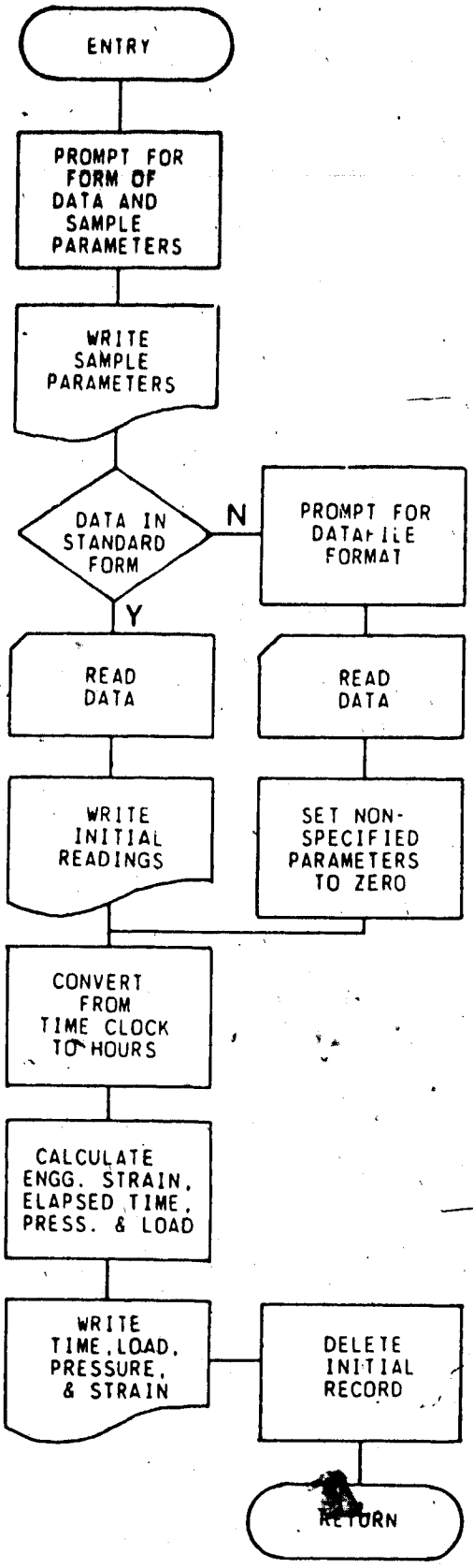

'igure A.2 Flow chart for the subroutine CRED2

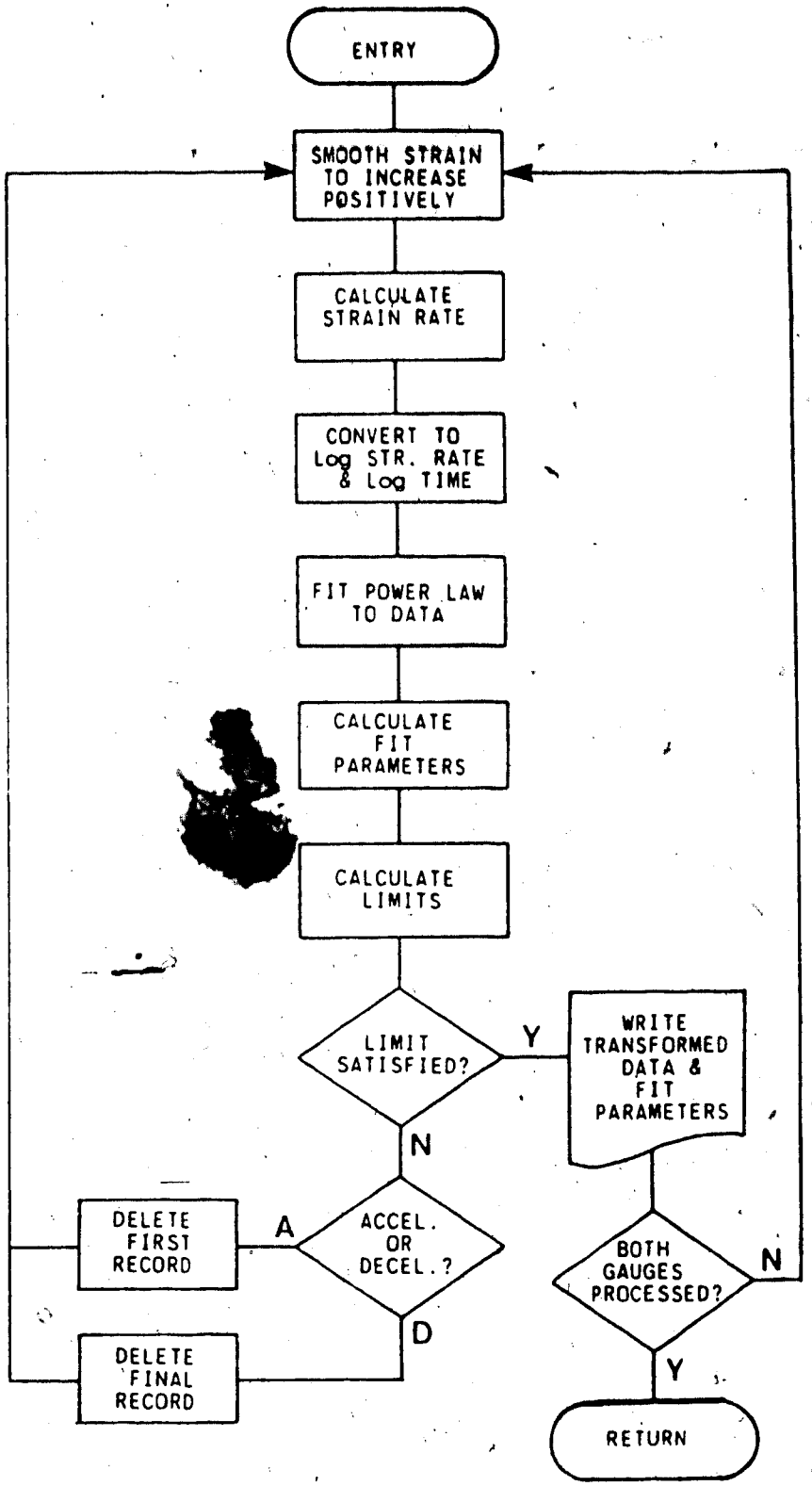

Figure A.3 Flow chart for the subroutine BFIT2

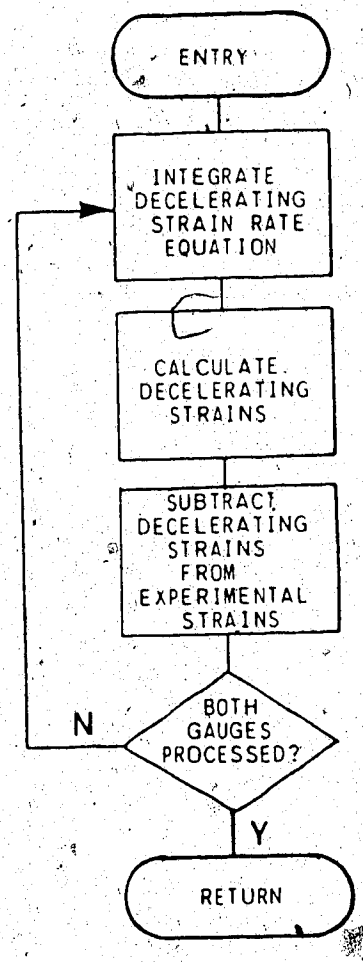

igure A.4 Flow chart for the subroutine INTEG2

Appendix B: Listing of CPACK2 Subroutines

```
      CCCCCCCCCCCCCCCCCCCCCCCCCCCCCCCCCCCCCCCCCCCCCCCCCCCCCCCCCCCCCCCCCCCC
      CCCCCCCCCCCCCCCCCCCCCCCCCCCCCCCCCCCCCCCCCCCCCCCCCCCCCCCCCCCCCCCCCCC
      CCCCC                                                          CCCCC
      CCCCC                      PROGRAM CPACK2                      CCCCC
      CCCCC                        IN MAIN2                          CCCCC
      CCCCC          A PACKAGE OF PROGRAMS THAT WILL REDUCE          CCCCC
      CCCCC          CREEP DATA, AND FIT A POWER LAW TO IT,          CCCCC
      CCCCC          SEPARATING THE DATA INTO ACCELERATING           CCCCC
      CCCCC                AND DECELERATING CREEP                    CCCCC
      CCCCC                                                          CCCCC
      CCCCCCCCCCCCCCCCCCCCCCCCCCCCCCCCCCCCCCCCCCCCCCCCCCCCCCCCCCCCCCCCCCCC
      CCCCCCCCCCCCCCCCCCCCCCCCCCCCCCCCCCCCCCCCCCCCCCCCCCCCCCCCCCCCCCCCCCC
C
C*****************************************************************
C  THIS VERSION WAS MODIFIED AND DOCUMENTED BY J.W.
C  CASSIE IN APRIL, 1987.
C*****************************************************************
C  THE PROGRAM IS INVOKED BY THE COMMAND:
C  $RUN CPACK2+CIVE:GRAPH+*IG+*PLOTLIB 4=INPUT 7=OUTPUT T=5S
C  THE PLOT (IF REQUIRED) WILL BE LOCATED IN THE FILE -PDF.
C  A HARDCOPY OF THE PLOT MAY BE OBTAINED BY RUNNING:
C  $RUN *CALCOMPQ PAR=FILE=-PDF T=2s
C*****************************************************************
C                      VARIABLE DOCUMENTATION
C  BBO: CONTAINS INTERCEPTS OF FITTED LINES.
C  BB1: CONTAINS SLOPES OF FITTED LINES.
C  ELPST: ELAPSED TIME IN HOURS COMPUTED BY SUBTRACTING.
C         THE TIME OF THE FIRST DEFLECTION READING.
C  TT: AS ABOVE BUT WITH THE FIRST RECORD DELETED.
C  ESTRN1: ENGINEERING STRAIN FOR LVDT#1.
C  E1:  AS ABOVE BUT WITH FIRST RECORD DELETED.
C  ESTRN2: ENGINEERING STRAIN FOR LVDT#2.
C  E2:  AS ABOVE BUT WITH THE FIRST RECORD DELETED.
C  LT:  CONTAINS THE LOGS OF TIME AS CALCULATED IN BFIT2.
C  LE:  CONTAINS THE LOGS OF STRAIN RATE AS CALCULATED IN BFIT2.
C  W1:  CONTAINS THE ABOVE RECORD WEIGHTINGS AS CALCULATED
C       IN BFIT2.
C  NC1:  NUMBER OF RECORDS IN THE ABOVE ARRAYS.
C  EEM1:  INTERMEDIATE VALUE USED IN CALCULATING THE
C         SLOPE SIGNIFICANCE STATISTIC.
C  TP:  TIMES OF THE TRANSFORMED DATA.
C  ERP:  STRAIN RATES OF THE TRANSFORMED DATA.
C  ANSM1:  INTERACTIVE RESPONSE THAT INDICATES WHETHER
C          TO PLOT THE DECELERATING DATA BEFORE THE
C          ACCELERATING DATA IS FIT.
C  ANSM3:  INTERACTIVE RESPONSE THAT INDICATES WHETHER OR NOT
C          TO USE CFIT.
C  K:  NUMBER OF THE FIRST RECORD USED IN THE FIT OF THE
C      ACCELERATING CREEP DATA.
C  L:  NUMBER TO INDICATE THE DECELERATING (L=1) AND THE
C      ACCELERATING (L=2) PHASES.
C  NFIT:  NUMBER USED TO INDICATE WHETHER ALL THE DATA
C         HAS BEEN FIT TO THE DECELERATING CURVE.
C*****************************************************************
C
      INTEGER N(1000),NC1(2)
      REAL BBO(2,2),BB1(2,2),E1(1000),E2(1000),TT(1000),
     *     ELPST(1000),ESTRN1(1000),ESTRN2(1000),LT(2,1000),
```

```
     *     LE(2,1000),W1(2,1000),EEM1(2),TP(1000),ERP(1000)
C
      CALL CRED (DIAM,XLEN,NRR,E1,E2,TT,XANS1,IANS3,
     *           ITN1,ITN2,ELPST,ESTRN1,ESTRN2)
C
      REAL Y/'Y'/
      DATA MMM/1/
      OOO=0
      OO=0
      K=0
      L=1
      NFIT=0
      WRITE(7,100)
  100 FORMAT(//20('*'),' FIT OF DECELERATING CREEP DATA TO ',
     *'POWER LAW ',20('*'))
C
C     INTERACTIVE PROMPT
C
      WRITE(6,200)
  200 FORMAT('WOULD YOU LIKE THE DECELERATING CREEP DATA'/
     *'PLOTTED BEFORE THE PROGRAM ATTEMPTS TO ISOLATE'/
     *'ACCELERATING CREEP?')
      READ(5,300) ANSM1
  300 FORMAT(A1)
      ANSM2=0.
C
      WRITE(6,202)
  202 FORMAT('WOULD YOU LIKE THE PROGRAM TO EXAMINE THE '/
     *'ACCELERATING DATA FOR AN OPTIMUM FIT?')
      READ(5,302) ANSM3
  302 FORMAT(A1)
C
C*************************************************************
C  FIRST CALL TO BFIT TO FIT THE DATA TO A DECELERATING
C  (OR TO AN ACCELERATING) LAW. THE VALUE OF THE PARAMETER
C  "L" IS EQUAL TO 1.
C*************************************************************
C
      CALL BFIT (NRR,E1,E2,TT,L,N,BBO,BB1,XANS1,IANS3,LT,LE,
     *           W1,EEM1,NC1,K,OO,FF,DW,MMM,ANSM3,NRF,NFIT,OOO,BCD,B1D,
     *           TP,ERP,NCP)
C
C*************************************************************
C  IF YOU WISH TO PLOT THE DECELERATING CREEP DATA, THE
C  PROGRAM WILL NOW GO TO SUBROUTINE CPLOT.
C*************************************************************
C
      IF(ANSM1.EQ.Y) GO TO 60
C
C*************************************************************
C  THE PROGRAM NOW GOES TO INTEG TO INTEGRATE THE POWER LAW
C  DETERMINED IN THE FIRST CALL TO BFIT ACCORDING TO THE
C  PROCEDURE OUTLINED IN THE PAPER, CRUDEN (1971),
C  "THE RECOVERY OF PENNANT SANDSTONE FROM A UNIAXIAL
C  COMPRESSIVE LOAD", CAN. J. E. SC., VOL.8,PP.518-522.
C  INTEG THEN SUBTRACTS THESE DECELERATING STRAINS FROM
C  THE OBSERVED STAINS TO GET THE ACCELERATING STRAINS
C  WHICH ARE PASSED ONTO BFIT.
```

```
106   C*****************************************************************
107   C
108      50 CALL INTEG(E1,E2,BBO,BB1,NRR,TT,L,XANS1,IANS3)
109   C
110   C*****************************************************************
111   C  THE ACCELERATING CREEP DATA WILL NOW BE FIT TO A POWER
112   C  LAW ON THE SECOND CALL TO BFIT. NOTICE THE VALUE OF
113   C  "L" NOW IS 2.
114   C*****************************************************************
115   C
116         L=2
117         WRITE(7,101)
118     101 FORMAT(//20('*'),' FIT OF ACCELERATING CREEP DATA TO ',
119        *'POWER LAW ',20('*'))
120      55 OOO=1.0
121         CALL BFIT (NRR,E1,E2,TT,L,N,BBO,BB1,XANS1,IANS3,LT,LE,
122        *        W1,EEM1,NC1,K,OO,FF,DW,MMM,ANSM3,NRF,NFIT,OOO,BOD,B1D,
123        *        TP,ERP,NCP)
124   C
125         IF(ANSM3.NE.Y) GO TO 60
126         IF(OO.EQ.2) GO TO 60
127   C
128   C*****************************************************************
129   C  CFIT IS NOW CALLED TO IDENTIFY THE BEST FIT OF THE
130   C  ACCELERATING CREEP AND THE BEST OVERALL FIT.
131   C*****************************************************************
132   C
133         CALL CFIT(EEM1,LT,LE,W1,BBO,BB1,NC1,K,OO,FF,DW,MMM,NRR,NRF,BOD
134        *        ,B1D)
135   C
136   C*****************************************************************
137   C  THE NUMBER OF THE FIRST RECORD USED IN THE FIT OF
138   C  THE ACCELERATING DATA IS INCREMENTED POSITIVELY TO
139   C  DECREASE THE SIZE OF THE DATA SET BEING FIT. THEN THE
140   C  PROGRAM RETURNS TO BFIT (GO TO 55) TO FIT THE NEW
141   C  REDUCED DATA SET.
142   C*****************************************************************
143   C
144         K=K+1
145         GO TO 55
146   C
147      60 CALL CPLOT(ESTRN1,ESTRN2,ELPST,BBO,BB1,NRR,
148        *   TP,ERP,NCP,ITN1,ITN2,XANS1,IANS3,ANSM1,ANSM2)
149   C
150         IF(ANSM1.NE.Y) GO TO 999
151         IF(NFIT.EQ.1) GO TO 555
152   C
153   C     INTERACTIVE PROMPT
154   C
155         WRITE(6,201)
156     201 FORMAT('WOULD YOU LIKE THE PROGRAM TO ATTEMPT TO FIT'/
157        *'YOUR DATA TO ACCELERATING CREEP AS WELL?')
158         READ(5,301) ANSM2
159     301 FORMAT(A1)
160         IF(ANSM2.NE.Y) GO TO 999
161         ANSM1=0.
162         GO TO 50
163     555 WRITE(6,401)
```

```
  164       401 FORMAT('THE ENTIRE SET OF DATA IS FITTED TO THE'/
  165          *'DECELERATING CREEP')
  166       999 STOP
  167           END
```

```
CCCCCCCCCCCCCCCCCCCCCCCCCCCCCCCCCCCCCCCCCCCCCCCCCCCCCCCCCCCCCCCC
CCCCCCCCCCCCCCCCCCCCCCCCCCCCCCCCCCCCCCCCCCCCCCCCCCCCCCCCCCCCCCCC
CCCCC                                                      CCCCC
CCCCC                  SUBROUTINE CRED2                    CCCCC
CCCCC              REDUCES EXPERIMENTAL DATA               CCCCC
CCCCC       IT ALSO WRITES SAMPLE PARAMETRES, INITIAL      CCCCC
CCCCC       READINGS, AND A TABLE OF TIMES AND STRAINS.    CCCCC
CCCCC                                                      CCCCC
CCCCCCCCCCCCCCCCCCCCCCCCCCCCCCCCCCCCCCCCCCCCCCCCCCCCCCCCCCCCCCCC
CCCCCCCCCCCCCCCCCCCCCCCCCCCCCCCCCCCCCCCCCCCCCCCCCCCCCCCCCCCCCCCC
C
C*****************************************************************
C                        VARIABLE DOCUMENTATION
C  DIAM:  SAMPLE DIAMETER.
C  XLEN:  SAMPLE LENGTH.
C  NRR: NUMBER OF RECORDS PASSED ONTO BFIT.
C       NRR=N-1 IN ORDER TO DELETE FIRST RECORD.
C  XANS1:  INTERACTIVE RESPONSE RE: IS DATA IN THE
C          STANDARD FORM?
C  IANS3:  NUMBER OF STRAIN GAUGES
C  ITN1 & ITN2:  INPUT TEST NUMBER. USED AS OUTPUT IN BFIT
C                & CPLOT AS IDENTIFICATION.
C  ISAM1 & ISAM2:  INPUT SAMPLE NUMBER. USED AS ABOVE.
C  NV:  NUMBER OF ELEMENTS ON EACH INPUT LINE.
C  XNAME:  ARRAY CONTAINING THE INPUT FORMAT OF NONSTANDARD
C          DATA. IT IS AN INTERACTVE RESPONSE.
C  VAR:  INTERMEDIATE VARIABLE USED FOR STORAGE WHILE
C        SORTING OF THE NONSTANDARD DATA OCCURS.
C  IMN:  INPUT TIME READINGS IN MONTHS.
C  IDY:  INPUT TIME READINGS IN DAYS.
C  IHR:  INPUT TIME READINGS IN HOURS.
C  IMI:  INPUT TIME READINGS IN MINUTES.
C  ISE:  INPUT TIME READINGS IN SECONDS.
C  RDEF1: DEFLECTION READINGS FOR LVDT#1.
C  RDEF2: DEFLECTION READINGS FOR LVDT#2.
C  VDEF1 & VDEF2:  VERTICAL DEFLECTION COMPUTED BY SUBTRACTING
C                  THE INITIAL RDEF RECORD.
C  FACT:  LVDT CALIBRATION FACTOR.
C  ESTRN: ENGINEERING MICROSTRAINS COMPUTED FROM;
C         ESTRN(J)=(VDEF(J)/XLEN)*1,000,000*FACT.
C  RCELLP:  CELL PRESSURE.
C  RILOAD: INTIAL LOAD ON SAMPLE.
C  ALVDT1 & BLVDT2: INITIAL READINGS FOR LVDTS #1 & #2
C                   RESPECTIVELY.
C*******************************************************************
C
      SUBROUTINE CRED (DIAM,XLEN,NRR,E1,E2,TT,XANS1,IANS3,
     *ITN1,ITN2,ELPST,ESTRN1,ESTRN2)
C
      REAL RLOAD(1000),RDEF1(1000),RDEF2(1000),IMN(1000),
     *     TIME(1000),VDEF1(1000),VDEF2(1000),IDY(1000),
     *     ESTRN2(1000),RCELLP(1000),ESTRN1(1000),
     *     IHR(1000),IMI(1000),ISE(1000),ELPST(1000),
     *     E1(1000),E2(1000),TT(1000),VAR(12,1000),XNAME(12)
C
C
      REAL Y/'Y'/,H/'H'/,M/'M'/,TH/'TH,'/,R1/'R1,'/,R2/'R2,'/,
     *DU/'DU,'/,TM/'TM,'/,TN/'TN,'/,TD/'TD,'/,TS/'TS,'/,FACT/1.0/,
```

```
      *YYY/'y'/,NNN/'n'/
C
C*****************************************************************
C  INITIALIZE ALL THE TIME ARRAYS WITH REAL VALUE ZEROS.
C*****************************************************************
C
      DATA IMN/1000*0./,IDY/1000*0./,IHR/1000*0./,
     *     IMI/1000*0./,ISE/1000*0./
C
C*****************************************************************
C  PROMPTS FOR INPUT PARAMETERS.
C*****************************************************************
C
      WRITE(6,150)
  150 FORMAT('THIS PROGRAM ACCEPTS DATA IN THE FOLLOWING FORMAT:'/
     *'LABEL,TIME CLOCK,3 COUNTERS,LOAD,CELL PRESSURE,DEF.1,DEF.2'
     */'IS YOUR DATA IN THIS FORM? (Y,N)')
   11 READ(5,250)XANS1
  250 FORMAT(A1)
      IF(XANS1.NE.YYY.AND.XANS1.NE.NNN) GO TO 12
      WRITE(6,261)
  261 FORMAT('*ERROR* ALL RESPONSES MUST BE IN UPPER CASE LETTERS.'
     */'RE-ENTER RESPONSE TO PREVIOUS QUESTION:')
      GO TO 11
   12 WRITE(6,151)
  151 FORMAT('DO YOU HAVE AN LVDT CALIBRATION FACTOR?')
      READ(5,251)XANS2
  251 FORMAT(A1)
      IF(XANS2.NE.Y) GO TO 199
      WRITE(6,160)
  160 FORMAT('INPUT THE LVDT CALIBRATION FACTOR (MULTIPLIER):')
      READ(5,260)FACT
  260 FORMAT(F10.5)
  199 WRITE(6,152)
  152 FORMAT('INPUT DIAMETER(MM),LENGTH(MM),AND WEIGHT(GM),'
     */'SEPARATED BY COMMAS:')
      READ(5,252)DIAM,XLEN,WEIG
  252 FORMAT(3F10.3)
      WRITE(6,153)
  153 FORMAT('INPUT SAMPLE NUMBER (8 CHARACTER MAX.):')
      READ(5,253)ISAM1,ISAM2
  253 FORMAT(2A4)
      WRITE(6,154)
  154 FORMAT('INPUT TEST NUMBER (8 CHARACTER MAX.):')
      READ(5,254)ITN1,ITN2
  254 FORMAT(2A4)
C
C*****************************************************************
C  WRITE INPUT PARAMETERS.
C*****************************************************************
C
      WRITE(7,20)ITN1,ITN2
   20 FORMAT(/,'TEST NUMBER     = ',2A4)
      WRITE(7,21) ISAM1,ISAM2
   21 FORMAT(/,'SAMPLE NUMBER   = ',2A4)
      WRITE(7,22) XLEN,DIAM,WEIG
   22 FORMAT(/,'SAMPLE LENGTH   = ',F10.3,' mm',
     *       /,'SAMPLE DIAMETER = ',F10.3,' mm',
```

```
117          *       /,'SAMPLE WEIGHT   = ',F10.3,' gm')
118           IF(XANS1.EQ.Y) GO TO 23
119     C
120     C*****************************************************************
121     C  PROMPT FOR INPUT FORMAT (NON-STANDARD).
122     C*****************************************************************
123     C
124           WRITE(6,155)
125       155 FORMAT('INPUT NUMBER OF ELEMENTS IN EACH LINE (+ COMMA):')
126           READ(5,255)NV
127       255 FORMAT(I2)
128           WRITE(6,156)
129       156 FORMAT('INPUT NUMBER OF STRAIN GAUGES (LVDTS);(1 OR 2):')
130           READ(5,256)IANS3
131       256 FORMAT(I1)
132           WRITE(6,157)
133       157 FORMAT(5X,'THE ONLY DATA THAT THIS PROGRAM REQUIRES FOR INPUT'
134          */'IN DEVICE 4, IS TIME AND DISPLACEMENT. LIST THE ELEMENTS IN'/
135          *'ONE LINE OF YOUR INPUT DATA, IN PROPER ORDER, USING "R1"'/
136          *'FOR THE FIRST STRAIN GAUGE READING, "R2" FOR THE SECOND (IF'/
137          *'THERE IS ONE), AND "TN","TD","TH","TM","TS", FOR THE TIME'/
138          *'IN: MONTHS,DAYS,HOURS,MINUTES,AND SECONDS (YOU MAY HAVE ONLY'
139          */'ONE OF THESE TIME PARAMETERS). USE THE DUMMY VARIABLE "DU"'/
140          *'FOR ALL OTHER VALUES. (SEPARATE THE ELEMENTS WITH COMMAS)')
141     C
142     C*****************************************************************
143     C  READS NON-STANDARD DATA FORMAT AND THE DATA FROM DEVICE 4
144     C  UNTIL THE END OF THE INPUT FILE IS REACHED.
145     C*****************************************************************
146     C
147           READ(5,257)(XNAME(J),J=1,NV)
148       257 FORMAT(12A3)
149     C
150     C*****************************************************************
151     C  FOR SOME REASON L IS DEFINED AGAIN AS L=1 WHEN IT HAS BEEN
152     C  PREVIOUSLY DEFINED AS THE ABOVE VALUE AT IS#0009 IN MAIN2.
153     C*****************************************************************
154     C
155           L=0
156         5 L=L+1
157           READ(4,300,END=8)(VAR(K,L),K=1,NV)
158           N=L
159           GO TO 5
160         8 K=0
161         9 K=K+1
162           IF(XNAME(K).NE.TH) GO TO 6
163           DO 16 L=1,N
164        16 IHR(L)=VAR(K,L)
165           GO TO 39
166         6 IF(XNAME(K).NE.R1) GO TO 7
167           DO 17 L=1,N
168        17 RDEF1(L)=VAR(K,L)
169           GO TO 39
170         7 IF(XNAME(K).NE.R2) GO TO 31
171           DO 18 L=1,N
172        18 RDEF2(L)=VAR(K,L)
173           GO TO 39
174        31 IF(XNAME(K).NE.TN) GO TO 32
```

```
      DO 42 L=1,N
   42 IMN(L)=VAR(K,L)
      GO TO 39
   32 IF(XNAME(K).NE.TD) GO TO 33
      DO 43 L=1,N
   43 IDY(L)=VAR(K,L)
      GO TO 39
   33 IF(XNAME(K).NE.TH) GO TO 34
      DO 44 L=1,N
   44 IHR(L)=VAR(K,L)
      GO TO 39
   34 IF(XNAME(K).NE.TM) GO TO 35
      DO 45 L=1,N
   45 IMI(L)=VAR(K,L)
      GO TO 39
   35 IF(XNAME(K).NE.TS) GO TO 39
      DO 46 L=1,N
   46 ISE(L)=VAR(K,L)
   39 IF(K.LT.NV) GO TO 9
  300 FORMAT(12G20)
C
C*****************************************************************************
C  INITIALIZES SOME OF THE DEFLECTION VARIABLES.
C*****************************************************************************
C
   56 DO 51 K=1,N
      RLOAD(K)=0.0
   51 RCELLP(K)=0.0
      IF(IANS3.EQ.2) GO TO 55
      DO 52 K=1,N
   52 RDEF2(K)=0.0
      GO TO 55
C
C*****************************************************************************
C  READS STANDARD FORMAT DATA.
C*****************************************************************************
C
   23 J=0
      WRITE(6,158)
  158 FORMAT('DOES YOUR TIME CLOCK HAVE A DOUBLE DIGIT MONTH?')
      READ(5,258)XANS3
  258 FORMAT(A1)
   30 J=J+1
      IF(XANS3.EQ.Y)GO TO 47
      READ(4,40,END=55) IMN(J),IDY(J),IHR(J),IMI(J),ISE(J),ICTR,
     *          I1,I0,RLOAD(J),RCELLP(J),RDEF1(J),RDEF2(J)
   40 FORMAT(7X,5G2,1X,I5,2I3,4G20)
      GO TO 48
   47 READ(4,49,END=55) IMN(J),IDY(J),IHR(J),IMI(J),ISE(J),ICTR,
     *          I1,I0,RLOAD(J),RCELLP(J),RDEF1(J),RDEF2(J)
   49 FORMAT(8X,5G2,1X,I5,2I3,4G20)
   48 N=J
      GO TO 30
C
C*****************************************************************************
C  ASSIGNS THE FIRST RECORD TO EACH OF THE FOLLOWING VARIABLES.
C*****************************************************************************
C
```

```
      55 RILOAD=RLOAD(1)
         RCELLP(1)=RCELLP(1)
         ALVDT1=RDEF1(1)
         BLVDT2=RDEF2(1)
C
C*****************************************************************
C  WRITES INITIAL READINGS ONTO UNIT 7.
C*****************************************************************
C
      WRITE(7,70) RILOAD,RCELLP(1),ALVDT1,BLVDT2
   70 FORMAT(/,'INITIAL LOAD                = ',F10.3,' KN',
     *       /,'INITIAL CELL PRESSURE      = ',F10.3,' KPA',
     *       /,'INITIAL READING FOR LVDT1 = ',F17.10,' mm',
     *       /,'INITIAL READING FOR LVDT2 = ',F17.10,' mm')
C
C*****************************************************************
C  CONVERTS TIME FROM CLOCK READING TO **HOURS** WHICH BFIT
C  WILL BE EXPECTING AS THE INPUT UNITS AS SEEN ON IS#33.
C*****************************************************************
C
      59 IMNST=IMN(1)
         DO 50 J=1,N
      60 TIME(J)=(IDY(J)*24.)+IHR(J)+((IMI(J)+ISE(J)/60.)/60.)
         IF(IMN(J).EQ.IMN(1)) GO TO 50
         IF(IMN(1).NE.4.OR.IMN(1).NE.6.OR.IMN(1).NE.9.OR.IMN(1).NE.11)
        *GO TO 61
         IDY(J)=IDY(J)+30
         GO TO 63
      61 IF(IMN(1).NE.2)GO TO 62
         IDY(J)=IDY(J)+28
         GO TO 63
      62 IDY(J)=IDY(J)+31
         IF(IMN(1).EQ.12)GO TO 64
      63 IMN(J)=IMN(J)-1
         GO TO 60
      64 IMN(J)=12
         GO TO 60
      50 CONTINUE
C
C*****************************************************************
C  INITIALIZES VARIABLES.
C*****************************************************************
C
      ELPST(1)=0.
      VDEF1(1)=0.
      VDEF2(1)=0.
      ESTRN1(1)=0.
      ESTRN2(1)=0.
C
C*****************************************************************
C  CALCULATES ELAPSED TIME, LOAD, CELL P., AND ENGG. STRAIN.
C*****************************************************************
C
      DO 80 J=2,N
      VDEF1(J)=RDEF1(J)-RDEF1(1)
      VDEF2(J)=RDEF2(J)-RDEF2(1)
      ELPST(J)=TIME(J)-TIME(1)
      RLOAD(J)=RLOAD(J)-RILOAD
```

```
      RCELLP(J)=RCELLP(J)-RCELLP(1)
      ESTRN1(J)=(VDEF1(J)/XLEN)*1000000.*FACT
      ESTRN2(J)=(VDEF2(J)/XLEN)*1000000.*FACT
   80 CONTINUE
      RLOAD(1)=0.
C
C*****************************************************************
C  WRITES TIME, LOAD, CELL P., AND ENGG. STRAIN ONTO UNIT 7.
C*****************************************************************
C
      WRITE(7,90)
   90 FORMAT(/,1X,'NUMBER',4X,'TIME',9X,'LOAD',8X,'CELL PRESSURE',
     *       2(3X,'ENGG. STRAIN  '),/,11X,'HOURS',9X,'KN',14X,
     *       'KPA',9X,'#1 (MICRO)',7X,'#2 (MICRO)')
      DO 100 J=1,N
      WRITE(7,110) J,ELPST(J),RLOAD(J),RCELLP(J),ESTRN1(J),ESTRN2(J)
  110 FORMAT(2X,I3,3X,F9.3,3X,E13.6,2X,E13.6,3X,F11.3,6X,F11.3)
  100 CONTINUE
C
C*****************************************************************
C  FIRST LINE OF DATA IS NOW DELETED WHEN PASSING ON TIME
C  STRAIN RECORDS TO FURTHER SUBROUTINES.
C*****************************************************************
C
      NRR=0
      NRR=N-1
      DO 85 I=1,NRR
      E1(I)=ESTRN1(I+1)
      E2(I)=ESTRN2(I+1)
   85 TT(I)=ELPST(I+1)
      RETURN
      END
```

```
      1     ccccccccccccccccccccccccccccccccccccccccccccccccccccccccccccccccc
      2     ccccccccccccccccccccccccccccccccccccccccccccccccccccccccccccccccc
      3     ccccc                                                         ccccc
      4     ccccc                    SUBROUTINE BFIT2                     ccccc
      5     ccccc          FITS A POWER LAW TO THE DATA                   ccccc
      6     ccccc            BY RESTRICTION ON DW & FF                    ccccc
      7     ccccc                                                         ccccc
      8     ccccccccccccccccccccccccccccccccccccccccccccccccccccccccccccccccc
      9     ccccccccccccccccccccccccccccccccccccccccccccccccccccccccccccccccc
     10     C
     11     C*****************************************************************
     12     C                      VARIABLE DOCUMENTATION
     13     C  NRR:  NUMBER OF RECORDS PASSED ONTO BFIT.
     14     C  E1 & E2:  ENGG. STRAINS FOR LVDT #1&#2.
     15     C  TT:  TIMES FOR THE ABOVE RECORDS.
     16     C  DUMMY: INTERMEDIATE ARRAY USED TO STORE INPUT STRAIN VALUES.
     17     C  AE:  INTERMEDIATE ARRAY CONTAINING STRAIN VALUES USED IN
     18     C       BFIT DURING THE SMOOTHING OF THE STRAIN DATA TO
     19     C       INCREASINGLY POSITIVE.
     20     C  AT:  INTERMEDIATE ARRAY CONTAINING TIME RECORDS IN MINUTES
     21     C       DURING THE SMOOTHING PROCESS.
     22     C  ER:  ARRAY CONTAINING THE STRAIN RATES COMPUTED FROM
     23     C       THE ABOVE VALUES.
     24     C  TP:  ARRAY CONTAINING THE AVERAGE TIME VALUES FOR THE ABOVE
     25     C       STRAIN RATES. ALSO REFERRED TO AS THE TRANSFORMED DATA.
     26     C  T:  CONTAINS THE LOGS OF THE AVERAGE TIMES.
     27     C  E:  CONTAINS THE LOGS OF THE STRAIN RATES.
     28     C  L:  INDICATES TYPE OF DATA.
     29     C  N:  RECORD NUMBER.
     30     C  BBO:  ARRAY CONTAINING INTERCEPTS OF FITTED LINES.
     31     C  BB1:  ARRAY CONTAINING SLOPES OF FITTED LINES.
     32     C  OO:  COUNTER USED TO TERMINATE CFIT.
     33     C  FF:  SLOPE SIGNIFICANCE STATISTIC.
     34     C  FFL:  INPUT LIMIT FOR THE ABOVE. NULL ENTRY WILL ASSIGN
     35     C        THE VALUE TO BE 10.0.
     36     C  DW:  DURBIN WATSON STATISTIC.
     37     C  DU:  SIGNIFICANCE LIMIT FOR THE ABOVE VARIABLE WHICH IS
     38     C       CALCULATED FROM THE FORMULAE ON IS#118 TO #124 AND
     39     C       IS DEPENDENT ON THE DEGREES OF FREEDOM.
     40     C  NDF:  NUMBER OF DEGREES OF FREEDOM FOR DW.
     41     C  MMM:  LVDT COUNTER.
     42     C  NRF:  NUMBER OF LAST RECORD USED IN THE FIT OF THE
     43     C        CFIT.
     44     C  OOO:  VARIABLE USED TO KEEP TRACK OF THE NUMBER OF
     45     C        CALLS MADE TO BFIT. OOO=0 ON THE FIRST CALL TO BFIT
     46     C        WHILE OOO=1 ON THE SECOND CALL.
     47     C*****************************************************************
     48     C
     49           SUBROUTINE BFIT (NRR,E1,E2,TT,L,N,BBO,BB1,XANS1,XANS3,LT,
     50          *     LE,W1,EEM1,NC1,K,OO,FF,DW,MMM,ANS3,NRF,NFIT,OOO,B0D,B1D,
     51          *  TP,ERP,NCP)
     52     C
     53     C
     54           REAL LT(2,1000),LE(2,1000)
     55           REAL Y/'Y'/,BLANK/'    '/
     56     C
     57     C
     58           DIMENSION T(1000),AA(10),AT(1000),E1(1000),E2(1000),
```

```
     *W(1000),B(1000),EA(1000),AE(1000),N(1),BBO(2,2),BB1(2,2),
     *DENT(48),VDEF(1000),DLOAD(1000),TT(1000),DUMMY(1000),
     *E(1000),EE(1000),ER(1000),W1(2,1000),
     *EEM1(2),NC1(2),NRF(2),TP(1000),ERP(1000)
C
C
      Z=0
      IF(OO.GT.0) Z=1
      IF(OO.EQ.0) K=1
      MM=0
      NR1=NRR
  700 MM=MM+1
      IF(ANSM3.EQ.Y.AND.L.EQ.2) MM=MMM
      NR=NRR
      IF(MM.EQ.1)GO TO 710
C
C*************************************************************************
C  ASSIGNING STRAIN VALUES TO INTERMEDIATE DUMMY VARIABLES.
C*************************************************************************
C
      DO 705 II=1,NR
      N(II)=II
  705 DUMMY(II)=E2(II)
      GO TO 720
  710 DO 715 II=1,NR
      N(II)=II
  715 DUMMY(II)=E1(II)
  720 CONTINUE
C
C*************************************************************************
C  PROMPT TO DETERMINE THE LIMIT FOR SLOPE SIGNIFICANCE.
C  NULL ENTRY WILL ASSIGN IT TO A VALUE OF 10.0.
C*************************************************************************
C
      IF(L.EQ.2.OR.MM.EQ.2) GO TO 515
      WRITE(6,200)
  200 FORMAT('INPUT DESIRED LIMIT FOR TEST OF SLOPE SIGNIFICANCE IF'
     */'OTHER THAN 10. (REAL NUMBER, TERMINATED WITH A COMMA):')
      READ(5,100)FFL
  100 FORMAT(G4)
      IF(FFL.LT.0.1) FFL=10.
C
C*************************************************************************
C  SMOOTHS DATA TO INCREASING POSITIVELY BY THE USE OF THE
C  RECURSION FORMULAE REFERENCED IN CRUDEN (1971).
C*************************************************************************
C
  515 I=K-1
      J=K-1
   12 I=I+1
      J=J+1
      AE(I)=DUMMY(J)
C
C*************************************************************************
C  PLEASE NOTE THAT THE INPUT TIME IN HOURS IS NOW BEING
C  CHANGED TO MINUTES.
C*************************************************************************
C
```

```
      AT(I)=TT(J)*60.
      W(I)=1.0
   11 IF(I .EQ.K) GO  TO 12
   14 IF(AE(I)-AE(I-1)) 13, 13, 4
   13 AE(I-1)=(AE(I)*W(I)+AE(I-1)*W(I-1))/(W(I)+W(I-1))
      AT(I-1)=(AT(I)*W(I)+AT(I-1)*W(I-1))/(W(I)+W(I-1))
      W(I-1)=W(I)+W(I-1)
      I=I-1
      IF(I-K-1) 12,14,14
    4 CONTINUE
      IF(J.LT.NR)GO TO 12
C
C*************************************************************************
C  INITIALIZE VARIABLES.
C*************************************************************************
C
      WW=0.
      BB=0.
      CONB1=0.
      CONBO=0.
      TE=0.
      DW=0.
      EER=0.
      EEM=0.
      EES=0.
      SUMT=0.
      SUMET=0.
      SUMT2=0.
      SUME=0.
      SUME2=0.
      SXX=0.0
      DWW=0.
      SXY=0.0
      WWA=0.
      AF=0.
      M=K+1
      NC=I
      IF(L.EQ.1.AND.NR.EQ.NR1) NCP=NC-1
C
C*************************************************************************
C  CALCULATES THE STRAIN RATE WITH THE SMOOTHED DATA AND THEN
C  TAKES LOGS OF THIS STRAIN RATE AND THE AVERAGE TIMES.
C*************************************************************************
C
      DO 1 J=M,NC
      ER(J)=(AE(J)-AE(J-1))/(AT(J)-AT(J-1))
      IF(L.NE.1.OR.NR.NE.NR1) GO TO 3
      TP(J-1)=(AT(J)+AT(J-1))/2.0
      ERP(J-1)=ER(J)
    3 CONTINUE
      T(J)=ALOG10((AT(J)+AT(J-1))/2.0)
    6 W(J)=(W(J)+W(J-1))/2.
      E(J)=ALOG10(ER(J))
      WW=WW+W(J)
      EE(J)=0.
      SUMT=SUMT+T(J)*W(J)
      SUME=SUME+E(J)*W(J)
      SUMET=SUMET+E(J)*T(J)*W(J)
```

```
      SUME2=SUME2+E(J)*E(J)*W(J)
    1 SUMT2=SUMT2+T(J)*T(J)*W(J)
      SUME2=SUME2-SUME*SUME/WW
      SUMT2=SUMT2-SUMT*SUMT/WW
      SUMET=SUMET-SUME*SUMT/WW
      FME=SUME/WW
      FMT=SUMT/WW
      DO 7 J=M,NC
      SXY=SXY+(T(J)-FMT)*(E(J)-FME)*W(J)
    7 SXX=SXX+W(J)*(T(J)-FMT)**2
C
C*****************************************************************
C  USES LEAST SQUARES TO FIT THE TRANSFORMED DATA TO A POWER
C  LAW.
C*****************************************************************
C
      B1=SXY/SXX
      BO=FME-FMT*B1
      DO 2 J=M,NC
      EE(J)=BO+B1*T(J)
      EES=EES+(EE(J)-E(J))*W(J)
      EA(J)=E(J)-EE(J)
      EER=EER+W(J)*(EA(J))**2
      EEM=EEM+W(J)*(EE(J)-FME)**2
      IF(J.LE.M)GO TO 2
      DW=DW+(EA(J)-EA(J-1))**2
      DWW=DWW+EA(J)*EA(J)
    2 CONTINUE
      SSDYX=EER
      EER=EER/(WW-2.)
      IF(EER.EQ.0) EER=10**(-6)
      FF=EEM/EER
      CONB1=SQRT(EER/SUMT2)
      CONBO=CONB1*SQRT((SUMT2*WW+SUMT*SUMT)/(WW*WW))
      DW=DW/DWW
C
C*****************************************************************
C  TRANSFER VARIABLES FOR SUBROUTINE CFIT.
C*****************************************************************
C
      IF(OO.EQ.2.AND.Z.EQ.0) OO=0
C
      IF(NR.NE.NRR.OR.L.NE.1) GO TO 111
      EEM1(MM)=EEM
      NC1(MM)=NC
      DO 21 J=1,NC
      LE(MM,J)=E(J)
      LT(MM,J)=T(J)
   21 W1(MM,J)=W(J)
C
C*****************************************************************
C  CHECKS DW AND FF TO SEE IF THE FIT OF THE POWER LAW TO THE
C  DATA IS SATISFACTORY.
C*****************************************************************
C
  111 NDF=NR-K+1
      IF(NDF.LE.20) DU=1.36+(NDF-15)*0.01
      IF(NDF.GT.20.AND.NDF.LE.30) DU=1.41+(NDF-20)*0.008
```

```
      IF(NDF.GT.30.AND.NDF.LE.40) DU=1.49+(NDF-30)*0.005
      IF(NDF.GT.40.AND.NDF.LE.50) DU=1.54+(NDF-40)*0.005
      IF(NDF.GT.50.AND.NDF.LE.60) DU=1.59+(NDF-50)*0.003
      IF(NDF.GT.60.AND.NDF.LE.95) DU=1.62+(NDF-60)*0.002
      IF(NDF.GT.95) DU=1.69
      IF(DW.GT.DU.AND.FF.GT.FFL) GO TO 817
      IF(L.EQ.1) NR=NR-1
      IF(L.EQ.2) GO TO 817
      GO TO 515
C
C
  817 NDIFF=NRR-NR
      IF(NDIFF.EQ.0) NFIT=1
      IF(ANSM3.NE.Y) GO TO 8
      IF(L.EQ.1) GO TO 8
      IF(OO.EQ.2) GO TO 8
      BBO(L,MM)=BO
      BB1(L,MM)=B1
      GO TO 702
C
C*************************************************************************
C  WRITES THE DATA AND THE STATISTICS.
C*************************************************************************
C
    8 WRITE(7,206)MM
  206 FORMAT(///30X,'       DATA FROM LVDT NO.',I2,//)
  416 CONTINUE
      WRITE(7,208)
  208 FORMAT(9X,'TRANSFORMED DATA')
      WRITE(7,209)
  209 FORMAT(11X,'TIME',5X,'STR RATE, E',5X,'LOG E',9X,'LOG EE',4X,
     *'LOG E - LOG EE',4X,'W')
      WRITE(7,216)
  216 FORMAT(11X,'(MIN)',3X,'(MICRO.E/MIN)')
      DO 9 J=M,NC
C
C*************************************************************************
C  THE LOG OF THE AVERAGE TIME T(J) IS NOW TAKEN AS A POWER
C  OF 10 IN ORDER TO GET TIME BACK FOR WRITING.
C*************************************************************************
C
      T(J)=10**(T(J))
C
C
      WRITE(7,106)T(J),ER(J),E(J),EE(J),EA(J),W(J)
  106 FORMAT(7X,F12.4,2X,F12.6,3(1X,E13.6),F7.2)
    9 CONTINUE
      WRITE(7,210)
  210 FORMAT(//,9X,'FIT PARAMETERS')
      A=10**BO
      CONBO=2*CONBO
      CONBO=10**CONBO
      CONB1=2*CONB1
      A1=A+CONBO
      A2=A-CONBO
      B1=B1+CONE1
      B11=B1-CONB1
      IF(OOO.EQ.1)GO TO 19
```

```
      BOD=BO
      B1D=B1
      WRITE(7,157)A
      WRITE(7,158)B1
      WRITE(7,105)A1,A2
      WRITE(7,115)BI,BII
  105 FORMAT(11X,' RANGE FOR A  ',16X,E15.6,3X,E15.6)
  157 FORMAT(11X,' A                                ',E15.6)
  115 FORMAT(11X,' RANGE FOR SLOPE, B               ',F12.7,3X,F12.7)
  158 FORMAT(11X,' SLOPE, B                         ',F12.7)
      GO TO 29
   19 CONTINUE
      WRITE(7,357)A
      WRITE(7,358)B1
      WRITE(7,305)A1,A2
      WRITE(7,315)BI,BII
  305 FORMAT(11X,' RANGE FOR C  ',16X,E15.6,3X,E15.6)
  357 FORMAT(11X,' C                                ',E15.6)
  315 FORMAT(11X,' RANGE FOR SLOPE, D               ',F12.7,3X,F12.7)
  358 FORMAT(11X,' SLOPE, D                         ',F12.7)
   29 CONTINUE
      WRITE (7,159)DW
  159 FORMAT(11X,' DURBIN WATSON STATISTIC          ',F7.3)
      WRITE(7,180) NDF
  180 FORMAT(11X,' DEGREE OF FREEDOM FOR DW         ',I3)
      WRITE(7,181) DU
  181 FORMAT(11X,' UPPER BOUND FOR DW               ',F7.3)
      WRITE(7,156)FF
  156 FORMAT(11X,' TEST OF SLOPE SIGNIFICANCE       ',F9.3)
      WRITE (7,211)
  211 FORMAT(//,9X,'DATA FOR COMPARISON TESTS')
      WW=WW-2.
      WRITE(7,122)WW
  122 FORMAT(11X,' WEIGHTING ',F6.1)
      WRITE(7,104)FME,FMT
      WRITE(7,214)SUME2,SUMT2
  104 FORMAT(11X,' MEAN STRAIN  ',F11.3,
     *'   MEAN TIME ',F11.3)
      WRITE(7,213)SUMET,SSDYX
  214 FORMAT(11X,' SSDY ',5X,F11.3,' SSDX      ',F11.3)
  213 FORMAT(11X,' SPDXY',5X,F11.3,' SSDYX     ',F11.3)
      WRITE(7,212)
  212 FORMAT(/,9X,'CHECK')
      WRITE(7,107)EES
  107 FORMAT(11X,' SUM OF RESIDUALS',14X,F12.6)
      WRITE(7,124) K
  124 FORMAT(///,11X,' DATA STARTS AT #',I3)
      WRITE(7,125) NR
  125 FORMAT(11X,' DATA ENDS AT #',I3)
C
C*****************************************************************
C  INITIALIZES COUNTERS FOR SUBROUTINE CFIT, IF USED.
C*****************************************************************
C
      IF(L.EQ.1)NRF(MM)=NR
      IF(ANSM3.EQ.Y.AND.L.EQ.2) GO TO 704
      GO TO 703
  704 MMM=2
```

```
      K=1
      Z=0
C
C*************************************************************
C  DIRECTS PROGRAM ACCORDING TO PROGRAM OPTIONS IN EFFECT.
C*************************************************************
C
  703 BBO(L,MM)=BO
      BB1(L,MM)=B1
      IF(XANS1.EQ.Y) GO TO 701
      IF(IANS3.EQ.1) GO TO 702
  701 IF(MM.EQ.2)GO TO 702
      GO TO 700
  702 CONTINUE
      RETURN
      END
```

```
      CCCCCCCCCCCCCCCCCCCCCCCCCCCCCCCCCCCCCCCCCCCCCCCCCCCCCCCCCCCCCCCCCCCCCC
      CCCCCCCCCCCCCCCCCCCCCCCCCCCCCCCCCCCCCCCCCCCCCCCCCCCCCCCCCCCCCCCCCCCCCC
      CCCCC                                                           CCCCC
      CCCCC                    SUBROUTINE INTEG2                      CCCCC
      CCCCC          INTEGRATES STRAIN RATE TO DETERMINE              CCCCC
      CCCCC       DECELERATING STRAINS WHICH ARE SUBTRACTED           CCCCC
      CCCCC     FROM TOTAL STRAINS TO GET ACCELERATING STRAINS        CCCCC
      CCCCC                                                           CCCCC
      CCCCCCCCCCCCCCCCCCCCCCCCCCCCCCCCCCCCCCCCCCCCCCCCCCCCCCCCCCCCCCCCCCCCCC
      CCCCCCCCCCCCCCCCCCCCCCCCCCCCCCCCCCCCCCCCCCCCCCCCCCCCCCCCCCCCCCCCCCCCCC
C
C*****************************************************************
C                    VARIABLE DOCUMENTATION
C  TT: INPUT TIME IN HOURS.
C  E:  ARRAY CONTAINING THE OBSERVED INPUT STRAINS.
C  TERM: INTERMEDIATE VARIABLE USED IN THE CALCULATIONS.
C  EE:  DECELERATING STRAINS COMPUTED THRU INTEGRATION
C       OF THE POWER LAW.
C  EDIFF:  ACCELERATING STRAINS COMPUTED. LATER PLACED
C          INTO ARRAY E1 OR E2 TO PASS ONTO BFIT.
C*****************************************************************
C
      SUBROUTINE INTEG(E1,E2,BBO,BB1,NRR,TT,L,XANS1,IANS3)
C
C
      DIMENSION EDIFF(1000),E(1000),EE(1000),E1(1000),E2(1000),
     *          BBO(2,2),BB1(2,2),TT(1000)
C
C
      REAL Y/'Y'/
C
C
      MM=0
      NR=NRR
   20 MM=MM+1
      IF(MM.EQ.2) GO TO 43
      DO 40 I=1,NR
   40 E(I)=E1(I)
C
C*****************************************************************
C  INTEGRATES STRAIN RATE EQUATION FROM BFIT TO GET
C  DECELERATING STRAINS FROM THE FORMULAE OUTLINED IN
C  CRUDEN (1971). TWO FORMULAE ARE PRESENT DEPENDENT ON
C  WHETHER OR NOT B1 IS POSITIVE OR NOT. THE TIME VARIABLE
C  TT MUST BE IN THE UNITS ON MINUTES FOR THESE EQUATIONS TO BE
C  VALID. THE TIME ARRAY TT MUST BE RETURNED TO BFIT IN HOURS.
C*****************************************************************
C
   43 BO=BBO(L,MM)
      B1=BB1(L,MM)
      BO=10.**BO
      B1=B1+1.
      BO=BO/B1
C
C*****************************************************************
C  DECISION IS MADE DEPENDENT UPON THE VALUE OF B1.
C*****************************************************************
```

```
      C
            IF(B1)12,12,13
         12 DO 9 I=1,NR
            TERM=0.000001/(TT(I)*60.0)
          9 EE(I)=-(BO)*(10**(-6*B1))*(1-(TERM**(-B1)))
            GO TO 2
         13 DO 1 I=1,NR
            TT(I)=TT(I)*60.0
            EE(I)=BO*((TT(I)**B1)-(10**(-6*B1)))
          1 TT(I)=TT(I)/60.0
      C
      C*****************************************************************
      C  SUBTRACTS DECELERATING STRAINS FROM EXPERIMENTAL STRAINS
      C  IN ORDER TO GET ACCELERATING STRAINS.
      C*****************************************************************
      C
          2 DO 21 I=1,NR
         21 EDIFF(I)=E(I)-EE(I)
      C
      C*****************************************************************
      C  ASSIGN ACCEL. STRAINS TO THE ARRAY BEING PASSED TO BFIT.
      C*****************************************************************
      C
            IF(MM.EQ.2) GO TO 15
            DO 30 I=1,NR
            E1(I)=EDIFF(I)
         30 E(I)=E2(I)
            IF(IANS1.EQ.Y) GO TO 20
            IF(IANS3.EQ.1) GO TO 999
            GO TO 20
         15 DO 31 I=1,NR
         31 E2(I)=EDIFF(I)
        999 RETURN
            END
```

```
      CCCCCCCCCCCCCCCCCCCCCCCCCCCCCCCCCCCCCCCCCCCCCCCCCCCCCCCCCCCCCCCCCCCC
      CCCCCCCCCCCCCCCCCCCCCCCCCCCCCCCCCCCCCCCCCCCCCCCCCCCCCCCCCCCCCCCCCCC
      CCCCC                                                         CCCCC
      CCCCC                    SUBROUTINE CFIT2                     CCCCC
      CCCCC                OPTIMIZES THE FIT OF THE                 CCCCC
      CCCCC                POWER LAW EXPRESSION TO THE              CCCCC
      CCCCC                  ENTIRE RANGE OF DATA                   CCCCC
      CCCCC                                                         CCCCC
      CCCCCCCCCCCCCCCCCCCCCCCCCCCCCCCCCCCCCCCCCCCCCCCCCCCCCCCCCCCCCCCCCCCC
      CCCCCCCCCCCCCCCCCCCCCCCCCCCCCCCCCCCCCCCCCCCCCCCCCCCCCCCCCCCCCCCCCCC
C
C*****************************************************************
C                      VARIABLE DOCUMENTATION
C  LT:  CONTAINS LOG TIME.
C  LE:  CONTAINS LOG STRAIN.
C  BBO:  CONTAINS INTERCEPTS OF FITTED LINES.
C  BB1:  CONTAINS SLOPES OF FITTED LINES.
C  R:  RATIO OF THE SQUARE OF THE SCATTER OF THE DATA POINTS
C      ABOUT THEIR MEAN TO THE SQUARES OF THE SCATTER ABOUT
C      THE OVERALL FIT. IT IS A MEASURE OF THE GOODNESS OF FIT.
C  DE, AE, EE, EER, :  LOCAL VARIABLES USED IN
C                      THE CALCULATION OF R.
C*****************************************************************
C
      SUBROUTINE CFIT(EEM1,LT,LE,W1,BBO,BB1,NC1,K,OO,
     *                FF,DW,MMM,NRR,NRF,BOD,B1D)
C
C
      REAL LT(2,1000),LE(2,1000)
C
C
      DIMENSION W1(2,1000),BBO(2,2),BB1(2,2),
     *          EEM1(2),NC1(2),NRF(2)
C
C
      MM=MMM
      WW=0
      M=0
      M=K+1
      NC=NC1(MM)
      EER=0
C
C*****************************************************************
C  CALCULATES R FOR CURRENT ACCELERATING CREEP PARAMETERS.
C*****************************************************************
C
      DO 1 J=2,NC
      DE=BBO(1,MM)+(LT(MM,J)*BB1(1,MM))
      AE=BBO(2,MM)+(LT(MM,J)*BB1(2,MM))
      EE=ALOG10((10**AE)+(10**DE))
      EER=EER+W1(MM,J)*(EE-LE(MM,J))**2
    1 WW=WW+W1(MM,J)
      EER=EER/(WW-2.)
      R=EEM1(MM)/EER
      IF(OO.NE.0) GO TO 2
C
C*****************************************************************
C  WRITES A TABLE OF FIT STATISTICS.
```

```
C*************************************************************************
C
      WRITE(7,100)MM
  100 FORMAT(//,22X,'PARAMETERS FOR EVALUATING TOTAL FIT,',
     *' LVDT NO.: ',I1,//
     *34X,'ACCELERATING CREEP',33X,'TOTAL FIT'/
     *16X,'RANGE              C     SLOPE,D ',6X,'R1',8X,'DW',3X,
     *'DAYS TO INFLEXION',6X,'R')
    2 DTI=10**((BOD-BBO(2,MM))/(BB1(2,MM)-B1D))
      DTI=(DTI/60)/24
      C=10**BBO(2,MM)
      WRITE(7,101)K,NRR,C,BB1(2,MM),FF,DW,DTI,R
  101 FORMAT(14X,I3,' - ',I3,E15.6,F12.7,2F9.3,4X,F9.3,7X,F9.3)
C
C*************************************************************************
C  TESTS TO SEE IF DATA MEETS TERMINATING CRITERIA.
C*************************************************************************
C
      EA=BBO(2,MM)+(LT(MM,M)*BB1(2,MM))
      ED=BBO(1,MM)+(LT(MM,M)*BB1(1,MM))
      EA=EA-0.5
      OO=1
      IF(EA.GE.ED.OR.M.GE.NRF(MM))GO TO 3
      GO TO 4
    3 OO=2
C
C*************************************************************************
C  RANGE OF DATA IS NOW DECREASED AND CONTROL IS TRANFERRED TO
C  BFIT TO FIT A POWER LAW TO THIS NEW DATA RANGE.
C*************************************************************************
C
      K=K-1
    4 RETURN
      END
```

```
      CCCCCCCCCCCCCCCCCCCCCCCCCCCCCCCCCCCCCCCCCCCCCCCCCCCCCCCCCCCCCCCCCCCC
      CCCCCCCCCCCCCCCCCCCCCCCCCCCCCCCCCCCCCCCCCCCCCCCCCCCCCCCCCCCCCCCCCCC
      CCCCC                                                          CCCCC
      CCCCC                  SUBROUTINE CPLOTI.2                     CCCCC
      CCCCC                  MAKES PLOTS OF :                        CCCCC
      CCCCC                 STRAIN RATE VS TIME                      CCCCC
      CCCCC                       AND                                CCCCC
      CCCCC             LOG STRAIN RATE VS LOG TIME                  CCCCC
      CCCCC                                                          CCCCC
      CCCCCCCCCCCCCCCCCCCCCCCCCCCCCCCCCCCCCCCCCCCCCCCCCCCCCCCCCCCCCCCCCCCC
      CCCCCCCCCCCCCCCCCCCCCCCCCCCCCCCCCCCCCCCCCCCCCCCCCCCCCCCCCCCCCCCCCCC
      C
      C*****************************************************************
      C  THIS SUBROUTINE MAKES USE OF THE PROGRAM CIVE:GRAPH.
      C  PLEASE SEE THE WRITE-UP IN THE CIVE FILES FOR MORE INFO.
      C*****************************************************************
      C
      C*****************************************************************
      C                      VARIABLE DOCUMENTATION
      C  OPTNS:  OPTIONS WHICH ARE CALLED FOR THE PLOTTING OF
      C         THE GRAPHS.
      C  LABELS:  LABELS USED WHEN PLOTTING.
      C*****************************************************************
      C
            SUBROUTINE CPLOT(ESTRN1,ESTRN2,ELPST,BBO,BB1,NRR,
           *  TP,ERP,NCP,ITN1,ITN2,XANS1,IANS3,ANSM1,ANSM2)
      C
      C
            DIMENSION ESTRN1(1000),ESTRN2(1000),ELPST(1000),BBO(2,2),
           *  BB1(2,2),AE(1000),E(1000),T(1000),AT(1000),DX(4),DY(4),
           *          LABELS(24),OPTNS(25),TE(1000),TP(1000),ERP(1000),
           *         XD(2),YD(2)
      C
      C
            REAL LOG/'LOG '/,Y/'Y'/,TWO/'TWO '/,ONE/'ONE '/,BLANK/'     '/
      C
      C*****************************************************************
      C  INITIALIZE ALL THE LABELS AND THE OPTIONS FOR CIVE:GRAPH.
      C*****************************************************************
      C
            REAL LABELS/'TEST',' NO.',':   ',2*'    ',' LVD','T NO',
           *'.:  ',',    ',4*'    ','TIME',3*'    ','STRA','IN R',
           *'ATE ',4*'    '/,ITN1,ITN2
            REAL OPTNS /1.0,24*'NO  '/
      C
      C*****************************************************************
      C  DETERMINE IF IN BATCH MODE.
      C*****************************************************************
      C
            CALL CREPLY(&8)
            GO TO 9
          8 OPTNS(4)=1
      C
      C*****************************************************************
      C   PROMPTS TO DETERMINE DESIRED PLOTS.
      C*****************************************************************
      C
          9 WRITE(6,200)
```

```
  200 FORMAT('  WOULD YOU LIKE A LOG STRAIN RATE - LOG TIME PLOT?(Y,N)')
      READ(5,300)ANS1
  300 FORMAT(A1)
      WRITE(6,201)
  201 FORMAT('  WOULD YOU LIKE A STRAIN RATE - TIME PLOT?(Y,N)')
      READ(5,301)ANS2
  301 FORMAT(A1)
      IF(ANS1.NE.Y.AND.ANS2.NE.Y) GO TO 1000
      IF(ANSM2.EQ.Y) GO TO 111
C
C*****************************************************************
C  LOAD GRAPH.
C*****************************************************************
C
  111 MM=0
   50 MM=MM+1
      IF(MM.EQ.2)GO TO 1
      LABELS(4)=ITN1
      LABELS(5)=ITN2
    1 CONTINUE
C
C*****************************************************************
C  TRANSFERS STRAIN RATE AND TIME.
C*****************************************************************
C
      DO 10 J=1,NCP
      E(J)=ERP(J)
      TE(J)=TP(J)
   10 T(J)=TP(J)
      IF(MM.EQ.1) GO TO 15
      XX=TWO
      GO TO 16
   15 XX=ONE
   16 CONTINUE
      LABELS(9)=XX
C
C*****************************************************************
C  DETERMINE MAXIMUM AND MINIMUM VALUES.
C*****************************************************************
C
      J=0
   25 J=J+1
      EMIN=E(J)
      EMAX=E(J)
      IF(E(J).LE.0.0)GO TO 25
   20 J=J+1
      IF(EMIN.LE.E(J).OR.E(J).LE.0.0)GO TO 21
      EMIN=E(J)
   21 IF(EMAX.GE.E(J))GO TO 22
      EMAX=E(J)
   22 IF(J.LT.NCP) GO TO 20
C    DELETES NEGATIVE STRAIN RATES
      IF(ANS2.NE.Y) GO TO 4
C
C*****************************************************************
C  PROMPT FOR STRAIN RATE - TIME PLOT PARAMETERS
C*****************************************************************
C
```

```
117           WRITE(6,202)
118           WRITE(6,203)EMIN
119           WRITE(6,204)EMAX
120           WRITE(6,205)T(NCP)
121         202 FORMAT('  FOLLOWING ARE THE EXTREME VALUES IN THE T VS E PLOT:')
122         203 FORMAT('  MINIMUM STRAIN RATE: ',F12.6)
123         204 FORMAT('  MAXIMUM STRAIN RATE: ',F15.6)
124         205 FORMAT('  FINAL TIME:          ',F10.3)
125           WRITE(6,206)
126         206 FORMAT(' INPUT DESIRED STRAIN RATE VALUE AT ORIGIN OF Y AXIS
127          *(TERMINATE WITH COMMA):')
128           READ(5,302)OPTNS(11)
129         302 FORMAT(E20.0)
130           6 WRITE(6,207)
131         207 FORMAT(' INPUT DESIRED Y AXIS SCALE (UNITS/INCH):')
132           READ(5,303)OPTNS(12)
133         303 FORMAT(E20.0)
134           IF(OPTNS(12).LT.1000000) GO TO 7
135           WRITE(6,220)
136         220 FORMAT('*** ERROR *** ALL INPUT VALUES MUST BE TERMINATED BY A
137          *COMMA')
138           GO TO 6
139           7 WRITE(6,208)
140         208 FORMAT(' INPUT DESIRED LENGTH OF Y AXIS (INCHES):')
141           READ(5,304)OPTNS(13)
142         304 FORMAT(E20.0)
143           WRITE(6,209)
144         209 FORMAT(' INPUT DESIRED X AXIS (TIME) SCALE (UNITS/INCH):')
145           READ(5,305)OPTNS(9)
146         305 FORMAT(E20.0)
147           WRITE(6,210)
148         210 FORMAT(' INPUT DESIRED LENGTH OF X AXIS (INCHES):')
149           READ(5,306)OPTNS(10)
150         306 FORMAT(E20.0)
151       C
152       C*****************************************************************
153       C  DEFINE DESIRED OPTIONS.
154       C*****************************************************************
155       C
156           OPTNS(6)=1.0
157           OPTNS(7)=1.0
158           OPTNS(16)=0.
159           OPTNS(21)=1.0
160           OPTNS(24)=BLANK
161           OPTNS(8)=0
162           OPTNS(22)=1
163           OPTNS(23)=0.04
164           LABELS(13)=BLANK
165           LABELS(17)=BLANK
166           ND=NCP
167       C
168           CALL GRAPH (TE,E,ND,LABELS,-1,OPTNS)
169       C
170           4 IF(ANS1.EQ.Y)GO TO 5
171           GO TO 60
172       C
173       C*****************************************************************
174       C  CALCULATES AXIS VALUES FOR LOG E - LOG T PLOT.
```

```
175     C*****************************************************************
176     C
177          5 XA=ALOG10(T(2))
178            OPTNS(8)=FLOAT(IFIX(XA))-1
179            XE=0
180            XE=ALOG10(T(NCP))
181            XE=FLOAT(IFIX(XE))+1
182            OPTNS(9)=XE-OPTNS(8)
183            XC=10.
184            YA=ALOG10(EMIN)
185            OPTNS(11)=FLOAT(IFIX(YA))-1
186            YE=ALOG10(EMAX)
187            YE=FLOAT(IFIX(YE))+1
188            OPTNS(12)=YE-OPTNS(11)
189            OPTNS(6)=2.0
190            OPTNS(7)=2.0
191            OPTNS(17)=1.0
192            OPTNS(18)=2.0
193            OPTNS(20)=0.08
194            OPTNS(21)=1.0
195            OPTNS(22)=1
196            OPTNS(23)=0.04
197            LABELS(13)=LOG
198            LABELS(17)=LOG
199     C
200            CALL GRAPH(TE,E,NE,LABELS,1,OPTNS)
201     C
202     C*****************************************************************
203     C  CALCULATES AND PLOTS BEST FIT LINES FOR LOG E - LOG T PLOT.
204     C*****************************************************************
205     C
206            K=0
207         40 K=K+1
208            IF(ANSW1.NE.Y) GO TO 41
209            IF(K.EQ.2) GO TO 60
210            NC=-2
211            GO TO 42
212         41 NC=K+1
213            IF(K.EQ.2)NC=-2
214         42 ND=4
215            OPTNS(21)=2.0
216            OPTNS(22)=4
217            OPTNS(23)=0.01
218            D=0
219            DX(1)=T(1)
220            D=BB1(K,MM)*ALOG10(DX(1))+BB0(K,MM)
221            DY(1)=10**D
222            DX(2)=T(NCP)
223            D=BB1(K,MM)*ALOG10(DX(2))+BB0(K,MM)
224            DY(2)=10**D
225            DY(3)=EMIN
226            D=(ALOG10(DY(3))-BB0(K,MM))/BB1(K,MM)
227            DX(3)=10**D
228            DY(4)=EMAX
229            D=(ALOG10(DY(4))-BB0(K,MM))/BB1(K,MM)
230            DX(4)=10**D
231     C
232            DO 43 KK=1,4
```

```
233         43 IF(DY(KK).LT.0.0000001) DY(KK)=0.0000001
234      C
235      C
236             DO 45 L=1,4
237             WRITE(7,8070) DX(L),DY(L)
238      8070   FORMAT(2G15.6)
239        45   CONTINUE
240             CALL GRAPH (DX,DY,ND,LABELS,NC,OPTNS)
241      C
242             IF(K.LT.2)GO TO 40
243      C
244      C
245         60 IF(MM.EQ.2)GO TO 999
246             IF(XANS1.EQ.Y) GO TO 50
247             IF(IANS3.EQ.1) GO TO 999
248             GO TO 50
249      C
250      C
251        999 CALL GRAPH (TE,E,ND,LABELS,0,OPTNS)
252      C
253      C
254       1000 RETURN
255             END
```

Appendix C: Assessing the Fitting Ability of CPACK2

The author could not locate any previous work where the fitting ability of CPACK or its versions had been tested. Hence, this appendix outlines the procedure followed and the results of such a study carried out on the latest version, CPACK2.

An equation was assumed with simple coefficients, such as:

$$\dot{\epsilon} = 1000\, t^{-1.0} + 10^{-10}\, t^{3.0}. \qquad [C.1]$$

Time intervals were chosen, and the strain rate was calculated with Equation C.1 at the time interval midpoint. The amount of displacement per time interval was computed by multiplying the midpoint strain rate by the elapsed time of the interval. The amount of total displacement was accumulated by successive summation of the interval displacements. The total displacements were then associated with the final time value of the interval. These two parameters were input into CPACK2 in order to see what equation was calculated by the program.

Three different values, 3.0, 6.0, and 9.0 were substituted for the exponential coeffient D in the second term of the equation. This was done to investigate the fitting ability of the program as the second term's slope became steeper and as the slope difference between the two terms became greater.

Tables C.1, C.2, and C.3 display the input files for the third-order, the sixth-order, and the ninth-order equations respectively. Figures C.1, C.2, and C.3 illustrate the fit of the program-derived equations in relation to the data points. The output for the three respective runs are located just past the above figures.

The three resultant equations from CPACK2 were;

$$\dot{\epsilon} = 939.7\ t^{-0.984} + 0.5316\times10^{-11}\ t^{3.360}, \qquad [C.2]$$

$$\dot{\epsilon} = 525.0\ t^{-0.793} + 0.3551\times10^{-11}\ t^{4.685}, \text{ and} \qquad [C.3]$$

$$\dot{\epsilon} = 734.1\ t^{-0.969} + 0.2894\times10^{-12}\ t^{10.759}. \qquad [C.4]$$

In all three cases, the values for the coefficients A, B, and C were less than the values assumed for calculation of the input points. Also, the exponent D value was greater than the assumed in all cases. It should also be noted that the Durbin Watson and the Test of Slope Significance statistics indicated a good fit to the data for all six terms.

Values for both A and B were all lower than assumed with the greatest deviation for both occurring with the sixth-order equation. The deviation from the assumed value of the C coeffient became greater (in absolute terms, C became smaller) as the order of the equation increased. This smaller-than-expected value for C can be correlated with the

larger-than-expected value observation for the exponent D. The program calculates a steeper slope (conservative error) for the second term of the equation. The amount of deviation, with respect to the assumed value for D was 12%, 11%, and 20% respectively.

The program seems to fit some of the effect of the second term to that of the first, before the statistics indicate a bad fit. This would explain the reasons for the lower values of both A and B. Because now, some of the second term has already been fit by the first term close to its start, the slope of the second term became steeper than the true case. Therefore D became larger while C decreased in value.

It is possible, that there may be some limits to the power difference of the two terms that the program can differentiate between. This phenomena requires more study and the program may have to be modified to "sharpen-up" the fitting procedure, by cutting-off the first term sooner, using stricter statistical criteria perhaps.

Table C.1 Input file for the third-order equation.

```
0,0,0,0,0,0,0,0,0,0,0,
0,0,0,0,10,0,2000.0,0,0,0,
0,0,0,0,20,0,2666.67,0,0,0,
0,0,0,0,30,0,3066.67,0,0,0,
0,0,0,0,50,0,3566.67,0,0,0,
0,0,0,0,70,0,3900.00,0,0,0,
0,0,0,0,90,0,4150.00,0,0,0,
0,0,0,0,100,0,4255.27,0,0,0,
0,0,0,0,120,0,4437.09,0,0,0,
0,0,0,0,200,0,4937.12,0,0,0,
0,0,0,0,800,0,6144.62,0,0,0,
0,0,0,0,1200,0,6584.62,0,0,0,
0,0,0,0,1400,0,6782.41,0,0,0,
0,0,0,0,1500,0,6881.86,0,0,0,
0,0,0,0,1700,0,7088.78,0,0,0,
0,0,0,0,2000,0,7440.89,0,0,0,
0,0,0,0,4000,0,13507.56,0,0,0,
0,0,0,0,8000,0,100574.22,0,0,0,1,
```

Table C.2 Input file for the sixth-order equation.

```
0,0,0,0,0,0,0,0,0,0,0,
0,0,0,0,10,0,2000.0,0,0,0,
0,0,0,0,20,0,2666.678,0,0,0,
0,0,0,0,30,0,3066.922,0,0,0,
0,0,0,0,40,0,3354.475,0,0,0,
0,0,0,0,50,0,3585.001,0,0,0,
0,0,0,0,60,0,3794.50,0,0,0,
0,0,0,0,70,0,4023.77,0,0,0,
0,0,0,0,80,0,4335.08,0,0,0,
0,0,0,0,100,0,5620.18,0,0,0,
0,0,0,0,200,0,120193.10,0,0,0,0,1,
```

Table C.3 Input file for the ninth-order equation.

```
0,0,0,0,0,0,0,0,0,0,0,
0,0,0,0,6,0,2000.0,0,0,0,
0,0,0,0,10,0,2500.054,0,0,0,
0,0,0,0,14,0,2835.451,0,0,0,
0,0,0,0,18,0,3112.939,0,0,0,
0,0,0,0,20,0,3282.74,0,0,0,
0,0,0,0,22,0,3536.83,0,0,0,
0,0,0,0,24,0,3984.02,0,0,0,
0,0,0,0,30,0,8781.6,0,0,0,
0,0,0,0,40,0,87882.95,0,0,0,1,
```

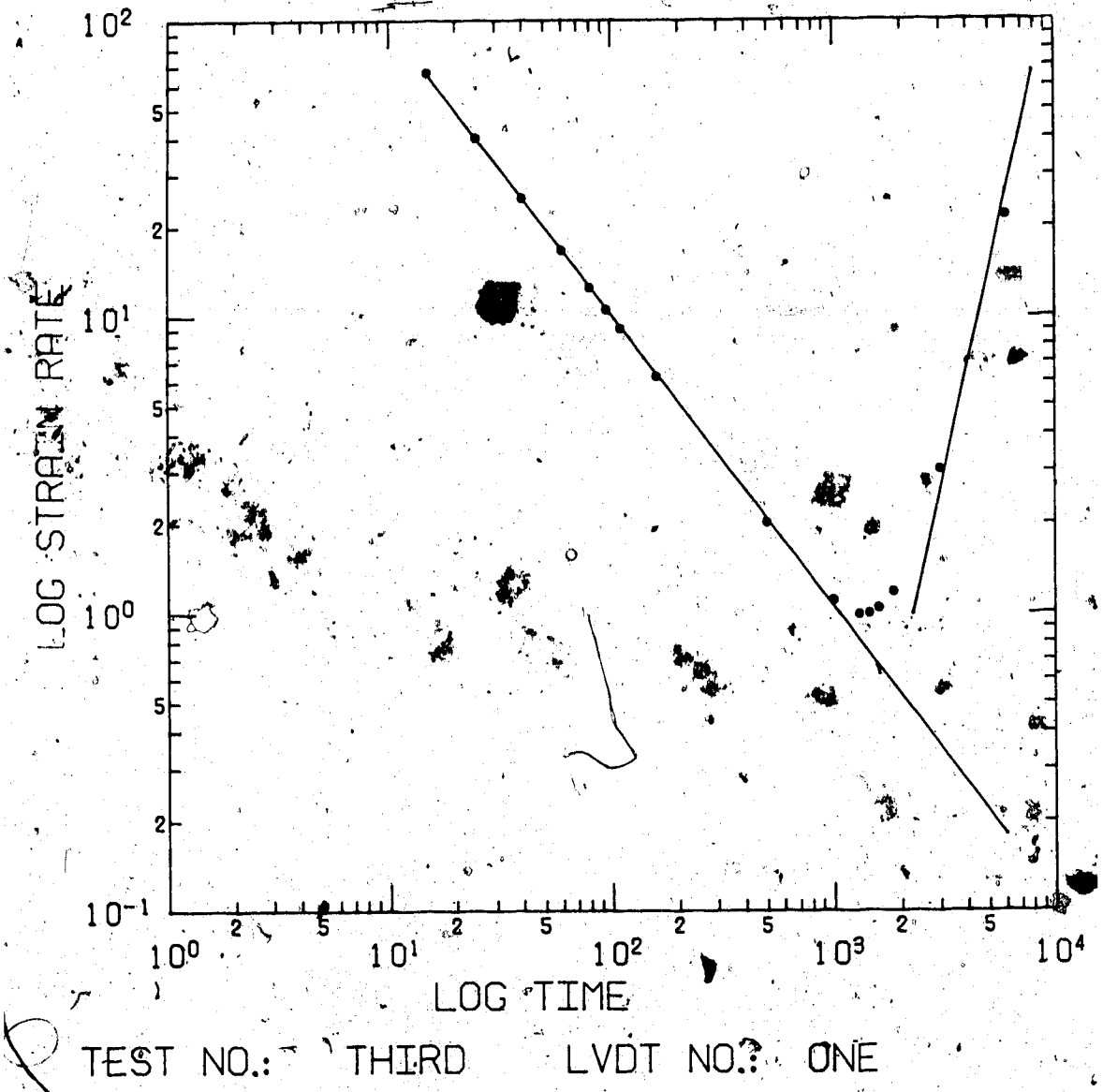

Figure C.1 Fit of the resultant equation to the data points of the third-order equation.

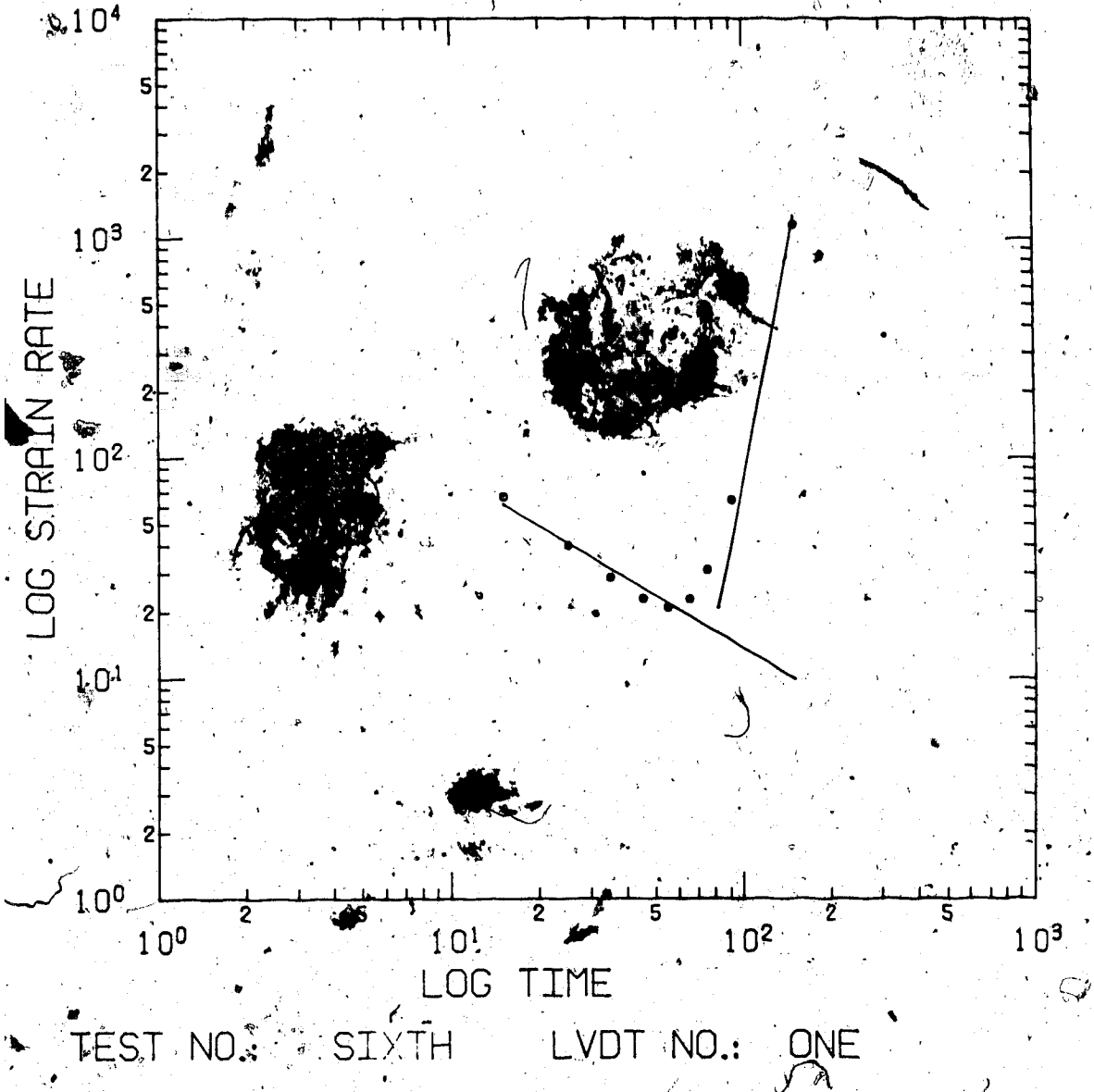

Figure C.2 Fit of the resultant equation to the data points of the sixth-order equation.

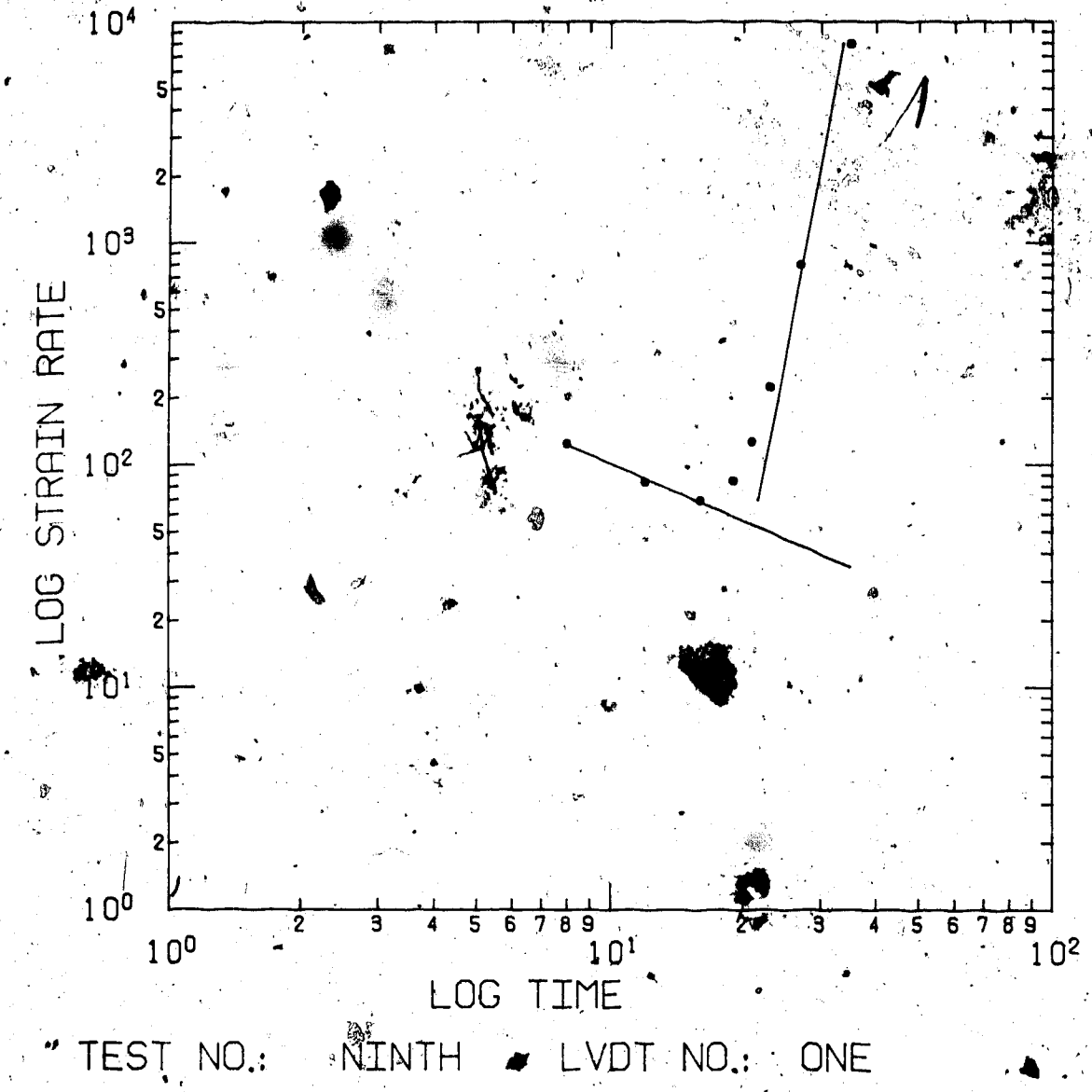

Figure C.3 Fit of the resultant equation to the data points of the ninth-order equation.

TEST NUMBER = THIRD

SAMPLE NUMBER = CRACK2N

SAMPLE LENGTH = 1000.000 mm
SAMPLE DIAMETER = 1.000 mm
SAMPLE WEIGHT = 1.000 gm

INITIAL LOAD = 0.0 KN
INITIAL CELL PRESSURE = 0.0 KPA
INITIAL READING FOR LVDT1 = 0.0 mm
INITIAL READING FOR LVDT2 = 0.0 mm

NUMBER	TIME HOURS	LOAD KN	CELL PRESSURE KPA	ENGG. STRAIN #1 (MICRO)	ENGG. STRAIN #2 (MICRO)
1	0.0	0.0	0.0	0.0	0.0
2	0.167	0.0	0.0	2000.000	0.0
3	0.333	0.0	0.0	2666.669	0.0
4	0.500	0.0	0.0	3066.669	0.0
5	0.833	0.0	0.0	3566.669	0.0
6	1.167	0.0	0.0	3899.999	0.0
7	1.500	0.0	0.0	4149.996	0.0
8	1.667	0.0	0.0	4255.266	0.0
9	2.000	0.0	0.0	4437.086	0.0
10	3.333	0.0	0.0	4937.116	0.0
11	13.333	0.0	0.0	6144.617	0.0
12	20.000	0.0	0.0	6584.617	0.0
13	23.333	0.0	0.0	6782.406	0.0
14	25.000	0.0	0.0	6881.855	0.0
15	28.333	0.0	0.0	7088.777	0.0
16	33.333	0.0	0.0	7440.887	0.0
17	66.667	0.0	0.0	13507.555	0.0
18	133.333	0.0	0.0	100574.188	0.0

********** FIT OF DECELERATING CREEP DATA TO POWER LAW **********

DATA FROM LVDT NO. 1

TRANSFORMED DATA

TIME (MIN)	STR RATE, E (MICRO.E/MIN)	LOG E	LOG EE	LOG E - LOG EE	W
15.0000	66.666977	0.182391E+01	0.181558E+01	0.832844E-02	1.00
25.0000	39.999939	0.160206E+01	0.159726E+01	0.480175E-02	1.00
39.9999	25.000015	0.139794E+01	0.139638E+01	0.155830E-02	1.00
59.9998	16.666504	0.122184E+01	0.122309E+01	-0.124359E-02	1.00
79.9998	12.499849	0.109690E+01	0.110013E+01	-0.322914E-02	1.00
94.9997	10.527000	0.102230E+01	0.102669E+01	-0.438213E-02	1.00
109.9998	9.090994	0.958611E+00	0.964028E+00	-0.541705E-02	1.00
159.9996	6.250393	0.795907E+00	0.803886E+00	-0.797898E-02	1.00
499.9990	2.012501	0.303736E+00	0.316898E+00	-0.131623E-01	1.00
999.9988	1.099998	0.413921E-01	0.206509E-01	0.207412E-01	1.00

FIT PARAMETERS

A	-0.939691E+03	
SLOPE, B	-0.981118	
RANGE FOR A	0.940756E+03	0.938632E+03
RANGE FOR SLOPE, B	-0.9719620	-0.8962615
DURBIN WATSON STATISTIC	1.620	
DEGREE OF FREEDOM FOR DW	11	
UPPER BOUND FOR DW	1.320	
TEST OF SLOPE SIGNIFICANCE	26242.891	

DATA FOR COMPARISON TESTS

WEIGHTING 0.0

MEAN STRAIN	1.026	MEAN TIME	1.978
SSDY	2.699 SSDX	2.786	
SPDXY	-2.742 SSDYX	0.001	

CHECK

SUM OF RESIDUALS -0.000017

DATA STARTS AT # 1

DATA ENDS AT # 11

********** FIT OF ACCELERATING CREEP DATA TO POWER LAW **********

PARAMETERS FOR EVALUATING TOTAL FIT. LVDT NO.: 1

RANGE	ACCELERATING CREEP C	SLOPE,D	R1	DW	DAYS TO INFLEXION	TOTAL FIT R
1 - 17	0.124027E-11	3.5235806	3544.346	2.860	1.388	1940.891
2 - 17	0.143838E-11	3.5056763	3390.474	2.880	1.385	2074.621
3 - 17	0.164256E-11	3.4896088	3196.574	2.902	1.381	2205.808
4 - 17	0.192619E-11	3.4703569	3019.631	2.928	1.377	2382.022
5 - 17	0.303851E-25	7.3636484	44.513	2.261	1.797	39.256
6 - 17	0.467594E-16	4.7753353	97.411	2.324	1.560	198.288
7 - 17	0.401101E-14	4.2296171	132.204	2.404	1.490	391.700
8 - 17	0.871096E-13	3.8527327	183.370	2.504	1.433	785.133
9 - 17	0.577913E-16	4.7568159	31.537	2.269	1.542	192.803
10 - 17	0.531577E-11	3.3595886	274.548	3.358	1.323	4304.723

DATA FROM LVDT NO. 1

TRANSFORMED DATA

TIME (MIN)	STR RATE, E (MICRO.E/MIN)	LOG E	LOG EE	LOG E - LOG EE	W
999.9988	0.037207	-0.142938E+01	-0.119567E+01	-0.233701E+00	1.00
1299.9971	0.177286	-0.751325E+00	-0.842874E+00	0.615491E-01	1.00
1449.9958	0.266911	-0.573634E+00	-0.653547E+00	0.799134E-01	1.00
1599.9956	0.373557	-0.427643E+00	-0.[illegible]917E+00	0.822740E-01	1.00
1849.9978	0.599870	-0.221943E+00	-0.298088E+00	0.761451E-01	1.00
2999.9888	2.663833	0.425507E+00	0.407253E+00	0.182537E-01	1.00

```
117          5999.9766     21.579865  0.133405E+01  0.141859E+01 -0.845423E-01    1.00
118
119
120        FIT PARAMETERS
121           C                              0.531577E-11
122           SLOPE, D                       3.3595886
123           RANGE FOR C                   -0.216705E+02     -0.216705E+02
124           RANGE FOR SLOPE, D             3.7650185        2.9541578
125           DURBIN WATSON STATISTIC          3.358
126           DEGREE OF FREEDOM FOR DW         8
127           UPPER BOUND FOR DW               1.290
128           TEST OF SLOPE SIGNIFICANCE     274.548
129
130
131        DATA FOR COMPARISON TESTS
132           WEIGHTING     5.0
133           MEAN STRAIN        -0.235   MEAN TIME        3.286
134           SSDY            4.743 SSDX             0.413
135           SPDXY           1.387 SSDYX            0.085
136
137        CHECK
138           SUM OF RESIDUALS                0.000108
139
140
141
142           DATA STARTS AT # 10
143           DATA ENDS AT # 17
```

TEST NUMBER = SIXTH

SAMPLE NUMBER = CPACK2N

SAMPLE LENGTH = 1000.000 mm
SAMPLE DIAMETER = 1.000 mm
SAMPLE WEIGHT = 1.000 gm

INITIAL LOAD = 0.0 KN
INITIAL CELL PRESSURE = 0.0 KPA
INITIAL READING FOR LVDT1 = 0.0 mm
INITIAL READING FOR LVDT2 = 0.0 mm

NUMBER	TIME HOURS	LOAD KN	CELL PRESSURE KPA	ENGG. STRAIN #1 (MICRO)	ENGG. STRAIN #2 (MICRO)
1	0.0	0.0	0.0	0.0	0.0
2	0.167	0.0	0.0	2000.000	0.0
3	0.333	0.0	0.0	2666.677	0.0
4	0.500	0.0	0.0	3066.921	0.0
5	0.667	0.0	0.0	3354.475	0.0
6	0.833	0.0	0.0	3585.000	0.0
7	1.000	0.0	0.0	3794.499	0.0
8	1.167	0.0	0.0	4023.769	0.0
9	1.333	0.0	0.0	4335.074	0.0
10	1.667	0.0	0.0	5620.176	0.0
11	3.333	0.0	0.0	120193.063	0.0

********** FIT OF DECELERATING CREEP DATA TO POWER LAW **********

DATA FROM L[redacted] 1

TRANSFORMED DATA

TIME (MIN)	STR RATE, E (MICRO.E/MIN)	LOG E	LOG EE	LOG E - LOG EE	W
15.0000	66.667770	0.182392E+01	0.178784E+01	0.360727E-01	1.00
25.0000	40.024323	0.160232E+01	0.161199E+01	-0.966167E-02	1.00
34.9999	28.755432	0.135872E+01	0.149615E+01	-0.374317E-01	1.00
44.9998	23.052490	0.136272E+01	0.140963E+01	-0.469151E-01	1.00
54.9999	20.949860	0.132118E+01	0.134055E+01	-0.193691E-01	1.00
64.9999	22.927094	0.136035E+01	0.128304E+01	0.773096E-01	1.00

FIT PARAMETERS

A	0.524953E+03	
SLOPE, B	-0.7926929	
RANGE FOR A	0.527026E+03	0.522881E+03
RANGE FOR SLOPE, B	-0.5909653	-0.9944205
DURBIN WATSON STATISTIC	1.300	
DEGREE OF FREEDOM FOR DW	7	
UPPER BOUND FOR DW	1.280	
TEST OF SLOPE SIGNIFICANCE	61.764	

DATA FOR COMPARISON TESTS
WEIGHTING 4.0
MEAN STRAIN 1.488 MEAN TIME 1.554
SSDY 0.187 SSDX 0.279
SPDXY -0.221 SSDYX 0.011

CHECK
SUM OF RESIDUALS -0.000005

DATA STARTS AT # 1
DATA ENDS AT # 7

********** FIT OF ACCELERATING CREEP DATA TO POWER LAW **********

PARAMETERS FOR EVALUATING TOTAL FIT, LVDT NO : 1

RANGE	ACCELERATING CREEP C	SLOPE,D	R1	DW	DAYS TO INFLEXION	TOTAL FIT R
1 - 10	0.188953E-10	6.33992861784	2.355	3.203	0.053	295.375
2 - 10	0.941370E-11	6.4839067	4714.133	3.285	0.054	292.732
3 - 10	0.956718E-15	8.4313278	91.557	2.490	0.058	27.851
4 - 10	0.650473E-13	7.5316935	140.829	2.679	0.057	70.924
5 - 10	0.688955E-12	7.0304470	202.974	2.959	0.055	144.630
6 - 10	0.355059E-11	6.6846743	310.441	3.453	0.055	241.442

DATA FROM LVDT NO. 1

TRANSFORMED DATA

TIME (MIN)	STR RATE, E (MICRO.E/MIN)	LOG E	LOG EE	LOG E - LOG EE	W
64.9999	3.711806	0.569585E+00	0.669024E+00	-0.994391E-01	1.00
74.9997	13.982086	0.114557E+01	0.108446E+01	0.611143E-01	1.00
89.9997	49.386200	0.169361E+01	0.161376E+01	0.798445E-01	1.00
149.9994	1135.562012	0.305521E+01	0.309675E+01	-0.415344E-01	1.00

FIT PARAMETERS

C	0.355059E-11	
SLOPE, D	6.6846743	
RANGE FOR C	0.306732E+02	-0.306732E+02
RANGE FOR SLOPE, D	7.4434586	5.9258890
DURBIN WATSON STATISTIC	3.453	
DEGREE OF FREEDOM FOR DW	5	
UPPER BOUND FOR DW	1.260	
TEST OF SLOPE SIGNIFICANCE	310.441	

DATA FOR COMPARISON TESTS
WEIGHTING 2.0
MEAN STRAIN 1.646 MEAN TIME 1.955
SSDY 3.394 SSDX -0.075

```
117              SPDXY          0.504 SSDYX          0.022
118
119           CHECK
120              SUM OF RESIDUALS =                  0.000018
121
122
123
124              DATA STARTS AT #  6
125              DATA ENDS AT # 10
```

TEST NUMBER = NINTH

SAMPLE NUMBER = CPACK2

SAMPLE LENGTH = 1000.000 mm
SAMPLE DIAMETER = 1.000 mm
SAMPLE WEIGHT = 1.000 gm

INITIAL LOAD = 0.0 KN
INITIAL CELL PRESSURE = 0.0 KPA
INITIAL READING FOR LVDT1 = 0.0 mm
INITIAL READING FOR LVDT2 = 0.0 mm

NUMBER	TIME-HOURS	LOAD KN	CELL PRESSURE KPA	ENGG. STRAIN #1 (MICRO)	ENGG. STRAIN #2 (MICRO)
1	0.0	0.0	0.0	0.0	0.0
2	0.100	0.0	0.0	2000.000	0.0
3	0.167	0.0	0.0	2500.053	0.0
4	0.233	0.0	0.0	2835.450	0.0
5	0.300	0.0	0.0	3112.938	0.0
6	0.333	0.0	0.0	3282.739	0.0
7	0.367	0.0	0.0	3536.829	0.0
8	0.400	0.0	0.0	3984.010	0.0
9	0.500	0.0	0.0	8781.598	0.0
10	0.667	0.0	0.0	87882.875	0.0

********** FIT OF DECELERATING CREEP DATA TO POWER LAW **********

DATA FROM LVDT NO. 1

TRANSFORMED DATA

TIME (MIN)	STR RATE, E (MICRO.E/MIN)	LOG E	LOG EE	LOG E - LOG EE	W
8.0000	125.013245	0.209696E+01	0.209042E+01	0.653553E-02	1.00
12.0000	83.849243	0.192350E+01	0.193924E+01	-0.157413E-01	1.00
16.0000	69.372223	0.184119E+01	0.183198E+01	0.920963E-02	1.00

FIT PARAMETERS

A	0.734099E+03	
SLOPE, B	-0.8585355	
RANGE FOR A	0.735661E+03	0.732536E+03
RANGE FOR SLOPE, B	-0.6773785	-1.0396919
DURBIN WATSON STATISTIC	3.364	
DEGREE OF FREEDOM FOR DW	4	
UPPER BOUND FOR DW	1.250	
TEST OF SLOPE SIGNIFICANCE	89.838	

DATA FOR COMPARISON TESTS

WEIGHTING 1.0
MEAN STRAIN 1.954 MEAN TIME 1.062
SSDY 0.034 SSDX 0.046

SPDXY -0.039 SSDYX 0.000

CHECK
SUM OF RESIDUALS -0.000004

DATA STARTS AT # 1
DATA ENDS AT # 4

********** FIT OF ACCELERATING CREEP DATA TO POWER LAW **********

PARAMETERS FOR EVALUATING TOTAL FIT, LVDT NO. : 1

RANGE	ACCELERATING CREEP C	SLOPE, D	R1	DW	DAYS TO INFLEXION	TOTAL FIT R
1 - 9	0.528389E-10	9.1853409********		1.855	0.014	6516.391
2 - 9	0.191709E-10	9.4900071	4696.938	1.893	0.014	2858.759
3 - 9	0.289372E-12	10.7585983	137.141	2.941	0.015	197.215

DATA FROM LVDT NO. 1

TRANSFORMED DATA

TIME (MIN)	STR RATE, E (MICRO.E/MIN)	LOG E	LOG EE	LOG E - LOG EE	W
15.9999	1.171821	0.688611E-01	0.416078E+00	-0.347216E+00	1.00
18.9999	26.255981	0.141923E+01	0.121903E+01	0.200197E+00	1.00
20.9999	73.238281	0.186474E+01	0.168666E+01	0.178078E+00	1.00
22.9999	173.833252	0.224013E+01	0.211172E+01	0.128413E+00	1.00
26.9999	756.109863	0.287858E+01	0.286091E+01	0.176764E-01	1.00
34.9999	7875.265625	0.389627E+01	0.407345E+01	-0.177183E+00	1.00

FIT PARAMETERS

C	0.289372E-12	
SLOPE, D	10.7585983	
RANGE FOR C	0.317311E+03	-0.317311E+03
RANGE FOR SLOPE, D	12.5960226	8.9211740
DURBIN WATSON STATISTIC	2.941	
DEGREE OF FREEDOM FOR DW	7	
UPPER BOUND FOR DW	1.280	
TEST OF SLOPE SIGNIFICANCE	137.141	

DATA FOR COMPARISON TESTS

WEIGHTING 4.0
MEAN STRAIN 2.061 MEAN TIME 1.357
SSDY 8.488 SSDX 0.071
SPDXY 0.767 SSDYX 0.241

CHECK
SUM OF RESIDUALS 0.000035

```
117
118
119                DATA STARTS AT #  3
120                DATA ENDS AT #  9
```

Appendix D: Example Input File For CPACK2

The following contains two input files, one for the full Gregg River data set and one for the truncated case, Trun6.

```
 1    0,0,0,0,0,0,0,0.0,0,0,0,
 2    0,0,0,0,15,0,4.1,0,0,0,
 3    0,0,0,0,30,0,5.9,0,0,0,
 4    0,0,0,0,45,0,4.1,0,0,0,
 5    0,0,0,0,60,0,3.1,0,0,0,
 6    0,0,0,0,75,0,4.7,0,0,0,
 7    0,0,0,0,90,0,2.4,0,0,0,
 8    0,0,0,0,105,0,5.4,0,0,0,
 9    0,0,0,0,120,0,7.3,0,0,0,
10    0,0,0,0,135,0,9.9,0,0,0,
11    0,0,0,0,150,0,8.3,0,0,0,
12    0,0,0,0,165,0,9.4,0,0,0,
13    0,0,0,0,185,0,12.9,0,0,0,
14    0,0,0,0,195,0,13.0,0,0,0,
15    0,0,0,0,210,0,14.2,0,0,0,
16    0,0,0,0,255,0,16.8,0,0,0,
17    0,0,0,0,270,0,11.1,0,0,0,
18    0,0,0,0,285,0,9.4,0,0,0,
19    0,0,0,0,300,0,10.7,0,0,0,
20    0,0,0,0,315,0,8.6,0,0,0,
21    0,0,0,0,330,0,9.4,0,0,0,
22    0,0,0,0,345,0,10.3,0,0,0,
23    0,0,0,0,360,0,11.1,0,0,0,
24    0,0,0,0,375,0,11.6,0,0,0,
25    0,0,0,0,390,0,11.6,0,0,0,
26    0,0,0,0,405,0,11.6,0,0,0,
27    0,0,0,0,420,0,10.7,0,0,0,
28    0,0,0,0,435,0,11.6,0,0,0,
29    0,0,0,0,450,0,11.6,0,0,0,
30    0,0,0,0,465,0,11.6,0,0,0,
31    0,0,0,0,480,0,10.7,0,0,0,
32    0,0,0,0,495,0,11.2,0,0,0,
33    0,0,0,0,510,0,11.6,0,0,0,
34    0,0,0,0,525,0,11.2,0,0,0,
35    0,0,0,0,540,0,12.0,0,0,0,
36    0,0,0,0,555,0,12.9,0,0,0,
37    0,0,0,0,570,0,12.0,0,0,0,
38    0,0,0,0,585,0,12.0,0,0,0,
39    0,0,0,0,600,0,12.0,0,0,0,
40    0,0,0,0,615,0,12.0,0,0,0,
41    0,0,0,0,630,0,11.8,0,0,0,
42    0,0,0,0,645,0,13.4,0,0,0,
43    0,0,0,0,660,0,12.6,0,0,0,
44    0,0,0,0,675,0,13.4,0,0,0,
45    0,0,0,0,690,0,13.9,0,0,0,
46    0,0,0,0,705,0,13.4,0,0,0,
47    0,0,0,0,720,0,14.2,0,0,0,
48    0,0,0,0,735,0,12.6,0,0,0,
49    0,0,0,0,750,0,14.7,0,0,0,
50    0,0,0,0,765,0,14.2,0,0,0,
51    0,0,0,0,780,0,14.7,0,0,0,
52    0,0,0,0,795,0,13.9,0,0,0,
53    0,0,0,0,810,0,14.7,0,0,0,
54    0,0,0,0,825,0,13.9,0,0,0,
55    0,0,0,0,840,0,15.0,0,0,0,
56    0,0,0,0,855,0,13.9,0,0,0,
57    0,0,0,0,870,0,14.7,0,0,0,
58    0,0,0,0,885,0,13.9,0,0,0,
```

```
 59    0,0,0,0,910,0,13.9,0,0,0,
 60    0,0,0,0,930,0,14.7,0,0,0,
 61    0,0,0,0,945,0,14.7,0,0,0,
 62    0,0,0,0,960,0,16.9,0,0,0,
 63    0,0,0,0,975,0,16.1,0,0,0,
 64    0,0,0,0,990,0,17.9,0,0,0,
 65    0,0,0,0,1005,0,18.7,0,0,0,
 66    0,0,0,0,1020,0,18.5,0,0,0,
 67    0,0,0,0,1035,0,18.3,0,0,0,
 68    0,0,0,0,1050,0,17.8,0,0,0,
 69    0,0,0,0,1065,0,18.3,0,0,0,
 70    0,0,0,0,1080,0,16.4,0,0,0,
 71    0,0,0,0,1095,0,18.2,0,0,0,
 72    0,0,0,0,1110,0,17.1,0,0,0,
 73    0,0,0,0,1125,0,18.6,0,0,0,
 74    0,0,0,0,1140,0,18.4,0,0,0,
 75    0,0,0,0,1155,0,18.1,0,0,0,
 76    0,0,0,0,1170,0,17.9,0,0,0,
 77    0,0,0,0,1185,0,17.9,0,0,0,
 78    0,0,0,0,1200,0,18.2,0,0,0,
 79    0,0,0,0,1215,0,19.3,0,0,0,
 80    0,0,0,0,1230,0,18.7,0,0,0,
 81    0,0,0,0,1245,0,20.6,0,0,0,
 82    0,0,0,0,1260,0,20.6,0,0,0,
 83    0,0,0,0,1275,0,21.3,0,0,0,
 84    0,0,0,0,1290,0,19.6,0,0,0,
 85    0,0,0,0,1305,0,18.2,0,0,0,
 86    0,0,0,0,1320,0,17.1,0,0,0,
 87    0,0,0,0,1335,0,18.2,0,0,0,
 88    0,0,0,0,1350,0,17.5,0,0,0,
 89    0,0,0,0,1365,0,18.5,0,0,0,
 90    0,0,0,0,1380,0,18.7,0,0,0,
 91    0,0,0,0,1395,0,17.8,0,0,0,
 92    0,0,0,0,1410,0,19.2,0,0,0,
 93    0,0,0,0,1425,0,18.4,0,0,0,
 94    0,0,0,0,1440,0,17.9,0,0,0,
 95    0,0,0,0,1455,0,17.4,0,0,0,
 96    0,0,0,0,1470,0,17.7,0,0,0,
 97    0,0,0,0,1485,0,19.2,0,0,0,
 98    0,0,0,0,1500,0,19.8,0,0,0,
 99    0,0,0,0,1515,0,19.1,0,0,0,
100    0,0,0,0,1530,0,19.8,0,0,0,
101    0,0,0,0,1545,0,20.5,0,0,0,
102    0,0,0,0,1560,0,21.9,0,0,0,
103    0,0,0,0,1575,0,22.7,0,0,0,
104    0,0,0,0,1590,0,23.7,0,0,0,
105    0,0,0,0,1605,0,24.6,0,0,0,
106    0,0,0,0,1620,0,23.9,0,0,0,
107    0,0,0,0,1635,0,23.7,0,0,0,
108    0,0,0,0,1665,0,25.6,0,0,0,
109    0,0,0,0,1680,0,27.0,0,0,0,
110    0,0,0,0,1695,0,27.2,0,0,0,
111    0,0,0,0,1710,0,27.4,0,0,0,
112    0,0,0,0,1725,0,27.8,0,0,0,
113    0,0,0,0,1740,0,28.5,0,0,0,
114    0,0,0,0,1755,0,28.2,0,0,0,
115    0,0,0,0,1770,0,28.2,0,0,0,
116    0,0,0,0,1785,0,28.7,0,0,0,
```

```
117    0,0,0,0,1800,0,30.1,0,0,0,
118    0,0,0,0,1815,0,30.1,0,0,0,
119    0,0,0,0,1830,0,29.4,0,0,0,
120    0,0,0,0,1845,0,31.4,0,0,0,
121    0,0,0,0,1860,0,32.1,0,0,0,
122    0,0,0,0,1875,0,33.4,0,0,0,
123    0,0,0,0,1897,0,34.8,0,0,0,
124    0,0,0,0,1905,0,34.7,0,0,0,
125    0,0,0,0,1920,0,35.4,0,0,0,
126    0,0,0,0,1935,0,36.8,0,0,0,
127    0,0,0,0,1950,0,36.8,0,0,0,
128    0,0,0,0,1965,0,38.9,0,0,0,
129    0,0,0,0,1980,0,38.2,0,0,0,
130    0,0,0,0,1995,0,38.9,0,0,0,
131    0,0,0,0,2010,0,40.3,0,0,0,
132    0,0,0,0,2025,0,40.3,0,0,0,
133    0,0,0,0,2040,0,41.0,0,0,0,
134    0,0,0,0,2055,0,41.8,0,0,0,
135    0,0,0,0,2070,0,43.9,0,0,0,
136    0,0,0,0,2085,0,44.6,0,0,0,
137    0,0,0,0,2100,0,44.6,0,0,0,
138    0,0,0,0,2115,0,46.0,0,0,0,
139    0,0,0,0,2130,0,46.7,0,0,0,
140    0,0,0,0,2145,0,46.7,0,0,0,
141    0,0,0,0,2160,0,49.6,0,0,0,
142    0,0,0,0,2175,0,50.9,0,0,0,
143    0,0,0,0,2190,0,53.2,0,0,0,
144    0,0,0,0,2205,0,58.5,0,0,0,
145    0,0,0,0,2220,0,61.3,0,0,0,
146    0,0,0,0,2235,0,62.7,0,0,0,
147    0,0,0,0,2250,0,66.3,0,0,0,
148    0,0,0,0,2265,0,66.9,0,0,0,
149    0,0,0,0,2280,0,67.6,0,0,0,
150    0,0,0,0,2295,0,67.5,0,0,0,
151    0,0,0,0,2310,0,71.0,0,0,0,
152    0,0,0,0,2325,0,71.6,0,0,0,
153    0,0,0,0,2340,0,75.3,0,0,0,
154    0,0,0,0,2355,0,79.9,0,0,0,
155    0,0,0,0,2370,0,83.3,0,0,0,
156    0,0,0,0,2385,0,89.9,0,0,0,
157    0,0,0,0,2390,0,92.4,0,0,0,
158    0,0,0,0,2395,0,93.3,0,0,0,
159    0,0,0,0,2400,0,94.5,0,0,0,
160    0,0,0,0,2405,0,96.2,0,0,0,1,
```

```
 1  0,0,0,0,0,0,0.0,0,0,0,
 2  0,0,0,0,195,0,13.0,0,0,0,
 3  0,0,0,0,210,0,14.2,0,0,0,
 4  0,0,0,0,255,0,16.8,0,0,0,
 5  0,0,0,0,270,0,11.1,0,0,0,
 6  0,0,0,0,285,0,9.4,0,0,0,
 7  0,0,0,0,300,0,10.7,0,0,0,
 8  0,0,0,0,315,0,8.6,0,0,0,
 9  0,0,0,0,330,0,9.4,0,0,0,
10  0,0,0,0,345,0,10.3,0,0,0,
11  0,0,0,0,360,0,11.1,0,0,0,
12  0,0,0,0,375,0,11.6,0,0,0,
13  0,0,0,0,390,0,11.6,0,0,0,
14  0,0,0,0,405,0,11.6,0,0,0,
15  0,0,0,0,420,0,10.7,0,0,0,
16  0,0,0,0,435,0,11.6,0,0,0,
17  0,0,0,0,450,0,11.6,0,0,0,
18  0,0,0,0,465,0,11.6,0,0,0,
19  0,0,0,0,480,0,10.7,0,0,0,
20  0,0,0,0,495,0,11.2,0,0,0,
21  0,0,0,0 510,0,11.6,0,0,0,
22  0,0,0,0 525,0,11.2,0,0,0,
23  0,0,0,0 540,0,12.0,0,0,0,
24  0,0,0,0,555,0,12.9,0,0,0,
25  0,0,0,0,570,0,12.0,0,0,0,
26  0,0,0,0,585,0,12.0,0,0,0,
27  0,0,0,0,600,0,12.0,0,0,0,
28  0,0,0,0,615,0,12.0,0,0,0,
29  0,0,0,0,630,0,11.6,0,0,0,
30  0,0,0,0,645,0,13.4,0,0,0,
31  0,0,0,0,660,0,12.6,0,0,0,
32  0,0,0,0,675,0,13.4,0,0,0,
33  0,0,0,0,690,0,13.9,0,0,0,
34  0,0,0,0,705,0,13.4,0,0,0,
35  0,0,0,0,720,0,14.2,0,0,0,
36  0,0,0,0,735,0,12.6,0,0,0,
37  0,0,0,0,750,0,14.7,0,0,0,
38  0,0,0,0,765,0,14.2,0,0,0,
39  0,0,0,0,780,0,14.7,0,0,0,
40  0,0,0,0,795,0,13.9,0,0,0,
41  0,0,0,0,810,0,14.7,0,0,0,
42  0,0,0,0,825,0,13.9,0,0,0,
43  0,0,0,0,840,0,15.0,0,0,0,
44  0,0,0,0,855,0,13.9,0,0,0,
45  0,0,0,0,870,0,14.7,0,0,0,
46  0,0,0,0,885,0,13.9,0,0,0,
47  0,0,0,0,900,0,13.9,0,0,0,
48  0,0,0,0,930,0,14.7,0,0,0,
49  0,0,0,0,945,0,14.7,0,0,0,
50  0,0,0,0,960,0,16.9,0,0,0,
51  0,0,0,0,975,0,16.1,0,0,0,
52  0,0,0,0,990,0,17.9,0,0,0,
53  0,0,0,0,1005,0,18.7,0,0,0,
54  0,0,0,0,1020,0,18.5,0,0,0,
55  0,0,0,0,1035,0,18.3,0,0,0,
56  0,0,0,0,1050,0,17.8,0,0,0,
57  0,0,0,0,1065,0,18.3,0,0,0,
58  0,0,0,0,1080,0,16.4,0,0,0,
```

```
 59   0,0,0,0,1095,0,18.2,0,0,0,
 60   0,0,0,0,1110,0,17.1,0,0,0,
 61   0,0,0,0,1125,0,18.6,0,0,0,
 62   0,0,0,0,1140,0,18.4,0,0,0,
 63   0,0,0,0,1155,0,18.1,0,0,0,
 64   0,0,0,0,1170,0,17.9,0,0,0,
 65   0,0,0,0,1185,0,17.9,0,0,0,
 66   0,0,0,0,1200,0,18.2,0,0,0,
 67   0,0,0,0,1215,0,19.3,0,0,0,
 68   0,0,0,0,1230,0,18.7,0,0,0,
 69   0,0,0,0,1245,0,20.6,0,0,0,
 70   0,0,0,0,1260,0,20.6,0,0,0,
 71   0,0,0,0,1275,0,21.3,0,0,0,
 72   0,0,0,0,1290,0,19.6,0,0,0,
 73   0,0,0,0,1305,0,18.2,0,0,0,
 74   0,0,0,0,1320,0,17.1,0,0,0,
 75   0,0,0,0,1335,0,18.2,0,0,0,
 76   0,0,0,0,1350,0,17.5,0,0,0,
 77   0,0,0,0,1365,0,18.5,0,0,0,
 78   0,0,0,0,1380,0,18.7,0,0,0,
 79   0,0,0,0,1395,0,17.8,0,0,0,
 80   0,0,0,0,1410,0,19.2,0,0,0,
 81   0,0,0,0,1425,0,18.4,0,0,0,
 82   0,0,0,0,1440,0,17.9,0,0,0,
 83   0,0,0,0,1455,0,17.4,0,0,0,
 84   0,0,0,0,1470,0,17.7,0,0,0,
 85   0,0,0,0,1485,0,19.2,0,0,0,
 86   0,0,0,0,1500,0,19.8,0,0,0,
 87   0,0,0,0,1515,0,19.1,0,0,0,
 88   0,0,0,0,1530,0,19.8,0,0,0,
 89   0,0,0,0,1545,0,20.5,0,0,0,
 90   0,0,0,0,1560,0,21.9,0,0,0,
 91   0,0,0,0,1575,0,22.7,0,0,0,
 92   0,0,0,0,1590,0,23.7,0,0,0,
 93   0,0,0,0,1605,0,24.6,0,0,0,
 94   0,0,0,0,1620,0,23.9,0,0,0,
 95   0,0,0,0,1635,0,23.7,0,0,0,
 96   0,0,0,0,1665,0,25.6,0,0,0,
 97   0,0,0,0,1680,0,27.0,0,0,0,
 98   0,0,0,0,1695,0,27.2,0,0,0,
 99   0,0,0,0,1710,0,27.4,0,0,0,
100   0,0,0,0,1725,0,27.8,0,0,0,
101   0,0,0,0,1740,0,28.5,0,0,0,
102   0,0,0,0,1755,0,28.2,0,0,0,
103   0,0,0,0,1770,0,28.2,0,0,0,
104   0,0,0,0,1785,0,28.7,0,0,0,
105   0,0,0,0,1800,0,30.1,0,0,0,
106   0,0,0,0,1815,0,30.1,0,0,0,
107   0,0,0,0,1830,0,29.4,0,0,0,
108   0,0,0,0,1845,0,31.4,0,0,0,
109   0,0,0,0,1860,0,32.1,0,0,0,
110   0,0,0,0,1875,0,33.4,0,0,0,
111   0,0,0,0,1897,0,34.8,0,0,0,
112   0,0,0,0,1905,0,34.7,0,0,0,
113   0,0,0,0,1920,0,35.4,0,0,0,
114   0,0,0,0,1935,0,36.8,0,0,0,
115   0,0,0,0,1950,0,36.8,0,0,0,
116   0,0,0,0,1965,0,38.9,0,0,0,
```

```
117     0,0,0,0,1980,0,38.2,0,0,0,
118     0,0,0,0,1995,0,38.9,0,0,0,
119     0,0,0,0,2010,0,40.3,0,0,0,
120     0,0,0,0,2025,0,40.3,0,0,0,
121     0,0,0,0,2040,0,41.0,0,0,0,
122     0,0,0,0,2055,0,41.8,0,0,0,
123     0,0,0,0,2070,0,43.9,0,0,0,
124     0,0,0,0,2085,0,44.6,0,0,0,
125     0,0,0,0,2100,0,44.6,0,0,0,
126     0,0,0,0,2115,0,46.0,0,0,0,
127     0,0,0,0,2130,0,46.7,0,0,0,
128     0,0,0,0,2145,0,46.7,0,0,0,
129     0,0,0,0,2160,0,49.6,0,0,0,
130     0,0,0,0,2175,0,50.9,0,0,0,
131     0,0,0,0,2190,0,53.2,0,0,0,
132     0.0,0,0,2205,0,58.5,0,0,0,
133     0.0,0,0,2220,0,61.2,0,0,0,
134     0,0,0,0,2235,0,62.7,0,0,0,
135     0,0,0,0,2250,0,66.3,0,0,0,
136     0,0,0,0,2265,0,66.9,0,0,0,
137     0,0,0,0,2280,0,67.6,0,0,0,
138     0,0,0,0,2295,0,67.5,0,0,0,
139     0,0,0,0,2310,0,71.0,0,0,0,
140     0,0,0,0,2325,0,74.6,0,0,0,
141     0,0,0,0,2340,0,75.3,0,0,0,
142     0,0,0,0,2355,0,79.9,0,0,0,
143     0,0,0,0,2370,0,83.3,0,0,0,
144     0,0,0,0,2385,0,89.9,0,0,0,
145     0,0,0,0,2390,0,92.4,0,0,0,
146     0,0,0,0,2395,0,93.3,0,0,0,
147     0,0,0,0,2400,0,94.5,0,0,0,
148     0,0,0,0,2405,0,96.2,0,0,0,1,
```

Appendix E: Example Run with CPACK2

```
 1       University of Alberta - Computing Services   Device: Vβ31   Task:  4275
 2      # Terminal,Prime,Internal/Teaching,Research
 3      # $run cpack2*cive:graph+*ig+*plotlib 4-grrcp2 7=-7 t=3s
 4      # 14:43:56
 5        THIS PROGRAM ACCEPTS DATA IN THE FOLLOWING FORMAT:
 6        LABEL,TIME CLOCK,3 COUNTERS,LOAD,CELL PRESSURE,DEF.1,DEF.2
 7        IS YOUR DATA IN THIS FORM? (Y,N)
 8        N
 9        DO YOU HAVE AN LVDT CALIBRATION FACTOR?
10        Y
11        INPUT THE LVDT CALIBRATION FACTOR (MULTIPLIER):
12        0.001,
13        INPUT DIAMETER(MM),LENGTH(MM),AND WEIGHT(GM),
14        SEPARATED BY COMMAS:
15        1.,1000.,1.,
16        INPUT SAMPLE NUMBER (8 CHARACTER MAX.):
17        FULL
18        INPUT TEST NUMBER (8 CHARACTER MAX.):
19        GRR NO
20        INPUT NUMBER OF ELEMENTS IN EACH LINE (+ COMMA):
21        10,
22        INPUT NUMBER OF STRAIN GAUGES (LVDTS);(1 OR 2):
23        1,
24            THE ONLY DATA THAT THIS PROGRAM REQUIRES FOR INPUT
25        IN DEVICE 4, IS TIME AND DISPLACEMENT. LIST THE ELEMENTS IN
26        ONE LINE OF YOUR INPUT DATA, IN PROPER ORDER, USING "R1"
27        FOR THE FIRST STRAIN GAUGE READING, "R2" FOR THE SECOND (IF
28        THERE IS ONE), AND "TN","TD","TH","TM","TS", FOR THE TIME
29        IN: MONTHS,DAYS,HOURS,MINUTES,AND SECONDS (YOU MAY HAVE ONLY
30        ONE OF THESE TIME PARAMETERS). USE THE DUMMY VARIABLE "DU"
31        FOR ALL OTHER VALUES. (SEPARATE THE ELEMENTS WITH COMMAS)
32        DU,DU,DU,DU,TM,DU,R1,DU,DU,DU,
33        WOULD YOU LIKE THE DECELERATING CREEP DATA
34        PLOTTED BEFORE THE PROGRAM ATTEMPTS TO ISOLATE
35        ACCELERATING CREEP?
36        NO
37        WOULD YOU LIKE THE PROGRAM TO EXAMINE THE
38        ACCELERATING DATA FOR AN OPTIMUM FIT?
39        YES
40        INPUT DESIRED LIMIT FOR TEST OF SLOPE SIGNIFICANCE IF
41        OTHER THAN 10. (REAL NUMBER, TERMINATED WITH A COMMA):
42        9.0,
43         WOULD YOU LIKE A LOG STRAIN RATE - LOG TIME PLOT?(Y,N)
44        Y
45         WOULD YOU LIKE A STRAIN RATE - TIME PLOT?(Y,N)
46        Y
47         FOLLOWING ARE THE EXTREME VALUES IN THE T VS E PLOT:
48         MINIMUM STRAIN RATE:      0.000185
49         MAXIMUM STRAIN RATE:        0.500049
50         FINAL TIME:              2402.498
51        INPUT DESIRED STRAIN RATE VALUE AT ORIGIN OF Y AXIS      (TERMINATE WITH CO
52        0.0,
53        INPUT DESIRED Y AXIS SCALE (UNITS/INCH):
54        0.15,
55        INPUT DESIRED LENGTH OF Y AXIS (INCHES):
56        5.0,
57        INPUT DESIRED X AXIS (TIME) SCALE (UNITS/INCH):
58        500.,
```

```
INPUT DESIRED LENGTH OF X AXIS (INCHES):
5.0,

  GRAPH   VERSION 2  DEC. 1, 1983

  PLOT FILE NAME IS -PDF

  SUMMARY FILE NAME IS -SUMMARY
```

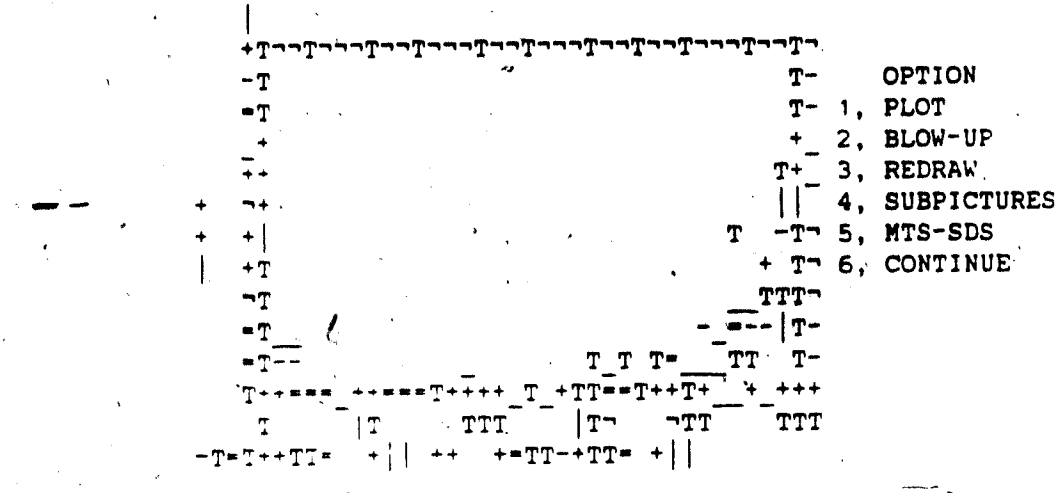


```
SELECT MENU OPTION
? 1

SELECT MENU OPTION
? 6

GRAPH   VERSION 2  DEC. 1, 1983

PLOT FILE NAME IS -PDF

SUMMARY FILE NAME IS -SUMMARY
```

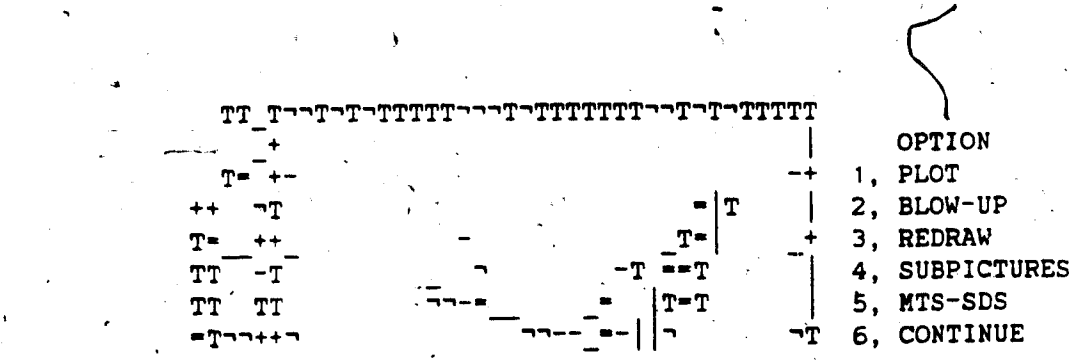

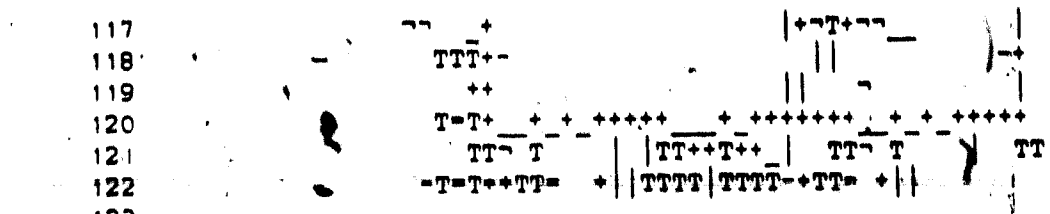

```
117
118
119
120
121
122
123
124
125
126
127
128
129
130          SELECT MENU OPTION
131       ? 1
132
133          SELECT MENU OPTION
134       ? 6
135       # 14:46:50  T=0.895  RC=0
```

Appendix F: Example Output File from CPACK2

The following contains the two output files from CPACK2 for the full and the truncated data sets.

TEST NUMBER = GRR NO

SAMPLE NUMBER = FULL

SAMPLE LENGTH = 1000.000 mm
SAMPLE DIAMETER = 1.000 mm
SAMPLE WEIGHT = 1.000 gm

INITIAL LOAD = 0.0 KN
INITIAL CELL PRESSURE = 0.0 KPA
INITIAL READING FOR LVDT1 = 0.0 mm
INITIAL READING FOR LVDT2 = 0.0 mm

NUMBER	TIME HOURS	LOAD KN	CELL PRESSURE KPA	ENGG. STRAIN #1 (MICRO)	ENGG. STRAIN #2 (MICRO)
1	0.0	0.0	0.0	0.0	0.0
2	0.250	0.0	0.0	4.100	0.0
3	0.500	0.0	0.0	5.900	0.0
4	0.750	0.0	0.0	4.100	0.0
5	1.000	0.0	0.0	3.100	0.0
6	1.250	0.0	0.0	4.700	0.0
7	1.500	0.0	0.0	2.400	0.0
8	1.750	0.0	0.0	5.400	0.0
9	2.000	0.0	0.0	7.300	0.0
10	2.250	0.0	0.0	9.900	0.0
11	2.500	0.0	0.0	8.300	0.0
12	2.750	0.0	0.0	9.400	0.0
13	3.083	0.0	0.0	12.900	0.0
14	3.250	0.0	0.0	13.000	0.0
15	3.500	0.0	0.0	14.200	0.0
16	4.250	0.0	0.0	16.800	0.0
17	4.500	0.0	0.0	11.100	0.0
18	4.750	0.0	0.0	9.400	0.0
19	5.000	0.0	0.0	10.700	0.0
20	5.250	0.0	0.0	8.600	0.0
21	5.500	0.0	0.0	9.400	0.0
22	5.750	0.0	0.0	10.300	0.0
23	6.000	0.0	0.0	11.100	0.0
24	6.250	0.0	0.0	11.600	0.0
25	6.500	0.0	0.0	11.600	0.0
26	6.750	0.0	0.0	11.600	0.0
27	7.000	0.0	0.0	10.700	0.0
28	7.250	0.0	0.0	11.600	0.0
29	7.500	0.0	0.0	11.600	0.0
30	7.750	0.0	0.0	11.600	0.0
31	8.000	0.0	0.0	10.700	0.0
32	8.250	0.0	0.0	11.200	0.0
33	8.500	0.0	0.0	11.600	0.0
34	8.750	0.0	0.0	11.200	0.0
35	9.000	0.0	0.0	12.000	0.0
36	9.250	0.0	0.0	12.900	0.0
37	9.500	0.0	0.0	12.000	0.0
38	9.750	0.0	0.0	12.000	0.0
39	10.000	0.0	0.0	12.000	0.0
40	10.250	0.0	0.0	12.000	0.0
41	10.500	0.0	0.0	11.800	0.0
42	10.750	0.0	0.0	13.400	0.0

59	43	11.000	0.0	0.0	12.600	0.0
60	44	11.250	0.0	0.0	13.400	0.0
61	45	11.500	0.0	0.0	13.900	0.0
62	46	11.750	0.0	0.0	13.400	0.0
63	47	12.000	0.0	0.0	14.200	0.0
64	48	12.250	0.0	0.0	12.600	0.0
65	49	12.500	0.0	0.0	14.700	0.0
66	50	12.750	0.0	0.0	14.200	0.0
67	51	13.000	0.0	0.0	14.700	0.0
68	52	13.250	0.0	0.0	13.900	0.0
69	53	13.500	0.0	0.0	14.700	0.0
70	54	13.750	0.0	0.0	13.900	0.0
71	55	14.000	0.0	0.0	15.000	0.0
72	56	14.250	0.0	0.0	13.900	0.0
73	57	14.500	0.0	0.0	14.700	0.0
74	58	14.750	0.0	0.0	13.900	0.0
75	59	15.167	0.0	0.0	13.900	0.0
76	60	15.500	0.0	0.0	14.700	0.0
77	61	15.750	0.0	0.0	14.700	0.0
78	62	16.000	0.0	0.0	16.900	0.0
79	63	16.250	0.0	0.0	16.100	0.0
80	64	16.500	0.0	0.0	17.900	0.0
81	65	16.750	0.0	0.0	18.700	0.0
82	66	17.000	0.0	0.0	18.500	0.0
83	67	17.250	0.0	0.0	18.300	0.0
84	68	17.500	0.0	0.0	17.800	0.0
85	69	17.750	0.0	0.0	18.300	0.0
86	70	18.000	0.0	0.0	16.400	0.0
87	71	18.250	0.0	0.0	18.200	0.0
88	72	18.500	0.0	0.0	17.100	0.0
89	73	18.750	0.0	0.0	18.600	0.0
90	74	19.000	0.0	0.0	18.400	0.0
91	75	19.250	0.0	0.0	18.100	0.0
92	76	19.500	0.0	0.0	17.900	0.0
93	77	19.750	0.0	0.0	17.900	0.0
94	78	20.000	0.0	0.0	18.200	0.0
95	79	20.250	0.0	0.0	19.300	0.0
96	80	20.500	0.0	0.0	18.700	0.0
97	81	20.750	0.0	0.0	20.600	0.0
98	82	21.000	0.0	0.0	20.600	0.0
99	83	21.250	0.0	0.0	21.300	0.0
100	84	21.500	0.0	0.0	19.600	0.0
101	85	21.750	0.0	0.0	18.200	0.0
102	86	22.000	0.0	0.0	17.100	0.0
103	87	22.250	0.0	0.0	18.200	0.0
104	88	22.500	0.0	0.0	17.500	0.0
105	89	22.750	0.0	0.0	18.500	0.0
106	90	23.000	0.0	0.0	18.700	0.0
107	91	23.250	0.0	0.0	17.800	0.0
108	92	23.500	0.0	0.0	19.200	0.0
109	93	23.750	0.0	0.0	18.400	0.0
110	94	24.000	0.0	0.0	17.900	0.0
111	95	24.250	0.0	0.0	17.400	0.0
112	96	24.500	0.0	0.0	17.700	0.0
113	97	24.750	0.0	0.0	19.200	0.0
114	98	25.000	0.0	0.0	19.800	0.0
115	99	25.250	0.0	0.0	19.100	0.0
116	100	25.500	0.0	0.0	19.800	0.0

117	101	25.750	0.0	0.0
118	102	26.000	0.0	0.0
119	103	26.250	0.0	0.0
120	104	26.500	0.0	0.0
121	105	26.750	0.0	0.0
122	106	27.000	0.0	0.0
123	107	27.250	0.0	0.0
124	108	27.750	0.0	0.0
125	109	28.000	0.0	0.0
126	110	28.250	0.0	0.0
127	111	28.500	0.0	0.0
128	112	28.750	0.0	0.0
129	113	29.000	0.0	0.0
130	114	29.250	0.0	0.0
131	115	29.500	0.0	0.0
132	116	29.750	0.0	0.0
133	117	30.000	0.0	0.0
134	118	30.250	0.0	0.0
135	119	30.500	0.0	0.0
136	120	30.750	0.0	0.0
137	121	31.000	0.0	0.0
138	122	31.250	0.0	0.0
139	123	31.617	0.0	0.0
140	124	31.750	0.0	0.0
141	125	32.000	0.0	0.0
142	126	32.250	0.0	0.0
143	127	32.500	0.0	0.0
144	128	32.750	0.0	0.0
145	129	33.000	0.0	0.0
146	130	33.250	0.0	0.0
147	131	33.500	0.0	0.0
148	132	33.750	0.0	0.0
149	133	34.000	0.0	0.0
150	134	34.250	0.0	0.0
151	135	34.500	0.0	0.0
152	136	34.750	0.0	0.0
153	137	35.000	0.0	0.0
154	138	35.250	0.0	0.0
155	139	35.500	0.0	0.0
156	140	35.750	0.0	0.0
157	141	36.000	0.0	0.0
158	142	36.250	0.0	0.0
159	143	36.500	0.0	0.0
160	144	36.750	0.0	0.0
161	145	37.000	0.0	0.0
162	146	37.250	0.0	0.0
163	147	37.500	0.0	0.0
164	148	37.750	0.0	0.0
165	149	38.000	0.0	0.0
166	150	38.250	0.0	0.0
167	151	38.500	0.0	0.0
168	152	38.750	0.0	0.0
169	153	39.000	0.0	0.0
170	154	39.250	0.0	0.0
171	155	39.500	0.0	0.0
172	156	39.750	0.0	0.0
173	157	39.833	0.0	0.0
174	158	39.917	0.0	0.0

20.500	0.0
21.900	0.0
22.700	0.0
23.700	0.0
24.600	0.0
23.900	0.0
23.700	0.0
25.600	0.0
27.000	0.0
27.200	0.0
27.400	0.0
27.800	0.0
28.500	0.0
28.200	0.0
28.200	0.0
28.700	0.0
30.100	0.0
30.100	0.0
29.400	0.0
31.400	0.0
32.100	0.0
33.400	0.0
34.800	0.0
34.700	0.0
35.400	0.0
36.800	0.0
36.800	0.0
38.900	0.0
38.200	0.0
38.900	0.0
40.300	0.0
40.300	0.0
41.000	0.0
41.800	0.0
43.900	0.0
44.600	0.0
44.600	0.0
46.000	0.0
46.700	0.0
46.700	0.0
49.600	0.0
50.900	0.0
53.200	0.0
58.500	0.0
61.300	0.0
62.700	0.0
66.300	0.0
66.900	0.0
67.600	0.0
67.500	0.0
71.000	0.0
71.600	0.0
75.300	0.0
79.900	0.0
83.300	0.0
89.900	0.0
92.400	0.0
93.300	0.0

159	40.000	0.0	0.0	94.500	0.0
160	40.083	0.0	0.0	96.200	0.0

********** FIT OF DECELERATING CREEP DATA TO POWER LAW **********

DATA FROM LVDT NO 1

TRANSFORMED DATA

TIME (MIN)	STR RATE, E (MICRO.E/MIN)	LOG E	LOG EE	LOG E - LOG EE	W
78.7500	0.025714	-0.158982E+01	-0.147676E+01	-0.113060E+00	3.50
112.4997	0.126667	-0.897338E+00	-0.160659E+01	0.709254E+00	2.25
131.2497	0.080000	-0.109691E+01	-0.166270E+01	0.565792E+00	2.13
153.7498	0.013334	-0.187506E+01	-0.172030E+01	-0.154759E+00	1.56
264.3171	0.010458	-0.198057E+01	-0.191752E+01	-0.630474E-01	11.78
451.8162	0.002964	-0.252813E+01	-0.211267E+01	-0.415461E+00	6.39
566.2485	0.002222	-0.265325E+01	-0.219484E+01	-0.458414E+00	6.20
622.4980	0.014722	-0.183202E+01	-0.222931E+01	0.397292E+00	4.10
663.7483	0.017778	-0.175012E+01	-0.225267E+01	0.502549E+00	2.55
693.7485	0.003333	-0.247712E+01	-0.226876E+01	-0.208365E+00	3.27
769.2024	0.006994	-0.215528E+01	-0.230634E+01	0.151065E+00	7.14
881.7024	0.003422	-0.246577E+01	-0.235603E+01	-0.109746E+00	4.57
952.4980	0.060000	-0.122185E+01	-0.238414E+01	0.116229E+01	3.28
978.7473	0.062222	-0.120606E+01	-0.239403E+01	0.118798E+01	2.14
1023.7480	0.000185	-0.373303E+01	-0.241040E+01	-0.132263E+01	5.07
1106.2498	0.002744	-0.256165E+01	-0.243861E+01	-0.123046E+00	5.04
1177.4978	0.000445	-0.335209E+01	-0.246133E+01	-0.890763E+00	3.02
1271.2471	0.003547	-0.245009E+01	-0.248921E+01	0.391245E-01	10.51
1413.7468	0.003470	-0.245966E+01	-0.252788E+01	0.682287E-01	5.75
1496.2461	0.011111	-0.195424E+01	-0.254853E+01	0.594287E+00	3.88
1518.7466	0.015556	-0.180811E+01	-0.255396E+01	0.745855E+00	2.44

FIT PARAMETERS

A	0.129582E+01	
SLOPE, B	-0.8381323	
RANGE FOR A	0.944789E+01	-0.685626E+01
RANGE FOR SLOPE, B	-0.5153224	-1.1609421
DURBIN WATSON STATISTIC	1.748	
DEGREE OF FREEDOM FOR DW	99	
UPPER BOUND FOR DW	1.690	
TEST OF SLOPE SIGNIFICANCE	26.962	

DATA FOR COMPARISON TESTS

WEIGHTING	94.6		
MEAN STRAIN	-2.236	MEAN TIME	2.802
SSDY	35.427	SSDX	11.190
SPDXY	-9.378	SSDYX	27.567

CHECK

SUM OF RESIDUALS	-0.000197

DATA STARTS AT # 1
DATA ENDS AT # 99

********** FIT OF ACCELERATING CREEP DATA TO POWER LAW **********

PARAMETERS FOR EVALUATING TOTAL FIT, LVDT NO.: 1

RANGE	ACCELERATING CREEP C	SLOPE,D	R1	DW	DAYS TO INFLEXION	TOTAL FIT R
1 - 159	0.858661E-07	1.6248941	62.915	0.903	0.570	13.418
2 - 159	0.703475E-07	1.6531563	61.507	0.950	0.573	13.502
3 - 159	0.168578E-06	1.5330820	51.786	0.783	0.557	13.175
4 - 159	0.104138E-06	1.6002188	53.458	0.787	0.564	13.365
5 - 159	0.447627E-07	1.7176752	59.787	0.808	0.577	13.696
6 - 159	0.194017E-07	1.8338804	65.598	0.832	0.589	14.023
7 - 159	0.294729E-08	2.0954199	87.866	1.311	0.614	14.755
8 - 159	0.441707E-09	2.3583984	115.500	1.150	0.636	15.478
9 - 159	0.160164E-18	5.3228436	462.729	1.713	0.814	21.540
10 - 159	0.196321E-10	2.7923365	227.066	1.168	0.664	16.622
11 - 159	0.156300E-16	4.7060394	401.385	1.590	0.782	20.631
12 - 159	0.493847E-16	4.5511274	378.597	1.550	0.773	20.361
13 - 159	0.331860E-14	3.9853296	301.711	1.391	0.736	19.237

DATA FROM LVDT NO. 1

TRANSFORMED DATA

TIME (MIN)	STR RATE, E (MICRO.E/MIN)	LOG E	LOG EE	LOG E - LOG EE	W
660.6790	0.000514	-0.328918E+01	-0.324046E+01	-0.487194E-01	24.00
905.2847	0.012683	-0.189677E+01	-0.269528E+01	0.798512E+00	13.00
1102.4971	0.003526	-0.245271E+01	-0.235417E+01	-0.985365E-01	23.50
1372.4973	0.000685	-0.316439E+01	-0.197503E+01	-0.118936E+01	12.75
1518.7466	0.012761	-0.189412E+01	-0.179978E+01	-0.943441E-01	6.88
1537.4978	0.043903	-0.135751E+01	-0.177854E+01	0.421031E+00	3.94
1552.4973	0.090590	-0.104292E+01	-0.176174E+01	0.718821E+00	2.47
1567.4978	0.050614	-0.129572E+01	-0.174509E+01	0.449369E+00	1.73
1582.4971	0.063968	-0.119404E+01	-0.172861E+01	0.534574E+00	1.37
1604.9961	0.009559	-0.201957E+01	-0.170418E+01	-0.315397E+00	2.18
1642.4934	0.031457	-0.150229E+01	-0.166420E+01	0.161919E+00	1.59
1672.4961	0.090757	-0.104212E+01	-0.163288E+01	0.590756E+00	1.30
1687.4954	0.010776	-0.196755E+01	-0.161742E+01	-0.350131E+00	1.15
1702.4995	0.010794	-0.196681E+01	-0.160210E+01	-0.364715E+00	1.07
1717.4961	0.024149	-0.161711E+01	-0.158692E+01	-0.301876E-01	1.04
1739.9966	0.014178	-0.184839E+01	-0.156439E+01	-0.283992E+00	2.02
1769.9968	0.010874	-0.196361E+01	-0.153481E+01	-0.428808E+00	1.51
1799.9976	0.036469	-0.143807E+01	-0.150571E+01	0.676432E-01	2.25
1829.9971	0.048719	-0.131230E+01	-0.147711E+01	0.164805E+00	1.63
1852.4976	0.044303	-0.135356E+01	-0.145596E+01	0.102392E+00	1.31
1867.4954	0.084318	-0.107408E+01	-0.144200E+01	0.367920E+00	1.16
1887.9956	0.049598	-0.130453E+01	-0.142310E+01	0.118568E+00	1.58
1910.4968	0.031904	-0.149616E+01	-0.140260E+01	-0.935612E-01	1.29
1931.2444	0.059941	-0.122228E+01	-0.138390E+01	0.161624E+00	1.64

291	1957.4990	0.056075	-0.125123E+01	-0.136053E+01	0.109303E+00	1.82
292	1983.7473	0.013322	-0.187544E+01	-0.133748E+01	-0.537967E+00	1.41
293	2006.2471	0.060012	-0.122176E+01	-0.131796E+01	0.961981E-01	1.71
294	2028.7444	0.[illegible]	-0.153883E+01	-0.129866E+01	-0.240178E+00	1.35
295	2047.4971	0.011161	-0.129106E+01	-0.128273E+01	-0.833225E-02	1.18
296	2062.4954	0.137839	-0.860629E+00	-0.127010E+01	0.409469E+00	1.09
297	2081.2446	0.028967	-0.153809E+01	-0.125443E+01	-0.283657E+00	1.54
298	2103.7463	0.060096	-0.122115E+01	-0.123582E+01	0.146685E-01	1.27
299	2126.2439	0.029006	-0.153751E+01	-0.121741E+01	-0.320101E+00	1.64
300	2148.7444	0.126800	-0.896881E+00	-0.119919E+01	0.302311E+00	1.32
301	2167.4917	0.084593	-0.107267E+01	-0.118416E+01	0.111489E+00	1.16
302	2182.4946	0.151274	-0.820237E+00	-0.117222E+01	0.351981E+00	1.08
303	2197.4944	0.351284	-0.454342E+00	-0.116036E+01	0.706021E+00	1.01
304	2212.4941	0.184628	-0.733702E+00	-0.114859E+01	0.411888E+00	1.02
305	2227.4939	0.091307	-0.103950E+01	-0.113689E+01	0.973969E-01	1.01
306	2242.4973	0.237983	-0.623454E+00	-0.112528E+01	0.501822E+00	1.00
307	2257.4917	0.037996	-0.142026E+01	-0.111374E+01	-0.306517E+00	1.00
308	2276.2437	0.026900	-0.157024E+01	-0.109942E+01	-0.470820E+00	1.50
309	2298.7437	0.151359	-0.819992E+00	-0.108240E+01	0.262408E+00	1.25
310	2317.4956	0.038041	-0.141975E+01	-0.106834E+01	-0.351408E+00	1.13
311	2332.4954	0.244716	-0.611337E+00	-0.105717E+01	0.445834E+00	1.06
312	2347.4939	0.304728	-0.516087E+00	-0.104608E+01	0.529990E+00	1.03
313	2362.4966	0.224739	-0.648322E+00	-0.103505E+01	0.386728E+00	1.02
314	2377.4951	0.438081	-0.358446E+00	-0.102410E+01	0.665651E+00	1.01
315	2387.4924	0.498214	-0.302584E+00	-0.101683E+01	0.714249E+00	1.00
316	2392.4888	0.178109	-0.749314E+00	-0.101322E+01	0.263901E+00	1.00
317	2397.4907	0.238011	-0.623403E+00	-0.100960E+01	0.386197E+00	1.00
318	2402.4917	0.338184	-0.470847E+00	-0.100599E+01	0.535147E+00	1.00

FIT PARAMETERS

C	0.331860E-14	
SLOPE, D	3.9853296,	
RANGE FOR C	0.269785E+02	-0.269785E+02
RANGE FOR SLOPE, D	4.4427414	3.5279169
DURBIN WATSON STATISTIC	1.391	
DEGREE OF FREEDOM FOR DW	147	
UPPER BOUND FOR DW	1.690	
TEST OF SLOPE SIGNIFICANCE	301.711	

DATA FOR COMPARISON TESTS

WEIGHTING 144.0

MEAN STRAIN -2.032 MEAN TIME 3.123

SSDY 111.798 SSDX 4.795

SPDXY 18.969 SSDYX 36.116

CHECK

SUM OF RESIDUALS 0.026526

DATA STARTS AT # 13

DATA ENDS AT #159

TEST NUMBER = GRR NO

SAMPLE NUMBER = TRUNG

SAMPLE LENGTH = 1000.000 mm
SAMPLE DIAMETER = 1.000 mm
SAMPLE WEIGHT = 1.000 gm

INITIAL LOAD = 0.0 KN
INITIAL CELL PRESSURE = 0.0 KPA
INITIAL READING FOR LVDT1 = 0.0 mm
INITIAL READING FOR LVDT2 = 0.0 mm

NUMBER	TIME HOURS	LOAD KN	CELL PRESSURE KPA	ENGG. STRAIN #1 (MICRO)	ENGG. STRAIN #2 (MICRO)
1	0.0	0.0	0.0	0.0	0.0
2	3.250	0.0	0.0	13.000	0.0
3	3.500	0.0	0.0	14.200	0.0
4	4.250	0.0	0.0	10.800	0.0
5	4.500	0.0	0.0	11.100	0.0
6	4.750	0.0	0.0	9.400	0.0
7	5.000	0.0	0.0	10.700	0.0
8	5.250	0.0	0.0	8.600	0.0
9	5.500	0.0	0.0	9.400	0.0
10	5.750	0.0	0.0	10.300	0.0
11	6.000	0.0	0.0	11.100	0.0
12	6.250	0.0	0.0	11.600	0.0
13	6.500	0.0	0.0	11.600	0.0
14	6.750	0.0	0.0	11.600	0.0
15	7.000	0.0	0.0	10.700	0.0
16	7.250	0.0	0.0	11.600	0.0
17	7.500	0.0	0.0	11.600	0.0
18	7.750	0.0	0.0	11.600	0.0
19	8.000	0.0	0.0	10.700	0.0
20	8.250	0.0	0.0	11.200	0.0
21	8.500	0.0	0.0	11.600	0.0
22	8.750	0.0	0.0	11.200	0.0
23	9.000	0.0	0.0	12.000	0.0
24	9.250	0.0	0.0	12.900	0.0
25	9.500	0.0	0.0	12.000	0.0
26	9.750	0.0	0.0	12.000	0.0
27	10.000	0.0	0.0	12.000	0.0
28	10.250	0.0	0.0	12.000	0.0
29	10.500	0.0	0.0	11.800	0.0
30	10.750	0.0	0.0	13.400	0.0
31	11.000	0.0	0.0	12.600	0.0
32	11.250	0.0	0.0	13.400	0.0
33	11.500	0.0	0.0	13.900	0.0
34	11.750	0.0	0.0	13.400	0.0
35	12.000	0.0	0.0	14.200	0.0
36	12.250	0.0	0.0	12.600	0.0
37	12.500	0.0	0.0	14.700	0.0
38	12.750	0.0	0.0	14.200	0.0
39	13.000	0.0	0.0	14.700	0.0
40	13.250	0.0	0.0	13.900	0.0
41	13.500	0.0	0.0	14.700	0.0
				13.900	0.0

59	43	14.000	0.0	0.0	15.000	0.0
60	44	14.250	0.0	0.0	13.900	0.0
61	45	14.500	0.0	0.0	14.700	0.0
62	46	14.750	0.0	0.0	13.900	0.0
63	47	15.167	0.0	0.0	13.900	0.0
64	48	15.500	0.0	0.0	14.700	0.0
65	49	15.750	0.0	0.0	14.700	0.0
66	50	16.000	0.0	0.0	16.900	0.0
67	51	16.250	0.0	0.0	16.100	0.0
68	52	16.500	0.0	0.0	17.900	0.0
69	53	16.750	0.0	0.0	18.700	0.0
70	54	17.000	0.0	0.0	18.500	0.0
71	55	17.250	0.0	0.0	18.300	0.0
72	56	17.500	0.0	0.0	17.800	0.0
73	57	17.750	0.0	0.0	18.300	0.0
74	58	18.000	0.0	0.0	16.[illegible]	0.0
75	59	18.250	0.0	0.0	18.200	0.0
76	60	18.500	0.0	0.0	17.100	0.0
77	61	18.750	0.0	0.0	18.600	0.0
78	62	19.000	0.0	0.0	18.400	0.0
79	63	19.250	0.0	0.0	18.100	0.0
80	64	19.500	0.0	0.0	17.900	0.0
81	65	19.750	0.0	0.0	17.900	0.0
82	66	20.000	0.0	0.0	18.200	0.0
83	67	20.250	0.0	0.0	19.300	0.0
84	68	20.500	0.0	0.0	18.700	0.0
85	69	20.750	0.0	0.0	20.600	0.0
86	70	21.000	0.0	0.0	20.600	0.0
87	71	21.250	0.0	0.0	21.300	0.0
88	72	21.500	0.0	0.0	19.600	0.0
89	73	21.750	0.0	0.0	18.200	0.0
90	74	22.000	0.0	0.0	17.100	0.0
91	75	22.250	0.0	0.0	18.200	0.0
92	76	22.500	0.0	0.0	17.500	0.0
93	77	22.750	0.0	0.0	18.500	0.0
94	78	23.000	0.0	0.0	18.700	0.0
95	79	23.250	0.0	0.0	17.800	0.0
96	80	23.500	0.0	0.0	19.200	0.0
97	81	23.750	0.0	0.0	18.400	0.0
98	82	24.000	0.0	0.0	17.900	0.0
99	83	24.250	0.0	0.0	17.400	0.0
100	84	24.500	0.0	0.0	17.700	0.0
101	85	24.750	0.0	0.0	19.200	0.0
102	86	25.000	0.0	0.0	19.800	0.0
103	87	25.250	0.0	0.0	19.100	0.0
104	88	25.500	0.0	0.0	19.800	0.0
105	89	25.750	0.0	0.0	20.500	0.0
106	90	26.000	0.0	0.0	21.900	0.0
107	91	26.250	0.0	0.0	22.700	0.0
108	92	26.500	0.0	0.0	23.700	0.0
109	93	26.750	0.0	0.0	24.600	0.0
110	94	27.000	0.0	0.0	23.900	0.0
111	95	27.250	0.0	0.0	23.700	0.0
112	96	27.750	0.0	0.0	25.600	0.0
113	97	28.000	0.0	0.0	27.000	0.0
114	98	28.250	0.0	0.0	27.200	0.0
115	99	28.500	0.0	0.0	27.400	0.0
116	100	28.750	0.0	0.0	27.800	0.0

117	101	29.000	0.0	0.0	28.500	0.0
118	102	29.250	0.0	0.0	28.200	0.0
119	103	29.500	0.0	0.0	28.200	0.0
120	104	29.750	0.0	0.0	28.700	0.0
121	105	30.000	0.0	0.0	30.100	0.0
122	106	30.250	0.0	0.0	30.100	0.0
123	107	30.500	0.0	0.0	29.400	0.0
124	108	30.750	0.0	0.0	31.400	0.0
125	109	31.000	0.0	0.0	32.100	0.0
126	110	31.250	0.0	0.0	33.400	0.0
127	111	31.617	0.0	0.0	34.800	0.0
128	112	31.750	0.0	0.0	34.700	0.0
129	113	32.000	0.0	0.0	35.400	0.0
130	114	32.250	0.0	0.0	36.800	0.0
131	115	32.500	0.0	0.0	36.800	0.0
132	116	32.750	0.0	0.0	38.900	0.0
133	117	33.000	0.0	0.0	38.200	0.0
134	118	33.250	0.0	0.0	38.900	0.0
135	119	33.500	0.0	0.0	40.300	0.0
136	120	33.750	0.0	0.0	40.300	0.0
137	121	34.000	0.0	0.0	41.000	0.0
138	122	34.250	0.0	0.0	41.800	0.0
139	123	34.500	0.0	0.0	43.900	0.0
140	124	34.750	0.0	0.0	44.600	0.0
141	125	35.000	0.0	0.0	44.600	0.0
142	126	35.250	0.0	0.0	46.000	0.0
143	127	35.500	0.0	0.0	46.700	0.0
144	128	35.750	0.0	0.0	46.700	0.0
145	129	36.000	0.0	0.0	49.600	0.0
146	130	36.250	0.0	0.0	50.900	0.0
147	131	36.500	0.0	0.0	53.200	0.0
148	132	36.750	0.0	0.0	58.500	0.0
149	133	37.000	0.0	0.0	61.300	0.0
150	134	37.250	0.0	0.0	62.700	0.0
151	135	37.500	0.0	0.0	66.300	0.0
152	136	37.750	0.0	0.0	66.900	0.0
153	137	38.000	0.0	0.0	67.600	0.0
154	138	38.250	0.0	0.0	67.500	0.0
155	139	38.500	0.0	0.0	71.000	0.0
156	140	38.750	0.0	0.0	71.600	0.0
157	141	39.000	0.0	0.0	75.300	0.0
158	142	39.250	0.0	0.0	79.900	0.0
159	143	39.500	0.0	0.0	83.300	0.0
160	144	39.750	0.0	0.0	89.900	0.0
161	145	39.833	0.0	0.0	92.400	0.0
162	146	39.917	0.0	0.0	93.300	0.0
163	147	40.000	0.0	0.0	94.500	0.0
164	148	40.083	0.0	0.0	96.200	

165
166
167 ********** FIT OF DECELERATING CREEP DATA TO POWER LAW **********
168
169
170
171 DATA FROM LVDT NO. 1
172
173
174 TRANSFORMED DATA

TIME (MIN)	STR RATE, E (MICRO.E/MIN)	LOG E	LOG EE	LOG E - LOG EE	W
456.0696	0.003518	-0.245373E+01	-0.253761E+01	0.838747E-01	11.00
566.2485	0.002222	-0.265325E+01	-0.233699E+01	-0.316265E+00	8.50
622.4980	0.014722	-0.183202E+01	-0.224918E+01	0.417163E+00	5.25
663.7483	0.017778	-0.175012E+01	-0.218970E+01	0.439580E+00	3.13
693.7485	0.003333	-0.247712E+01	-0.214872E+01	-0.328409E+00	3.59
769.2024	0.006994	-0.215528E+01	-0.205300E+01	-0.102280E+00	7.28
881.7024	0.003422	-0.246577E+01	-0.192644E+01	-0.539328E+00	4.64
952.4980	0.060000	-0.122185E+01	-0.185484E+01	0.632992E+00	3.32
978.7473	0.062222	-0.120606E+01	-0.182964E+01	0.623582E+00	2.16
1012.4978	0.009333	-0.202998E+01	-0.179821E+01	-0.231775E+00	3.58

FIT PARAMETERS

A	0.610978E-08	
SLOPE, B	2.1347523	
RANGE FOR A	0.278182E+03	0.278182E+03
RANGE FOR SLOPE, B	2.9991745	1.2700291
DURBIN WATSON STATISTIC	2.115	
DEGREE OF FREEDOM FOR DW	56	
UPPER BOUND FOR DW	1.608	
TEST OF SLOPE SIGNIFICANCE	24.363	

DATA FOR COMPARISON TESTS

WEIGHTING	50.4		
MEAN STRAIN	-2.185	MEAN TIME	2.824
SSDY	9.816	SSDY	0.702
SPDXY	1.498	SSDYY	6.618

CHECK

SUM OF RESIDUALS	0.000348

DATA STARTS AT # 1
DATA ENDS AT # 56

********** FIT OF ACCELERATING CREEP DATA TO POWER LAW **********

PARAMETERS FOR EVALUATING TOTAL FIT, LVDT NO : 1

	RANGE	ACCELERATING CREEP C	SLOPE, D	R1	DW	DAYS TO INFLEXION	TOTAL FIT R
BBO= -60.2928925	1 - 147	0.509473E-60	17.6471558	6027.129	1.987	1.581	81.170
BBO= -60.3189850	2 - 147	0.479769E-60	17.6548767	5892.172	1.987	1.581	81.171
BBO= -60.2922363	3 - 147	0.510244E-60	17.6469421	5748.762	1.987	1.581	81.170
BBO= -60.1392517	4 - 147	0.725712E-60	17.6016388	5585.559	1.988	1.581	81.161
BBO= -60.2590179	5 - 147	0.550805E-60	17.6371002	5478.590	1.987	1.581	81.168
BBO= -60.4591980							

233		6 - 147	0.347388E-60	17.6963959	5387.754	1.986	1.581	R1 179
234	BBO=	-60.6016693						
235		7 - 147	0.250234E-60	17.7386017	5286.793	1.986	1.581	R1 187
236	BBO=	-60.8437500						
237		8 - 147	0.143307E-60	17.8103180	5204.746	1.984	1.582	R1 199
238	BBO=	-61.0510101						
239		9 - 147	0.889218E-61	17.8717194	5116.867	1.983	1.582	R1 210
240	BBO=	-61.2193146						
241		10 - 147	0.603532E-61	17.9215698	5022.750	1.982	1.582	R1 219
242	BBO=	-61.3523712						
243		11 - 147	0.444263E-61	17.9609833	4923.699	1.982	1.582	R1 226
244	BBO=	-61.4660950						
245		12 - 147	0.341915E-61	17.9946594	4822.211	1.981	1.582	R1 232.
246	BBO=	-61.5821686						
247		13 - 147	0.261728E-61	18.0290375	4722.246	1.981	1.582	R1 238
248	BBO=	-61.7016602						
249		14 - 147	0.198772E-61	18.0644531	4624.367	1.980	1.583	R1 244
250	BBO=	-61.8652496						
251		15 - 147	0.136385E-61	18.1128998	4534.352	1.979	1.583	R1 252
252	BBO=	-61.9912720						
253		16 - 147	0.102034E-61	18.1502228	4439.430	1.979	1.583	R1 259
254	BBO=	-62.1204071						
255		17 - 147	0.757891E-62	18.1884766	4346.223	1.978	1.583	R1 265
256	BBO=	-62.2527313						
257		18 - 147	0.558834E-62	18.2276764	4254.598	1.977	1.583	R1 271
258	BBO=	-62.4295349						
259		19 - 147	0.371946E-62	18.2800293	4170.266	1.977	1.584	R1 280
260	BBO=	-62.5869904						
261		20 - 147	0.258837E-62	18.3266907	4084.141	1.976	1.584	R1 288
262	BBO=	-62.7303467						
263		21 - 147	0.186067E-62	18.3691559	3996.948	1.975	1.584	R1 295
264	BBO=	-62.8953705						
265		22 - 147	0.127247E-62	18.4180298	3913.753	1.974	1.584	R1 303
266	BBO=	-63.0279083						
267		23 - 147	0.937790E-63	18.4572754	3827.151	1.974	1.584	R1 309
268	BBO=	-63.1244965						
269		24 - 147	0.750792E-63	18.4859009	3737.223	1.973	1.584	R1 313
270	BBO=	-63.2660980						
271		25 - 147	0.541899E-63	18.5278320	3654.005	1.972	1.584	R1 320
272	BBO=	-63.4115601						
273		26 - 147	0.387662E-63	18.5709381	3572.344	1.971	1.585	R1 327
274	BBO=	-63.5612640						
275		27 - 147	0.274633E-63	18.6152649	3492.225	1.971	1.585	R1 334
276	BBO=	-169.205768						
277		28 - 147	0.0	49.949661323366	313.	1.060	1.617	R2 170
278	BBO=	-127.3952637						
279		29 - 147	0.0	37.555694615863	676.	1.333	1.608	R2 099
280	BBO=	-115.9178925						
281		30 - 147	0.0	31.153396613439	785.	1.120	1.605	R2 043
282	BBO=	-110.3871002						
283		31 - 147	0.0	32.513900812121	660.	1.464	1.603	R2 005
284	BBO=	-106.1502838						
285		32 - 147	0.0	31.257904111075	520.	1.500	1.601	R1 972
286	BBO=	-102.8280331						
287		33 - 147	0.0	30.273101810224	289.	1.526	1.600	R1 942
288	BBO=	-100.4600220						
289		34 - 147	0.0	29.5710754	9557.984	1.547	1.599	R1 918
290	BBO=	-98.2972870						

294		35 - 147	0.0	28.9299011	8951.152	1.566	1.598	R1 895
292	BBO=	-96.9817047						
293		36 - 147	0.0	28.5398865	8491.340	1.578	1.597	R1 880
294	BBO=	-95.3274384						
295		37 - 147	0.0	28.0494690	8003.734	1.593	1.597	R1 860
296	BBO=	-94.0510101						
297		38 - 147	0.0	27.6710510	7586.500	1.601	1.596	R1 843
298	BBO=	-92.8530579						
299		39 - 147	0.0	27.3159027	7195.961	1.615	1.595	R1 827
300	BBO=	-91.9765625						
301		40 - 147	0.0	27.0560303	6860.695	1.623	1.595	R1 815
302	BBO=	-91.0717010						
303		41 - 147	0.0	26.7877808	6534.523	1.631	1.594	R1 802
304	BBO=	-90.4199371						
305		42 - 147	0.0	26.5945282	6249.746	1.637	1.594	R1 793
306	BBO=	-89.6749878						
307		43 - 147	0.0	26.3736267	5964.246	1.645	1.594	R1 782
308	BBO=	-89.1914063						
309		44 - 147	0.0	26.2302704	5717.152	1.649	1.593	R1 774
310	BBO=	-88.6544495						
311		45 - 147	0.0	26.0710602	5472.598	1.655	1.593	R1 766
312	BBO=	-88.2997742						
313		46 - 147	0.0	25.9658508	5254.738	1.659	1.593	R1 761
314	BBO=	-88.0062256						
315		47 - 147	0.0	25.8787994	5050.832	1.662	1.593	R1 756
316	BBO=	-87.6564789						
317		48 - 147	0.0	25.7750549	4848.793	1.666	1.593	R1 751

DATA FROM LVDT NO. 1

TRANSFORMED DATA

TIME (MIN)	STR RATE, E (MICRO.E/MIN)	LOG E	LOG EE	LOG E - LOG EE	W
1987.4399	0.002258	-0.264628E+01	-0.264275E+01	-0.353813E-02	46.50
2347.4939	0.210831	-0.676066E+00	-0.778946E+00	0.102880E+00	23.75
2362.4966	0.129569	-0.887497E+00	-0.707642E+00	-0.179856E+00	12.38
2377.4951	0.341563	-0.466529E+00	-0.636795E+00	0.170266E+00	6.69
2387.4924	0.400589	-0.397301E+00	-0.589813E+00	0.192512E+00	3.84
2392.4888	0.080309	-0.109524E+01	-0.566422E+00	-0.528815E+00	2.42
2397.4907	0.139836	-0.854382E+00	-0.543045E+00	-0.311337E+00	1.71
2402.4917	0.239280	-0.621094E+00	-0.519714E+00	-0.101380E+00	1.36

FIT PARAMETERS

C	0.0	
SLOPE, D	25.7750549	
RANGE FOR C	0.276289E+03	-0.276289E+03
RANGE FOR SLOPE, D	26.5063782	25.0437164
DURBIN WATSON STATISTIC	1.666	
DEGREE OF FREEDOM FOR DW	100	
UPPER BOUND FOR DW	1.690	
TEST OF SLOPE SIGNIFICANCE	4848.793	

DATA FOR COMPARISON TESTS

Listing of -7 at 18:00:07 on JUN 24, 1987 for CCid-GSB7 on UALTAMTS

```
349                 WEIGHTING   96.6
350                 MEAN STRAIN          -1.619    MEAN TIME          3.338
351                 SSDY              94.443 SSDX                    0.143
352                 SPDXY              3.592 SSDYX                   1.846
353
354               CHECK
355                 SUM OF RESIDUALS                          0.019044
356
357
358
359                 DATA STARTS AT # 48
360                 DATA ENDS AT #147
```

Appendix G: Regression Plots from *STPK

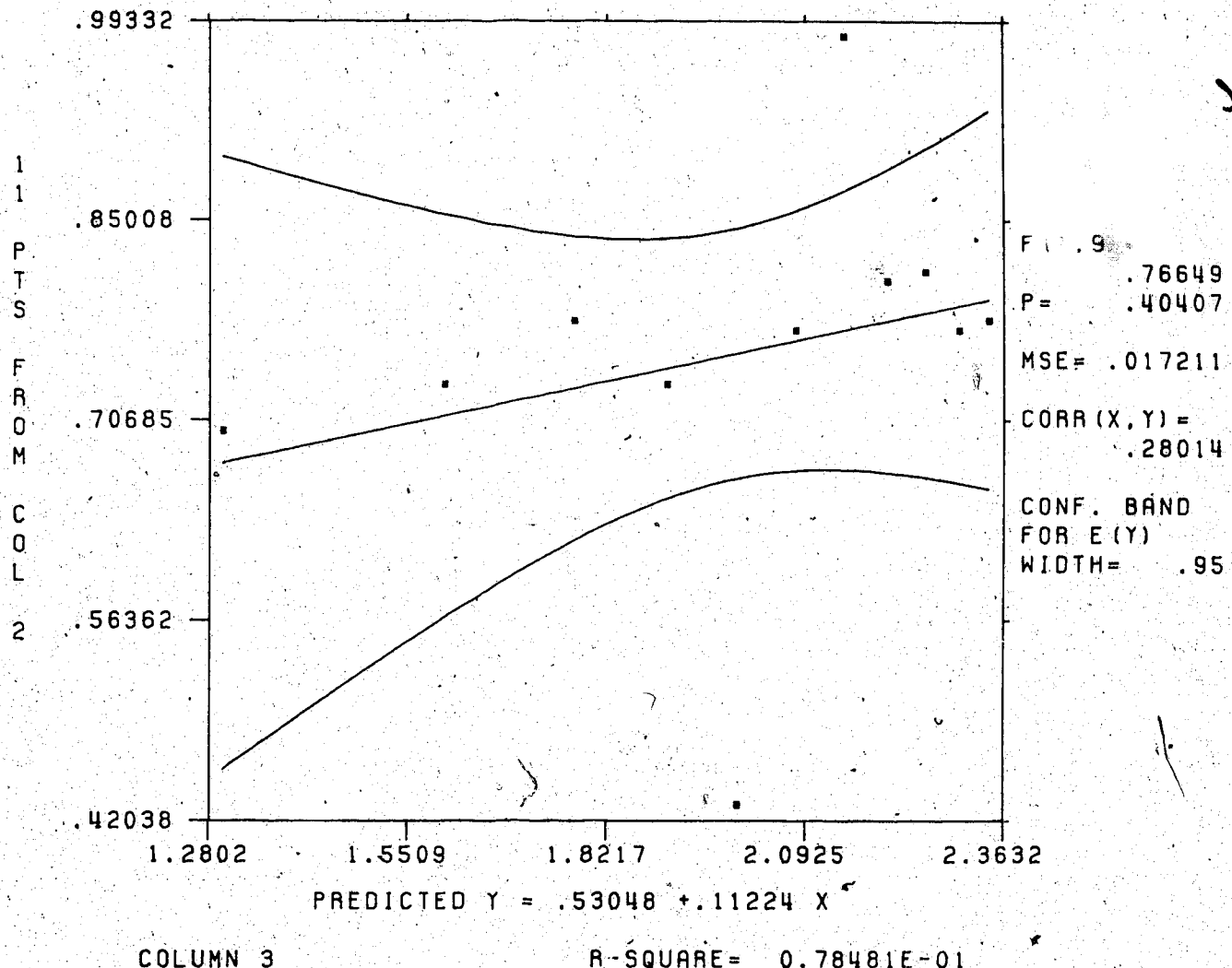

Figure G.1 Regression plot for sample #3.2

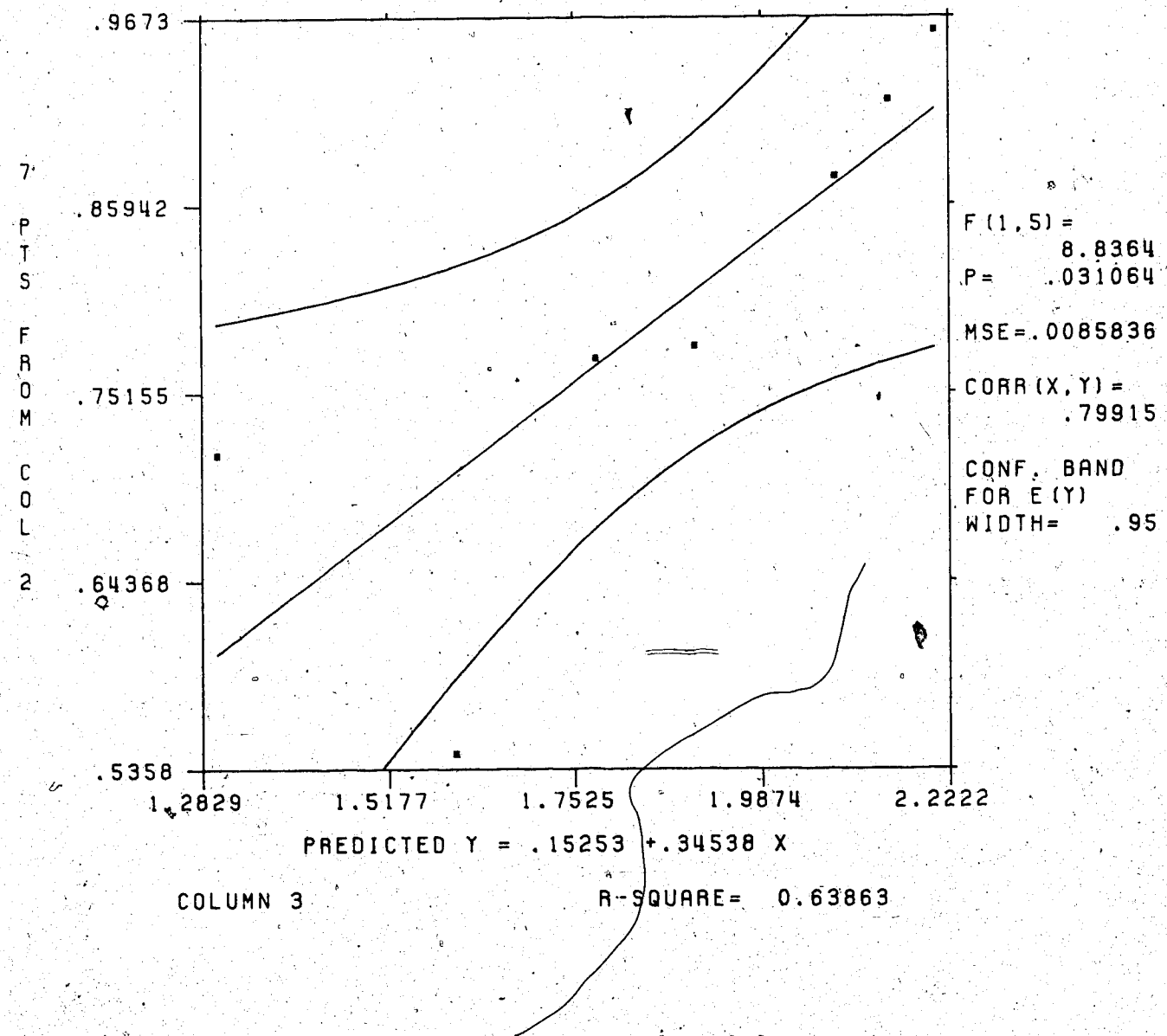

Figure G.2 Regression plot for sample #6.2

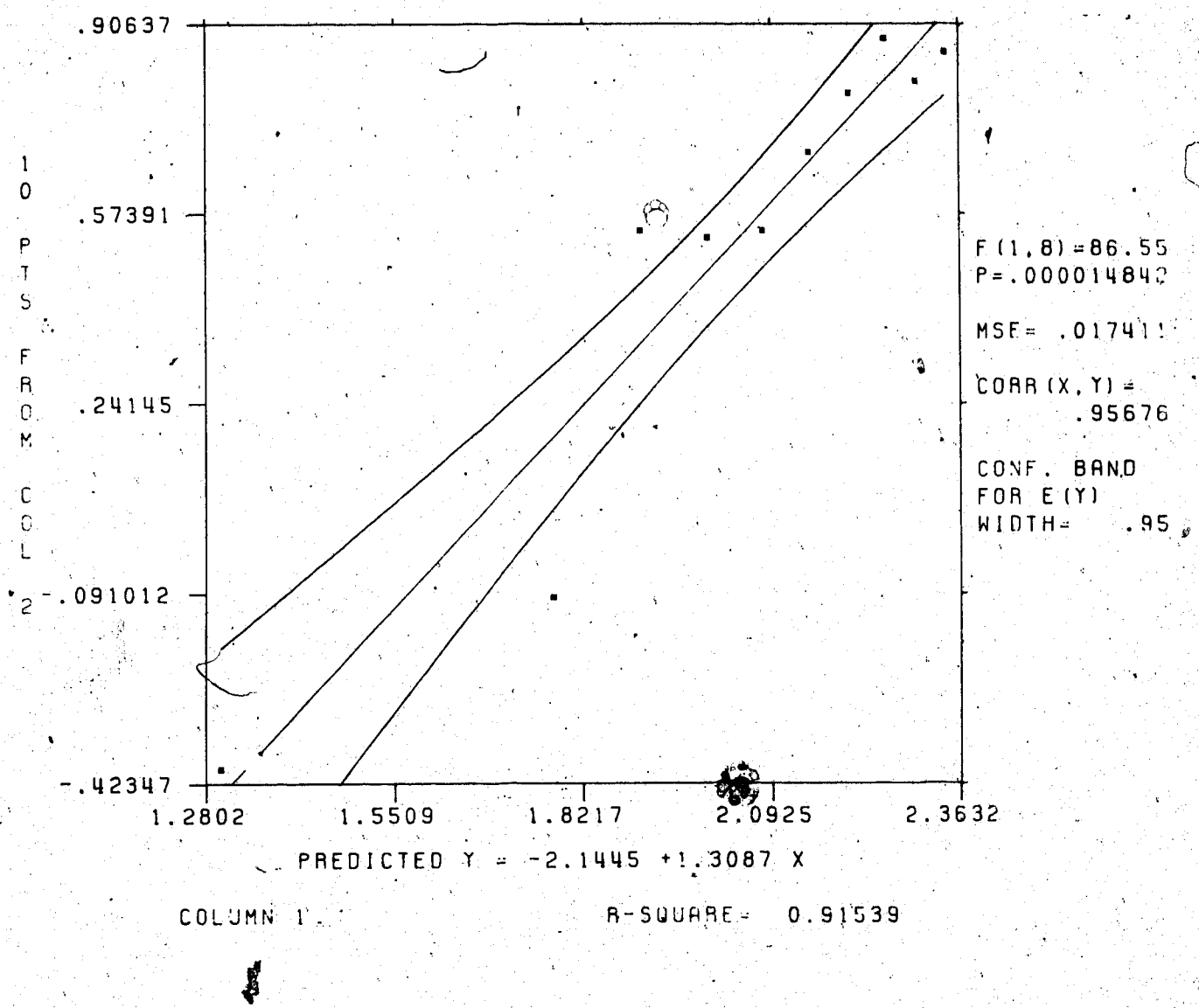

Figure G.3 Regression plot for sample #8.2

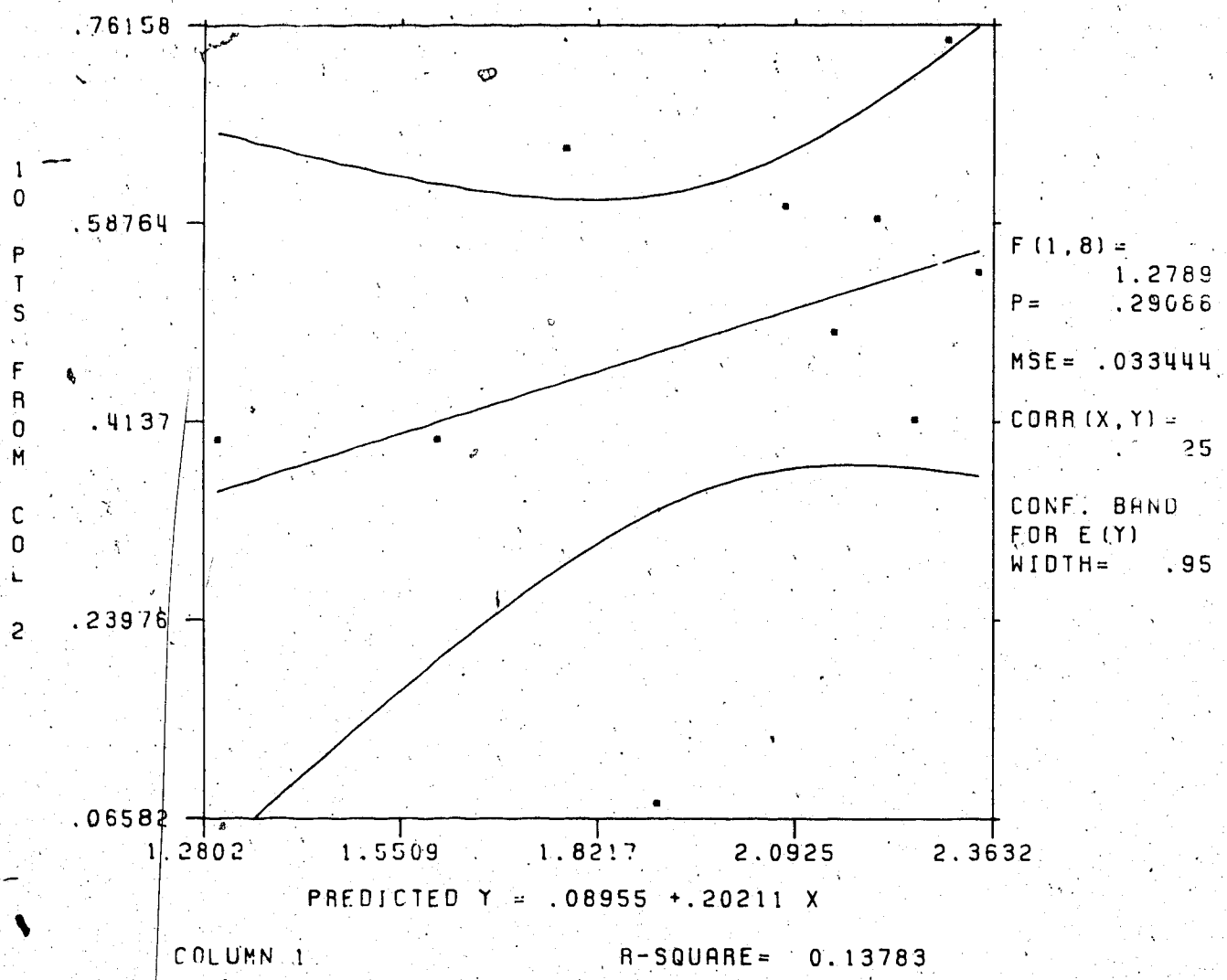

Figure G.4 Regression plot for sample #10.2

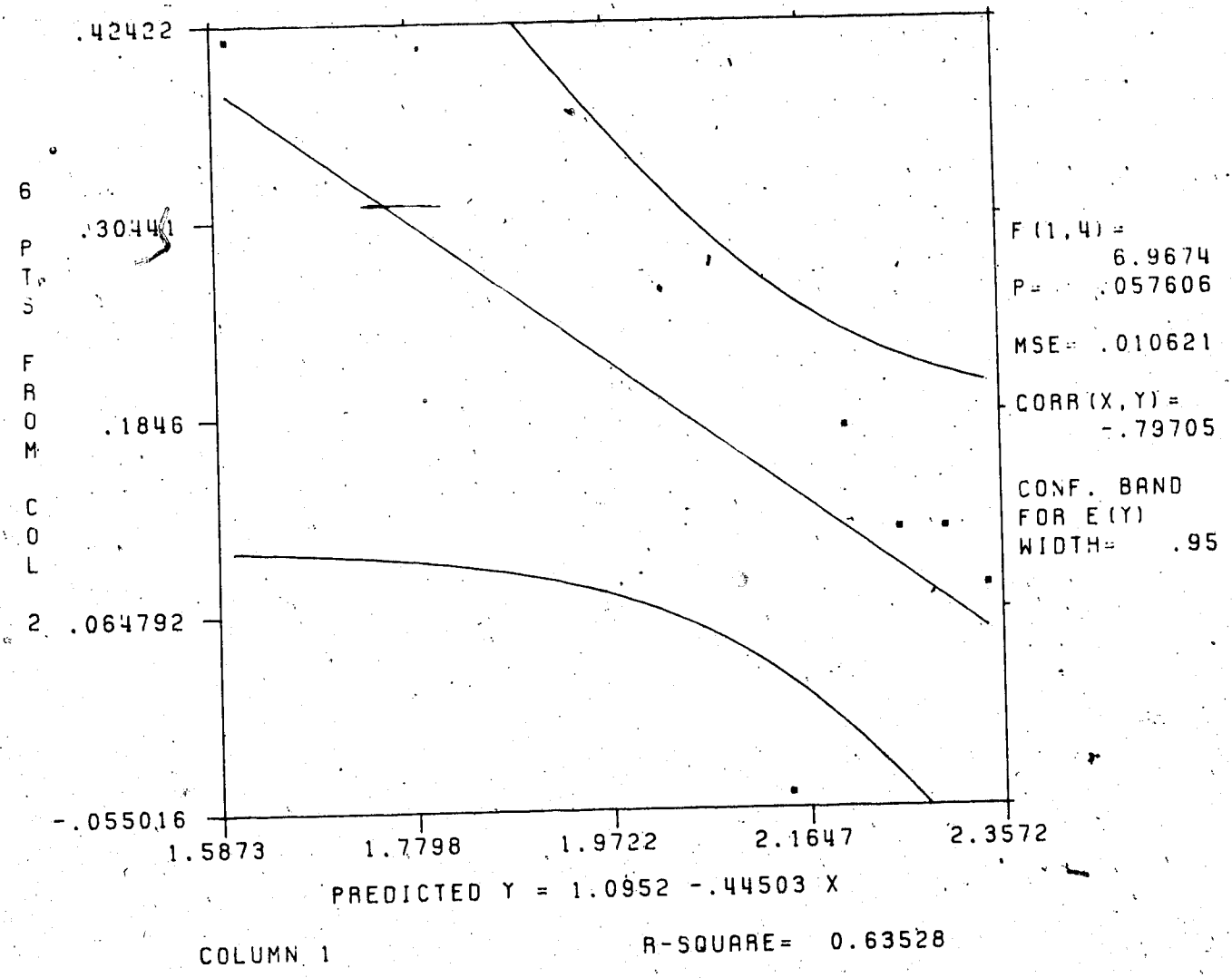

Figure G.5 Regression plot for sample #13.2

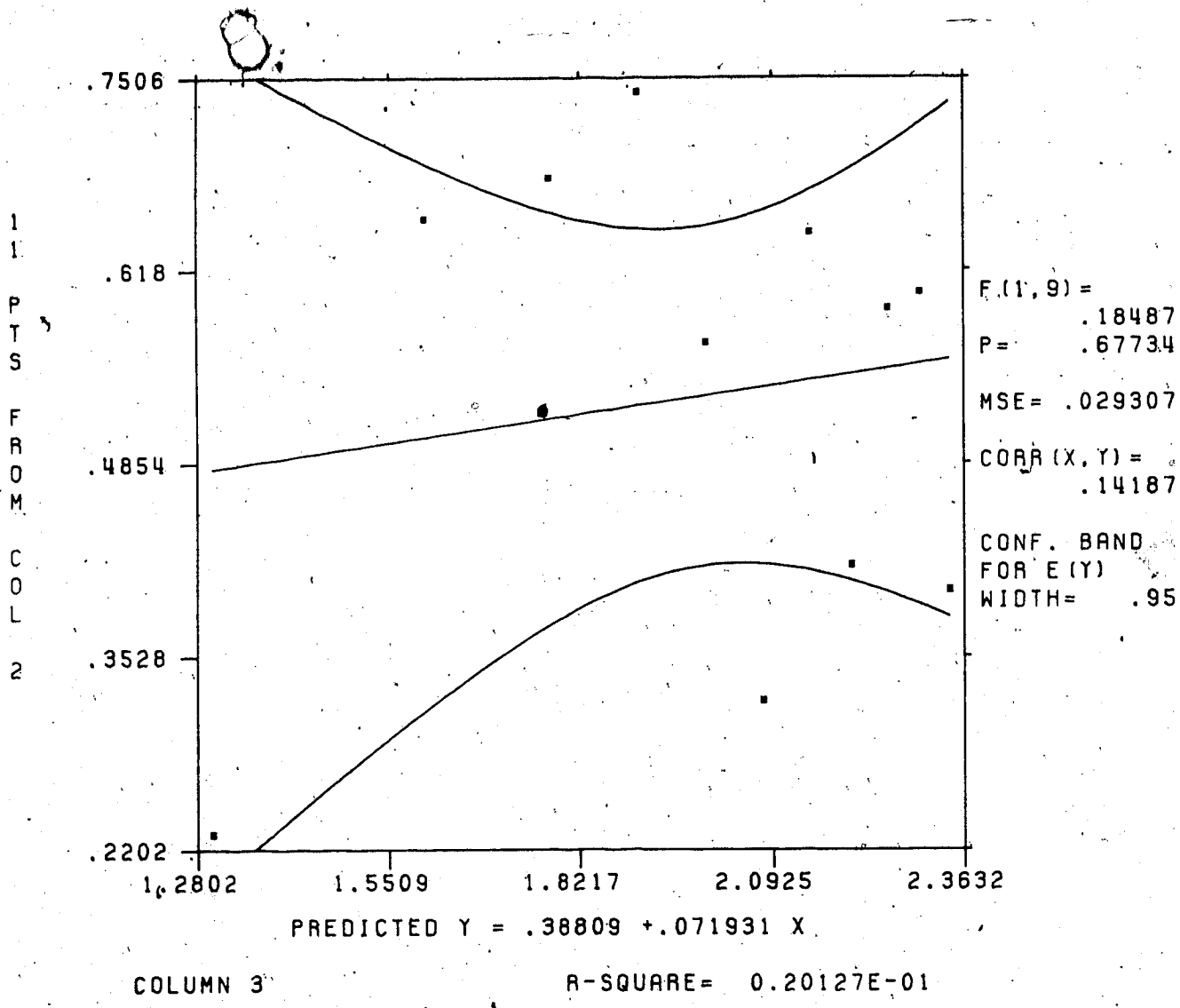

Figure G.6 Regression plot for sample #4.2

Appendix H: Finite Difference Program

The following contains an example listing of the finite difference program used to solve and plot the results of the sliding block modelling equation. The program is not interactive and hence any parameter changes have to made in the file before the program is compiled.

The program is invoked by typing in the following two commands:

```
$Run *Fortgtest Scards=Programfile T=0.3s

$Run -Load#+*Disspla 7=-Output 9=-Plotfile T=0.5s
```

An example output file is also included.

```
      REAL Y(500),YP(500),DIS(500),RATE(500)
C-- "A" is the inclination angle and must be expressed
C--    in radians. Note that "A" is equal to the
C--    inclination angle BETA for initial stability.
      DATA A/1.047198/
C-- "G" is the force of gravity in mm/min**2
      DATA G/3.5316E07/
C-- using raw data, upper limit, from the regressions.
      DATA B/0.00023203/
      DATA EXP/1.3087/
C-- "T" is the time step amount which can be varied.
      DATA T/0.0005/
C-- "N" is the number of points required.
      DATA N/200/
C-- zero the variables.
      DO 1 I=1,N
        Y(I)=0.
        YP(I)=0.
    1 CONTINUE
      DO 2 I=3,N
        E=Y(I-1)
        EQN=G*SIN(A)-G*COS(A)*TAN(A*(1.-B*E**EXP))
        Y(I)=T**2*EQN+2*E-Y(I-2)
        YP(I)=(Y(I)-E)/T
        DIS(I)=(Y(I)+E)/2.
    2 CONTINUE
      WRITE(7,105)
  105 FORMAT('DISPLACEMENT (MM)',4X,'RATE (MM/MIN)')
      DO 40 L=3,N
        DIS(L-2)=DIS(L)
        RATE(L-2)=YP(L)
   40 CONTINUE
      NN=N-2
      DO 3 I=1,NN
        WRITE(7,100)DIS(I),RATE(I)
    3 CONTINUE
  100 FORMAT(2(G13.4,5X))
      CALL DSPDEV('PLOTTER ')
      CALL PAGE(11.,8.5)
      CALL SIMPLX
      CALL INTAXS
      CALL AREA2D(8.,5.)
      CALL XNAME('Displacement (mm)$',100)
      CALL YNAME('Displacement Rate (mm/min)$',100)
      CALL GRAF(0.,25.,100.,0.,5000.,25000.)
      CALL THKFRM(0.03)
      CALL FRAME
      CALL CURVE(DIS,RATE,NN,0)
      CALL ENDPL(0)
      CALL DONEPL
      STOP
      END
```

53	DISPLACEMENT (MM)	RATE (MM/MIN)
54	0.2000E-05	0.8000E-02
55	0.8000E-05	0.1600E-01
56	0.1800E-04	0.2400E-01
57	0.3200E-04	0.3200E-01
58	0.5000E-04	0.4000E-01
59	0.7200E-04	0.4800E-01
60	0.9800E-04	0.5600E-01
61	0.1280E-03	0.6400E-01
62	0.1620E-03	0.7200E-01
63	0.2000E-03	0.8000E-01
64	0.2420E-03	0.8800E-01
65	0.2880E-03	0.9600E-01
66	0.3380E-03	0.1040
67	0.3920E-03	0.1120
68	0.4500E-03	0.1200
69	0.5120E-03	0.1280
70	0.5780E-03	0.1360
71	0.6480E-03	0.1440
72	0.7220E-03	0.1520
73	0.8000E-03	0.1600
74	0.8820E-03	0.1680
75	0.9680E-03	0.1760
76	0.1058E-02	0.1840
77	0.1152E-02	0.1920
78	0.1250E-02	0.2000
79	0.1352E-02	0.2080
80	0.1458E-02	0.2160
81	0.1568E-02	0.2240
82	0.1682E-02	0.2320
83	0.1800E-02	0.2400
84	0.1932E-02	0.2880
85	0.2088E-02	0.3360
86	0.2268E-02	0.3840
87	0.2472E-02	0.4320
88	0.2700E-02	0.4800
89	0.2952E-02	0.5280
90	0.3228E-02	0.5760
91	0.3528E-02	0.6239
92	0.3852E-02	0.6719
93	0.4200E-02	0.7199
94	0.4572E-02	0.7679
95	0.4968E-02	0.8159
96	0.5388E-02	0.8639
97	0.5832E-02	0.9119
98	0.6300E-02	0.9599
99	0.6791E-02	1.008
100	0.7307E-02	1.056
101	0.7847E-02	1.104
102	0.8411E-02	1.152
103	0.8999E-02	1.200
104	0.9611E-02	1.248
105	0.1025E-01	1.296
106	0.1091E-01	1.344
107	0.1159E-01	1.392
108	0.1230E-01	1.440
109	0.1303E-01	1.488
110	0.1379E-01	1.536

111	0.1457E-01	1.584
112	0.1537E-01	1.632
113	0.1620E-01	1.704
114	0.1707E-01	1.776
115	0.1798E-01	1.848
116	0.1892E-01	1.920
117	0.1990E-01	1.992
118	0.2091E-01	2.064
119	0.2196E-01	2.136
120	0.2305E-01	2.208
121	0.2417E-01	2.280
122	0.2533E-01	2.352
123	0.2653E-01	2.464
124	0.2779E-01	2.576
125	0.2911E-01	2.688
126	0.3048E-01	2.800
127	0.3191E-01	2.912
128	0.3339E-01	3.024
129	0.3494E-01	3.168
130	0.3656E-01	3.311
131	0.3825E-01	3.455
132	0.4002E-01	3.599
133	0.4185E-01	3.743
134	0.4377E-01	3.919
135	0.4577E-01	4.095
136	0.4786E-01	4.271
137	0.5004E-01	4.446
138	0.5232E-01	4.662
139	0.5470E-01	4.878
140	0.5720E-01	5.094
141	0.5980E-01	5.334
142	0.6253E-01	5.574
143	0.6538E-01	5.813
144	0.6835E-01	6.093
145	0.7147E-01	6.373
146	0.7474E-01	6.693
147	0.7816E-01	7.013
148	0.8176E-01	7.365
149	0.8553E-01	7.717
150	0.8948E-01	8.101
151	0.9363E-01	8.509
152	0.9799E-01	8.917
153	0.1026	9.365
154	0.1074	9.853
155	0.1124	10.36
156	0.1177	10.88
157	0.1233	11.43
158	0.1292	12.00
159	0.1353	12.62
160	0.1418	13.30
161	0.1486	14.01
162	0.1558	14.76
163	0.1634	15.59
164	0.1714	16.44
165	0.1799	17.36
166	0.1888	18.32
167	0.1982	19.34
168	0.2081	20.43

169	0.2187	21.59
170	0.2298	22.81
171	0.2415	24.13
172	0.2539	25.53
173	0.2670	27.02
174	0.2810	28.62
175	0.2957	30.32
176	0.3113	32.15
177	0.3279	34.11
178	0.3454	36.21
179	0.3641	38.44
180	0.3839	40.85
181	0.4050	43.43
182	0.4274	46.17
183	0.4512	49.11
184	0.4766	52.29
185	0.5036	55.70
186	0.5323	59.35
187	0.5630	63.27
188	0.5957	67.49
189	0.6306	72.04
190	0.6678	76.92
191	0.7076	82.19
192	0.7501	87.88
193	0.7956	94.02
194	0.8442	100.7
195	0.8964	107.8
196	0.9522	115.6
197	1.012	124.0
198	1.076	133.1
199	1.145	142.9
200	1.220	153.6
201	1.299	165.2
202	1.385	177.8
203	1.477	191.5
204	1.577	206.5
205	1.684	222.7
206	1.800	240.4
207	1.925	259.7
208	2.060	280.8
209	2.206	303.9
210	2.365	329.2
211	2.536	356.9
212	2.722	387.2
213	2.924	420.5
214	3.143	457.0
215	3.382	497.2
216	3.642	541.5
217	3.925	590.3
218	4.233	644.0
219	4.570	703.5
220	4.938	769.1
221	5.341	841.8
222	5.782	922.4
223	6.266	1012.
224	6.796	1111.
225	7.379	1222.
226	8.021	1345.

227	8.728	
228	9.507	1635.
229	10.37	1806.
230	11.32	1998.
231	12.37	2213.
232	13.54	2455.
233	14.83	2726.
234	16.27	3032.
235	17.87	3377.
236	19.66	3766.
237	21.65	4206.
238	23.88	4704.
239	26.37	5270.
240	29.17	5911.
241	32.31	6641.
242	35.84	7471.
243	39.81	8418.
244	44.29	9497.
245	49.34	0.1073E+05
246	55.06	0.1214E+05
247	61.53	0.1375E+05
248	68.87	0.1559E+05
249	77.19	0.1770E+05
250	86.64	0.2010E+05
251	97.38	0.2286E+05